

**EFFECTS OF *Centella asiatica* SAPONINS ON
TELOMERASE ACTIVATION AND WOUND
HEALING**

**A Thesis Submitted to
the Graduate School of Engineering and Sciences of
İzmir Institute of Technology
in Partial Fulfillment of the Requirements for the Degree of**

MASTER OF SCIENCE

in Biotechnology

**by
Devran DEMİRBAŞ**

**October 2021
İZMİR**

ACKNOWLEDGMENTS

Firstly, I would like to express my deep gratitude to my esteemed supervisor Prof. Dr. Erdal BEDİR for giving me a chance, his endless support, patience and guidance.

I would like to thank Prof. Dr. Petek BALLAR KIRMIZIBAYRAK for her valuable contributions to my thesis, patience, interest, and opening her laboratory for bioactivity studies.

I'm grateful to Gülten KURU and Sinem YILMAZ, for training me and assisting the bioactivity studies.

I'm also grateful to Ünver KURT for assisting structure elucidation studies and sharing his valuable comments.

I would like to thank Eyüp BİLGİ and Melis KÜÇÜKSOLAK for sharing their knowledge and experience during my research.

I want to thank all BEDİR group members for their help, friendship and wonderful time we spent together.

I'm grateful to my co-supervisor Assoc. Prof. Dr. Ali Oğuz BÜYÜKKİLEÇİ for his support.

I would like to thank my dearest friends Alper ULUBAŞ, Alperay TARIM, Betül KARAKUZU, Cemre ÖKSÜZ and Emre GEZER for their valuable friendship and all their support.

I would like to thank Büşra CERİT for her patience, support and love throughout this period.

I offer my endless thank to my aunts, Hamiyet YILMAZ, Sevda YILMAZ, Sibel SANLI, and my cousins, Busenur YENTÜR, Doğukan ŞANLI and Mehmet ÇELİKKOL, who have never given up supporting me during my thesis studies.

I would like to express my endless love to my dear family, my grandma Nezahat DEMİRBAŞ, my mother Hülya DEMİRBAŞ, my father Tarık DEMİRBAŞ, and my brother Emre DEMİRBAŞ, who have always stood by me through my career.

ABSTRACT

EFFECTS OF *Centella asiatica* SAPONINS ON TELOMERASE ACTIVATION AND WOUND HEALING

Centella asiatica L. is a well-known plant species endemic to Southeast Asia that has noteworthy biological effects. Triterpenoid saponins, comprising more than 80% of the content, are suggested to be the chief compounds responsible for the biological effects. A recent study has described that the extract of *Centella asiatica* exhibits telomerase activation. In line with these developments, as part of our studies on natural products demonstrating anti-aging properties, we decided to engage *Centella asiatica* and its components.

Within the scope of this thesis, four major compounds, viz. madecassoside, asiaticoside, madecassic acid, and asiatic acid were isolated from the standardized extract of *Centella asiatica*, and their structures were elucidated by spectroscopic methods. Using *in vitro* methods, the effects of the extract and purified compounds on cell proliferation under standard culture and oxidative stress (H₂O₂) conditions, wound healing, and human Telomerase Reverse Transcriptase (hTERT) protein level were investigated. Our experiments were conducted on MRC-5 and HEK293T cell lines. It was observed that the standardized extract of *Centella asiatica* increased the proliferation of the MRC-5 cells meaningfully between 5 to 100 µg/ml. Moreover, the extract showed protective effects on MRC-5 cells at 500 and 1000 ng/ml under oxidative stress conditions. Madecassoside, madecassic acid, asiaticoside, and asiatic acid exhibited the highest proliferative effects on MRC-5 cells at concentrations of 1000 nM (28%), 2 nM (66%), 300 nM (61%), and 300 nM (56%), respectively. Asiatic acid and the extract accelerated cell migration in wound areas that were made on MRC-5 cells up to 32% and 36% in the range of 10 to 300 nM or ng/ml, respectively. The immunoblotting assay studies showed that madecassoside and asiaticoside were increased the expression of hTERT protein level on HEK293T cell line by 3.16-fold and 5.62-fold, respectively, at 30 nM concentration. Furthermore, the extract was observed to increase the protein level by 2.62-fold at 300 ng/ml.

ÖZET

Centella asiatica SAPONİNLERİNİN TELOMERAZ AKTİVASYONU VE YARA İYİLEŞMESİ ÜZERİNE ETKİLERİ

Centella asiatica L., dikkate değer biyolojik etkilere sahip olan, Güneydoğu Asya'ya özgü, iyi bilinen bir bitki türüdür. İçeriğin %80'inden fazlasını oluşturan triterpenik saponinlerin, biyolojik etkilerden sorumlu başlıca bileşikler olduğu öne sürülmektedir. Yakın zamanda yapılmış bir çalışmada, *Centella asiatica* ekstraktının telomeraz aktivasyonu sergilediği açıklanmıştır. Bu gelişmeler doğrultusunda, yaşlanma karşıtı özellikler gösteren doğal ürünler ile ilgili araştırmalarımızın bir parçası olarak *Centella asiatica* ve bileşenlerini çalışmaya karar verdik.

Bu tez kapsamında, dört ana bileşik, madecassoside, asiaticoside, madecassic acid ve asiatic acid, standardize *Centella asiatica* ekstraktından izole edildi ve yapıları spektroskopik yöntemlerle aydınlatıldı. *In vitro* yöntemler kullanılarak, ekstrakt ve saflaştırılmış bileşiklerin standart kültür ve oksidatif stres (H₂O₂) koşulları altındaki hücre proliferasyonuna, yara iyileşmesi ve insan Telomeraz Ters Transkriptaz (hTERT) protein seviyesi üzerine etkileri araştırıldı. Deneylerimiz, MRC-5 ve HEK_n hücre hatları üzerinde gerçekleştirildi. Standartlaştırılmış *Centella asiatica* ekstraktının, MRC-5 hücrelerinin proliferasyonunu 5 ile 100 µg/ml konsantrasyon aralığında anlamlı bir şekilde arttırdığı gözlemlendi. Dahası, oksidatif stres koşulları altında, ekstrakt, 500 ve 1000 ng/ml konsantrasyonlarında MRC-5 hücreleri üzerinde koruyucu etkiler gösterdi. Madecassoside, madecassic acid, asiaticoside ve asiatic acid bileşikleri, MRC-5 hücreleri üzerine en yüksek proliferatif etkilerini sırasıyla, 1000 nM (%28), 2 nM (%66), 300 nM (%61) ve 300 nM (%56) konsantrasyonlarında sergilediler. Asiatic acid ve ekstrakt, MRC-5 hücrelerinde oluşturulan yara bölgelerinde, hücre göçünü 10 ile 300 nM veya ng/ml aralıklarında sırasıyla, %32 ve %36'ya kadar arttırdı. İmmünoablota çalışmaları, madecassoside ve asiaticoside bileşiklerinin, HEK_n hücre hattındaki hTERT protein seviyesi ekspresyonunu 30 nM konsantrasyonlarında sırasıyla 3.16 ile 5.62 kat arttırdığını gösterdi. Buna ek olarak, ekstrenin ise, 300 ng/ml konsantrasyonda protein seviyesini 2.62 kat arttırdığı tespit edildi.

TABLE OF CONTENTS

LIST OF FIGURES	ix
LIST OF TABLES	xii
LIST OF SPECTRA	xiii
ABBREVIATIONS	xiv
CHAPTER 1. INTRODUCTION	1
1.1. Natural Product Chemistry	2
1.2. Saponins.....	5
1.3. <i>Centella asiatica</i> L.....	7
1.3.1. Biological activities of <i>Centella asiatica</i>	10
CHAPTER 2. MATERIALS AND METHODS.....	17
2.1. Materials	17
2.1.1. Materials and equipment used in isolation studies.....	17
2.1.2. Materials for cell proliferation and wound healing studies.....	18
2.1.2.1. Chemicals used on cell proliferation and wound healing studies	19
2.1.2.2. Equipment used on cell proliferation and wound healing studies	19
2.1.3. Materials used in immunoblotting studies	19
2.1.3.1. Cells and antibodies.....	19
2.1.3.2. Chemicals and equipment used in immunoblotting studies ..	20
2.1.3.3. Buffers used in immunoblotting studies.....	21
2.2. Methods	22

2.2.1. Determination of proper solvent systems to be used in chromatographic separations	22
2.2.2. Alkaline hydrolysis and isolation studies.....	24
2.2.2.1. Alkaline hydrolysis step	24
2.2.2.2. The EtOAc partition of alkaline hydrolysis solution.....	24
2.2.2.3. Purification of the EtOAc phase obtained from alkaline hydrolysis.....	26
2.2.2.4. Isolation and purification of four major compounds from the standardized extract	28
2.2.3. Bioactivity Studies	33
2.2.3.1. Cell culture studies	33
2.2.3.2. Cell proliferation studies (MTT assay).....	34
2.2.3.3. Wound healing studies (Scratch assay)	34
2.2.3.4. Immunoblotting studies	35
2.2.3.4.1. Protein isolation.....	35
2.2.3.4.2. Determination of protein amount	35
2.2.3.4.3. Separation of proteins by SDS-PAGE.....	36
2.2.3.4.4. Transfer to Polyvinylidene Difluoride (PVDF) membrane	37
2.2.3.4.5. Blocking, primary and secondary antibodies labeling.....	37
2.2.4. Statistical analyses	38
CHAPTER 3. RESULTS AND DISCUSSION	39
3.1. Isolation and purification studies.....	39
3.1.1. Determination of proper solvent systems to be used in chromatographic separations	39
3.1.2. Alkaline hydrolysis of the standardized extract of <i>C. asiatica</i>	41
3.1.3. Isolation of DD-GK-S(74-168)-S(28-45)	42

3.1.4. Major compounds isolated by reverse phase silica gel (RP-C18) column system	43
3.2. Structure elucidation studies.....	48
3.2.1. Structure elucidation of DD-GK-01.....	49
3.2.2. Structure elucidation of DD-GK-02.....	52
3.2.3. Structure elucidation of DD-GK-03.....	56
3.2.4. Structure elucidation of DD-GK-04.....	59
3.3. Results of biological activity studies	62
3.3.1. Proliferative effects of DD-GK-S(74-168)-S(28-45) and the standardized extract of <i>C. asiatica</i> on MRC-5 cell line via MTT assay	62
3.3.2. Proliferative effects of DD-GK-S(74-168)-S(28-45) and the standardized extract of <i>C. asiatica</i> on MRC-5 cell line via MTT assay under oxidative stress conditions.....	64
3.3.3. Proliferative effects of major compounds (madecassoside, madecassic acid, asiaticoside, asiatic acid) on MRC-5 cell line via MTT assay	66
3.3.4. Wound closure effects of madecassic acid, asiatic acid, and the standardized extract of <i>C. asiatica</i> on MRC-5 cell line via Scratch assay.....	68
3.3.5. The effects of major compounds and the standardized extract of <i>C. asiatica</i> on hTERT protein level on HEK293 cell line via Immunoblotting assay.....	70
 CHAPTER 4. CONCLUSION.....	 77
 REFERENCES	 81
 APPENDICES	
APPENDIX A. SPECTRUMS OF DD-GK-01, DD-GK-02, DD-GK-03, DD-GK-04..	89

APPENDIX B. OPEN WOUND IMAGES OF MADECASSIC ACID, ASIATIC ACID AND THE EXTRACT	100
---	-----

LIST OF FIGURES

<u>Figures</u>	<u>Page</u>
Figure 1. Pathway summarizing the relationship between primary and secondary metabolites	3
Figure 2. Classification of secondary metabolites	4
Figure 3. Pie chart representing the major groups of secondary metabolite.....	4
Figure 4. Biosynthesis of steroidal and triterpenoidal saponins	5
Figure 5. Triterpenoid sapogenin skeletons	6
Figure 6. Image of <i>Centella asiatica</i>	7
Figure 7. Geographic distribution of <i>Centella asiatica</i>	8
Figure 8. Pharmacological activities of <i>Centella asiatica</i>	13
Figure 9. Alkaline hydrolysis of the standardized extract of <i>C. asiatica</i>	25
Figure 10. EtOAc partition of the alkaline hydrolysis reaction	26
Figure 11. Image of MPLC column system.....	28
Figure 12. The isolation scheme of DD-GK-S(74-168)-S(28-45).....	30
Figure 13. Image of VLC column system.....	31
Figure 14. The isolation scheme of DD-GK-01, DD-GK-02, DD-GK-03, and DD-GK-04	32
Figure 15. TLC chromatograms of the general phytochemical profiles of the extract dissolved in MeOH under UV ₃₆₅ , mobile phases; 90:10; CHCl ₃ :MeOH (A), 80:20:2; CHCl ₃ :MeOH:H ₂ O (B), 61:32:7; CHCl ₃ :MeOH:H ₂ O (C)	40
Figure 16. TLC chromatograms of the general phytochemical profiles of the extract dissolved in MeOH under UV ₃₆₅ , mobile phases; 80:25:20; EtOAc:MeOH:H ₂ O (A), 100:25:20; EtOAc:MeOH:H ₂ O (B), 8:4:2; EtOAc:2-propanol:H ₂ O (C).....	40
Figure 17. TLC chromatograms of the general phytochemical profiles of the extract dissolved in MeOH under UV ₃₆₅ using reverse phase (RP-C18) silica gel plate, mobile phases; 40:60; ACN:H ₂ O (A), 70:30; MeOH:H ₂ O (B), 40:60; MeOH:H ₂ O (C)	41
Figure 18. TLC chromatograms of the extract for alkaline hydrolysis residues after n-BuOH and EtOAc partitions	42
Figure 19. TLC chromatograms of combined fractions	43

<u>Figures</u>	<u>Page</u>
Figure 20. TLC chromatograms of S(74-168) combined fractions	44
Figure 21. TLC chromatograms of minor bands	45
Figure 22. TLC chromatogram of all fractions numbered.....	45
Figure 23. Image of lyophilized fractions (Fr. 64-74, Fr. 75-89, and Fr. 144-150).....	46
Figure 24. TLC chromatogram of alkaline hydrolysis residues	47
Figure 25. TLC chromatograms of EtOAc partition.....	48
Figure 26. Chemical structure of DD-GK-01	49
Figure 27. Chemical structure of DD-GK-02	52
Figure 28. Chemical structure of DD-GK-03	56
Figure 29. Chemical structure of DD-GK-04	59
Figure 30. Proliferative effects of DD-GK-S(74-168)-S(28-45) on MRC-5 cell line at 48 h.....	62
Figure 31. Proliferative effects of the standardized extract of <i>C. asiatica</i> on MRC-5 cell line at 48 h.....	63
Figure 32. Proliferative effects of DD-GK-S(74-168)-S(28-45) on the MRC-5 cell line under oxidative stress conditions at 24 h.	64
Figure 33. Proliferative effects of the standardized extract of <i>C. asiatica</i> on MRC-5 cell line under oxidative stress conditions at 24 h.	65
Figure 34. Proliferative effects of madecassoside (A) and madecassic acid (B) on MRC-5 cell line at 24 h.....	66
Figure 35. Proliferative effects of asiaticoside (A) and asiatic acid (B) on MRC-5 cell line at 24 h.....	67
Figure 36. Wound closure effect of madecassic acid on MRC-5 cell line at 24 h.	68
Figure 37. Wound closure effects of asiatic acid on MRC-5 cell line at 24 h.....	69
Figure 38. Wound closure effect of the standardized extract of <i>C. asiatica</i> on MRC- 5 cell line at 24 h.....	70
Figure 39. Effects of MS on hTERT protein level at 24 h.....	71
Figure 40. Effects of MA on hTERT protein level at 24 h.	72
Figure 41. Effect of AS on hTERT protein level at 24 h.....	73
Figure 42. Effects of AA on hTERT protein level at 24 h.....	74
Figure 43. Effects of the standardized extract of <i>C. asiatica</i> on hTERT protein level at 24 h.....	75
Figure 44. Open wound images of DMSO control at 0, 24, and 36 h	100

<u>Figures</u>	<u>Page</u>
Figure 45. Open wound images of MA (2nM) at 0, 24, and 36 h	101
Figure 46. Open wound images of MA (10nM) at 0, 24, and 36 h	101
Figure 47. Open wound images of MA (30nM) at 0, 24, and 36 h	102
Figure 48. Open wound images of MA (100nM) at 0, 24, and 36 h	102
Figure 49. Open wound images of MA (300 nM) at 0, 24, and 36 h	103
Figure 50. Open wound images of AA (2 nM) at 0, 24, and 36 h	103
Figure 51. Open wound images of AA (10 nM) at 0, 24, and 36 h	104
Figure 52. Open wound images of AA (30 nM) at 0, 24, and 36 h	104
Figure 53. Open wound images of AA (100 nM) at 0, 24, and 36 h	105
Figure 54. Open wound images of AA (300 nM) at 0, 24, and 36 h	105
Figure 55. Open wound images of the extract (2 nM) at 0, 24, and 36 h	106
Figure 56. Open wound images of the extract (10 nM) at 0, 24, and 36 h	106
Figure 57. Open wound images of the extract (30 nM) at 0, 24, and 36 h	107
Figure 58. Open wound images of the extract (100 nM) at 0, 24, and 36 h	107
Figure 59. Open wound images of the extract (300 nM) at 0, 24, and 36 h	108

LIST OF TABLES

<u>Table</u>	<u>Page</u>
Table 1. Systematic classification (Taxonomy) of <i>Centella asiatica</i>	8
Table 2. Some secondary metabolites of <i>Centella asiatica</i>	9
Table 3. Structure of ursane type pentacyclic triterpenoid compounds found in <i>Centella asiatica</i>	10
Table 4. Structure of oleanane type pentacyclic triterpenoid compounds found in <i>Centella asiatica</i>	11
Table 5. HEK293 growth medium.....	20
Table 6. The amounts of fractions	27
Table 7. The amounts of MPLC column fractions	29
Table 8. Fractions of metabolites collected from Sephadex LH-20 column and amounts of lyophilized substances	33
Table 9. Preparation of stacking and resolving gels	37
Table 10. ¹ H- and ¹³ C-NMR spectroscopic data of DD-GK-01, ^{a)} (in C ₅ D ₅ N, δ ppm, ¹ H: 500 MHz, ¹³ C:125 MHz).....	50
Table 11. ¹ H- and ¹³ C-NMR spectroscopic data of DD-GK-02, ^{a)} (in C ₅ D ₅ N, ¹ H:500 MHz, ¹³ C:125 MHz)	53
Table 12. ¹ H- and ¹³ C-NMR spectroscopic data of DD-GK-03, ^{a)} (in C ₅ D ₅ N, ¹ H: 500 MHz, ¹³ C:125 MHz)	57
Table 13. ¹ H and ¹³ C NMR spectroscopic data of DD-GK-04, ^{a)} (in C ₅ D ₅ N, ¹ H: 500 MHz, ¹³ C:125 MHz)	60

LIST OF SPECTRA

<u>Spectrum</u>	<u>Page</u>
Spectrum 1. ^1H -NMR spectrum of DD-GK-01	51
Spectrum 2. ^{13}C -NMR spectrum of DD-GK-01	52
Spectrum 3. ^1H -NMR spectrum of DD-GK-02	55
Spectrum 4. ^{13}C -NMR spectrum of DD-GK-02	55
Spectrum 5. ^1H -NMR spectrum of DD-GK-03	58
Spectrum 6. ^{13}C -NMR spectrum of DD-GK-03	58
Spectrum 7. ^1H -NMR spectrum of DD-GK-04.....	61
Spectrum 8. ^{13}C -NMR spectrum of DD-GK-04	61
Spectrum 9. DEPT135 spectrum of DD-GK-01	89
Spectrum 10. HSQC spectrum of DD-GK-01	90
Spectrum 11. HMBC spectrum of DD-GK-01	90
Spectrum 12. COSY spectrum of DD-GK-01	91
Spectrum 13. NOESY spectrum of DD-GK-01.....	91
Spectrum 14. DEPT135 spectrum of DD-GK-02.....	92
Spectrum 15. HSQC spectrum of DD-GK-02	92
Spectrum 16. HMBC spectrum of DD-GK-02	93
Spectrum 17. COSY spectrum of DD-GK-02	93
Spectrum 18. NOESY spectrum of DD-GK-02.....	94
Spectrum 19. DEPT135 spectrum of DD-GK-03.....	94
Spectrum 20. HSQC spectrum of DD-GK-03	95
Spectrum 21. HMBC spectrum of DD-GK-03	95
Spectrum 22. COSY spectrum of DD-GK-03	96
Spectrum 23. NOESY spectrum of DD-GK-03.....	96
Spectrum 24. DEPT135 spectrum of DD-GK-04	97
Spectrum 25. HSQC spectrum of DD-GK-04	97
Spectrum 26. HMBC spectrum of DD-GK-04	98
Spectrum 27. COSY spectrum of DD-GK-04	98
Spectrum 28. NOESY spectrum of DD-GK-04.....	99

ABBREVIATIONS

^{13}C NMR	Carbon Nuclear Magnetic Resonance
^1H NMR	Proton Nuclear Magnetic Resonance
1D-NMR	One-Dimensional Nuclear Magnetic Resonance
2D-NMR	Two-Dimensional Nuclear Magnetic Resonance
AA	Asiatic acid
ACN	Acetonitrile
AS	Asiaticoside
BCA	Bicinchoninic Acid
$\text{C}_5\text{D}_5\text{N}$	Pyridine
<i>C. asiatica</i>	<i>Centella asiatica</i>
CHCl_3	Chloroform
COSY	Correlation Spectroscopy
d	Doubled
DMEM	Dulbecco's Modified Eagle Medium
DMSO	Dimethyl Sulfoxide
EtOAc	Ethyl Acetate
Fr.	Fraction
FBS	Fetal Bovine Serum
GAPDH	Glyceraldehyde 3-phosphate Dehydrogenase
h	Hour
H_2O_2	Hydrogen Peroxide
HEK _n	Primary Human Keratinocyte Cells, neonatal
HMBC	Heteronuclear Multiple Bond Coherence
HR-ESI-MS	High-resolution Electrospray Ionisation Mass Spectrometry
HSQC	Heteronuclear Single Quantum Coherence
hTERT	Human Telomerase Reverse Transcriptase
m	Multiplied
MA	Madecassic acid
MeOH	Methanol
MPLC	Medium Pressure Liquid Chromatography
MRC-5	Human Lung Fibroblast cells

MS	Madecassoside
MTT	3-[4,5-dimethylthiazol-2-yl]-2,5-diphenyltetrazolium bromide
n-BuOH	Butanol
NaOH	Sodium Hydroxide
NOESY	Nuclear Overhauser Spectroscopy
PBS	Phosphate buffered saline
PIC	Protease Inhibitor Cocktail
PVDF	Polyvinylidene Difluoride
RP	Reversed Phase
s	Singled
SDS	Sodium Dodecyl Sulphate
TLC	Thin Layer Chromatography
UV	Ultraviolet
VLC	Vacuum Liquid Chromatography

CHAPTER 1

INTRODUCTION

Plants have been used as medicine to treat diseases since ancient times. Herbal medicine has been very important and popular in many ancient civilizations, especially in traditional Chinese medicine and Indian Ayurveda. In retrospect, archaeological excavations have shown that even the Sumerians, the known oldest society, used plants such as *Carum carvi* L. (Apiaceae) and *Thymus vulgaris* L. (Lamiaceae) for therapeutic purposes (Amiri et al., 2021). In line with this information, it can be deduced that plants have been used for therapeutic purposes since the beginning of humanity.

The pharmaceutical industry has gained great momentum in line with the developments in sciences such as pharmacy, chemistry, biology, and medicine since the 19th century. Many pharmacological properties of the plant have been enlightened, the isolation of active components of these plants have been successfully performed and resulting products have been put into use for humankind due to these scientific improvements (S.-Y. Pan et al., 2014). The concept of phytotherapy, introduced in the early 19th century, is a science and evidence-based definition of the use of plant sources in the therapy of diseases. The term phytochemistry is derived from the Greek word "Phyto" which means plant (Rao et al., 2012). Phytochemicals are naturally occurring non-nutritious biologically active molecules, found almost in any kind of plants, and protect their cells from diseases, animals, and environmental damages such as pollution, radiation, and stress. These molecules, known as secondary metabolites, have more than a thousand defined forms, are found in different parts of plants such as root, flower, fruit, seed, and leaf, and have many pharmacological properties (Saxena et al., 2013).

Centella asiatica L. (*C. asiatica*) is an herb with many valuable secondary metabolites. It has been used for the treatment of diseases for many years and hundreds of scientific studies have been published related to this plant or its derivatives (Chandrika & Kumara., 2015). Saponins which are major bioactive compounds of *C. asiatica* and particularly their biological effects have attracted attention from scientists. These scientific studies have led to many commercial products (Madecassol[®], Madelab, etc.) of *C. asiatica* in many fields such as medicine, cosmetics, food, etc (Rush et al., 1993).

Although *C. asiatica* has many important pharmacological effects such as anti-proliferative, anti-aging, and immunomodulator, its wound healing effect has always been prominent (B. Sun et al., 2020). *In vitro* and *in vivo* studies on many cell lines and living organisms have proven that *C. asiatica* has very effective wound healing activities (Azis et al., 2017).

Our research group has been studying in the field of natural product chemistry and telomerase activity for many years. In a recent study, telomerase activity of *C. asiatica* extract formulation in human peripheral blood mononuclear cells (PBMCs) was found as 3-4 times higher than *Astragalus* formulation and TA-65[®] (the only telomerase activator on the market) (Tsoukalas et al., 2019). This important finding encouraged us to focus on the telomerase activity of *C. asiatica*. In this thesis, major saponin glycosides (madecassoside, and asiaticoside) and their aglycone derivatives (madecassic acid, and asiatic acid) were isolated from the standardized extract of *C. asiatica*. The extract and major compounds were used to investigate the effects of the proliferation (MTT assay), and wound healing (scratch assay) on human lung fibroblast cell line (MRC-5), and human telomerase reverse transcriptase (hTERT) protein level on primary human keratinocyte cells, neonatal (HEKn).

1.1. Natural Product Chemistry

Natural products are organic molecules that contain at least one carbon atom in their structure, isolated from living organisms (Cooper & Nicola, 2014). They are often derived from plants, but they can also be isolated from fungi, animals, microorganisms, marine algae, marine sponges, and other marine environmental sources (Dias et al., 2012). These molecules are divided into primary metabolites, which are produced for vital activities like growth and reproduction, and secondary metabolites, which are mainly produced for non-vital purposes such as protection from environmental stress factors (Ray F. Evert, 2016). Pathways summarizing the relationship between primary and secondary metabolites were shown in Figure 1.

Secondary metabolites, rare in nature compared to primary metabolites, are biomolecules that protect plants against environmental hazards like UV, pathogens, oxidative stress, pH, sudden changes of temperature and ensure their survival (Anulika et al., 2016).

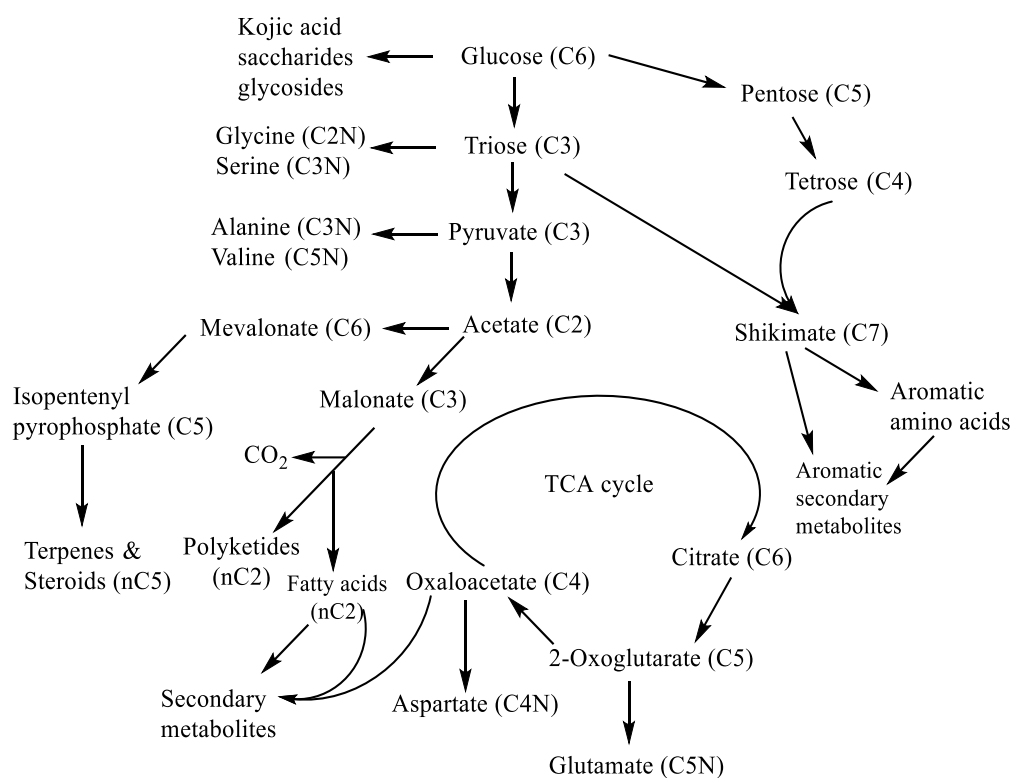


Figure 1. Pathway summarizing the relationship between primary and secondary metabolites

(Moore et al., 2020)

It has been described that there are more than a hundred thousand varieties in nature (Mazid et al., 2011). Secondary metabolites can most commonly be grouped into four different classes as terpenes, S- and N-containing molecules, and phenolics as seen in Figure 2. Secondary metabolites, which were considered worthless wastes of plants in the past, are used in different fields as important sources. Although there are many competing drug discovery methods, due to advances in biotechnology, secondary metabolites still have great potential for new drug discovery candidates for the treatment of many important diseases, especially cancer, anti-aging, heart disease, and wound healing. For these reasons, commercial uses of secondary metabolites in the pharmaceutical industry represent a huge economic market worldwide (Butler, 2004).

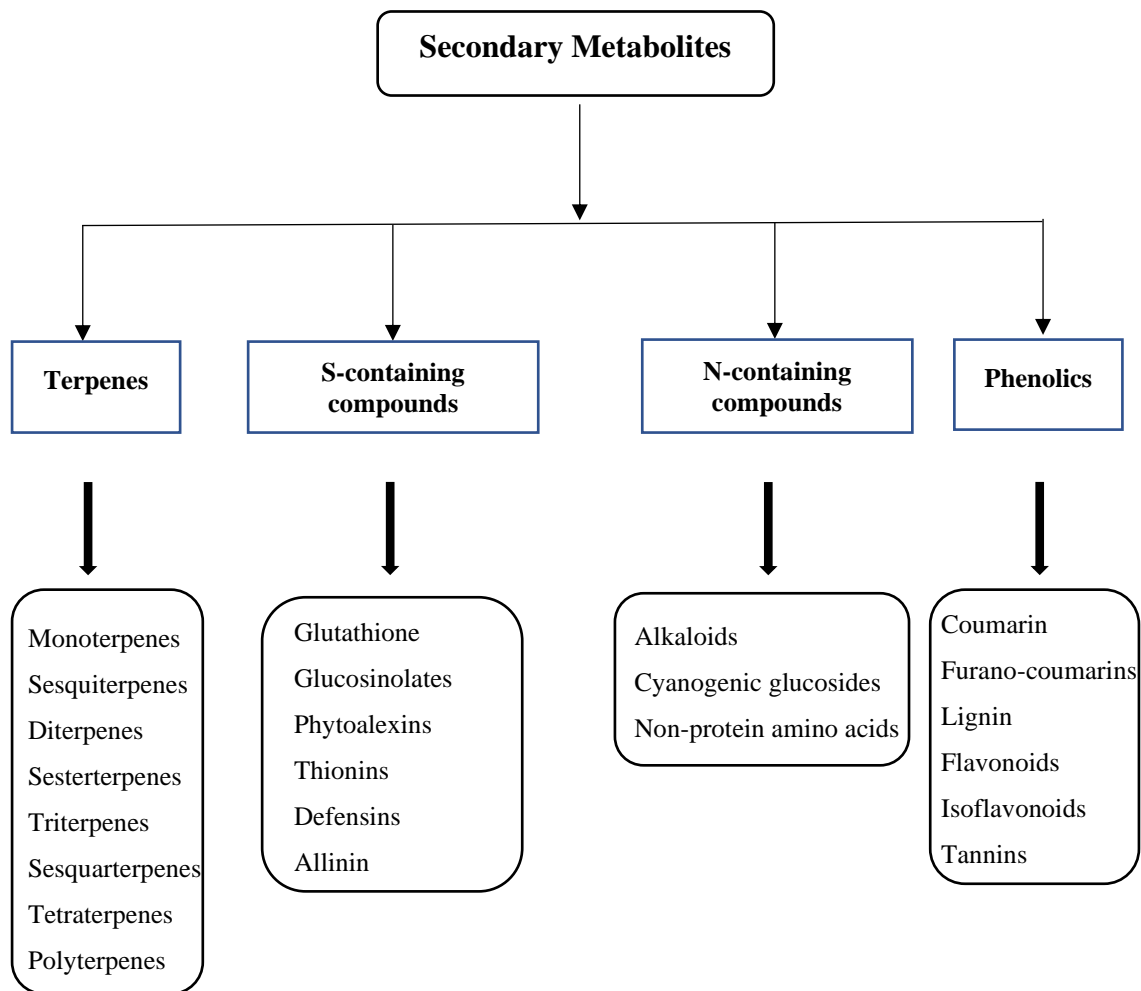


Figure 2. Classification of secondary metabolites
(Jamwal et al., 2018)

The ratio of major secondary metabolite groups found in nature were shown in Figure 3.

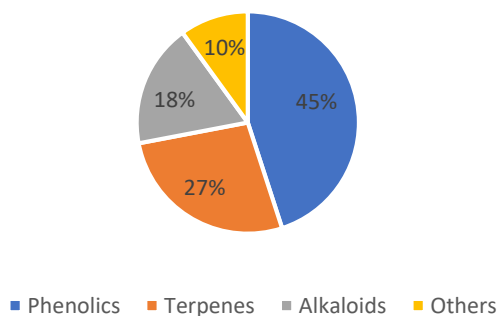


Figure 3. Pie chart representing the major groups of secondary metabolites
(Saxena et al., 2013)

1.2. Saponins

Saponins are high molecular weight secondary metabolites that have a lipophilic core and one or more oligosaccharide side chains, and their main sources are microorganisms, higher plants, and animals (Mahato, 2000). The name of saponin is derived from the Latin word "Sapo" which means soap since they exhibit strong soap-like foaming properties in aqueous solutions (Osbourn, 2003). Saponins have a bitter taste and are protective of plants against environmental threats. Even though it is used for treatment, it is known that its high doses are toxic to humans (Milgate & Roberts, 1995).

Saponins are synthesized from the mevalonic acid (MVA) pathway consisting of acetyl coenzyme-A. The main intermediate product is squalene consisting of geranyl pyrophosphate (GPP). Steroid or triterpenoid structures are formed by the cyclization of squalene-2,3 epoxide (Augustin et al., 2011; Haralampidis et al., 2002; Moses et al., 2014). The biosynthesis of saponins through the MVA pathway was shown in Figure 4 modified from literature (Augustin et al., 2011).

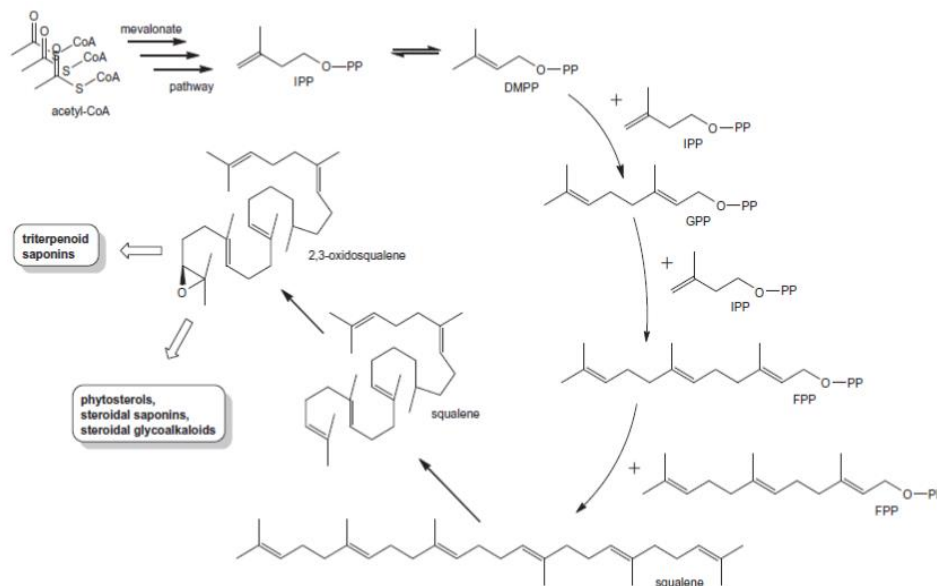


Figure 4. Biosynthesis of steroidal and triterpenoidal saponins

(Augustin et al., 2011)

Saponins are classified as steroidal (C-27) and triterpenoid (C-30) saponins according to the structure of the aglycone moieties which are called sapogenin (Faizal &

Geelen, 2013). Aglycone carbon backbone contains various functional groups such as -OH, -COOH, and -CH₃ (Oleszek, 2002). The glycone moieties are formed from branched or straight sugars such as glucose, galactose, fructose, rhamnose, arabinose, xylose, which are linked to hydroxyl or carboxyl groups of aglycone (Beserra et al., 2016; T. K. Das et al., 2012). Saponins are called monodesmoside (single point binding), bidesmoside (two different binding points), and tridesmoside saponins (three different binding points) according to the number of places where sugars are attached (Mahato et al., 1988; Oleszek, 2002). Steroidal saponins either called spirostane, which has a hexacyclic skeletal structure, due to the spiro structure of the C-22, or furostane, of which hydroxyl group at the C-26 forms a glycosidic bond which makes it a pentacyclic ring (Kräutler & Sahu, 2008; Sparg et al., 2004). Triterpenoid saponins, which are found more in nature than steroidal saponins, are also pentacyclic molecules. Oleananes (β -amirin derivatives) and ursanes (α -amirin derivatives), which are important triterpenoid saponin groups, were shown in Figure 5 (Augustin et al., 2011; Basu & Rastogi, 1967).

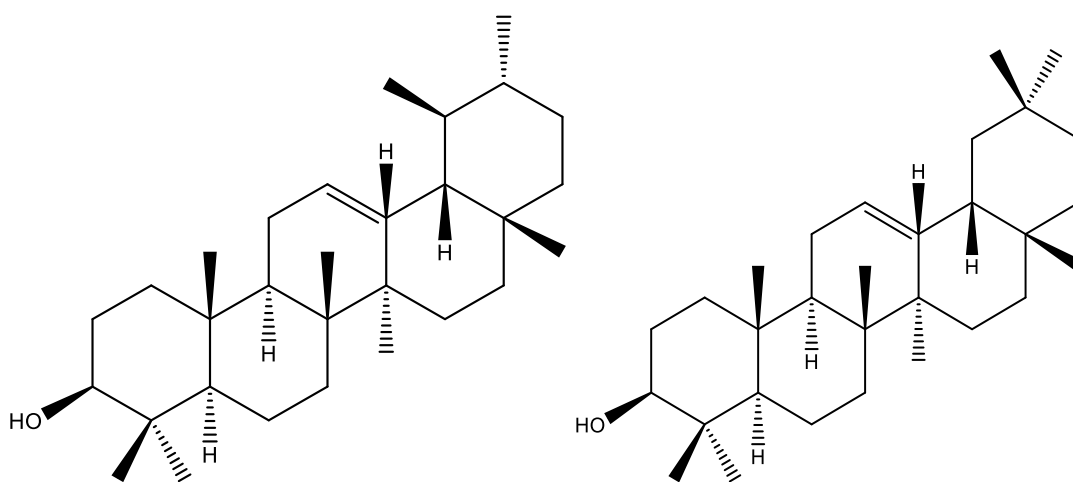


Figure 5. Triterpenoid saponin skeletons. (A) ursane type, (B) oleanane type

(H. Sun et al., 2006)

Saponins are used in personal care products, instant drinks, nutritional supplements due to their hydrophilic glycone and hydrophobic aglycone structure (Netala et al., 2015). Additionally, they have been reported to have various biological activities such as anti-tumor, anti-viral, anti-aging, anti-microbial, anti-inflammatory, antioxidant, anti-hypertensive, anti-hyperlipidemic, anti-hyperglycemic, and immunostimulant. These

pharmacological properties make saponins good candidates for the drug discovery processes (Thakur et al., 2011).

1.3. *Centella asiatica* L.

C. asiatica L. is a perennial herbaceous and tuberous plant of the Apiaceae (Umbelliferae) family (Figure 6). It can often be seen along the banks of rivers, streams, ponds, and irrigated fields. In the wild, it can grow (reaching 15 cm) in humid and shady places up to 7000 ft. According to morphological investigations, their roots are long knotted, stems are glabrous, leaves are greenish in a rosette form with long stems, flowers are pinkish to red and in the form of rounded bunches (umbels), and seeds have pendulous embryos (Chandrika & Kumara, 2015; James & Dubery, 2009; Seevaratnam et al., 2012).



Figure 6. Image of *Centella asiatica*

(Prasad et al., 2019)

C. asiatica has been widely used for thousands of years as a culinary vegetable and medicinal herb in the treatment of various diseases, especially in Ayurvedic medicine and traditional Chinese treatments (Mangas et al., 2009; Mathur et al., 2007). It was known as the "brain food" in India (Chandrika & Kumara, 2015) and was considered one of the "miracle elixirs of life" in China (Prakash et al., 2017). It was also well known for promoting longevity in these cultures. It was also used in the treatment of many diseases

such as nerve disorders, madness, skin diseases, asthma, leprosy, ulcer, eczema, rheumatism, inflammation, syphilis, mental illness, epilepsy, hysteria, dehydration, and diarrhea, etc. (Brinkhaus et al., 2000; Pittella et al., 2009; Schaneberg et al., 2003).

Apart from its taxonomic name of which classification was given in Table 1, *C. asiatica* is also known by many different names like Gotu Kola, *Hydrocotyle asiatica* L., Antanan, Pegagan, Brahmi, Indian Pennywort, Asiatic Pennywort, Thick-leaved Pennywort, etc. in various regions (Brinkhaus et al., 2000; Yu et al., 2006).

Table 1. Systematic classification (Taxonomy) of *Centella asiatica*

(A. J. Das, 2011)

Classification	Name
Kingdom	Plantae
Division	Angiosperm
Class	Dicotyledonous
Order	Umbelliferae
Family	Apiaceae
Genus	Centella
Species	Asiatica

C. asiatica is endemic to the Southeast Asia Region and most abundant in China, India, Sri Lanka, Indonesia, Malaysia, Oceania, Madagascar, Pakistan, and Bangladesh (Alfarra & Omar, 2013). On the other hand, it can also be found in South Africa, the U.S.A., Mexico, Colombia, and Venezuela, which are close to the equatorial region (Mangas et al., 2009). The geographical distribution of *C. asiatica* was shown in Figure 7.

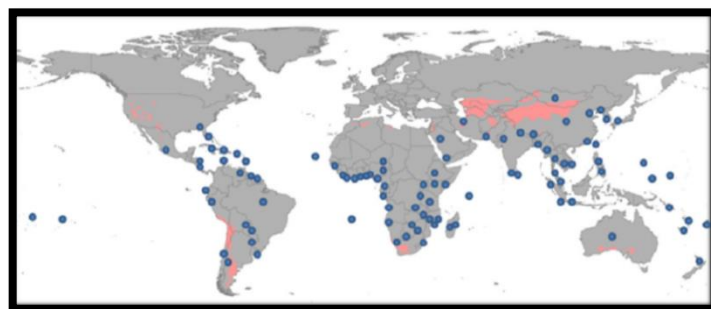


Figure 7. Geographic distribution of *Centella asiatica*

(Azerad, 2016)

C. asiatica is a rich source of secondary metabolites, some of which are listed in Table 2 (Puttarak & Panichayupakaranant, 2012).

Table 2. Some secondary metabolites of *Centella asiatica*
(Roy et al., 2013)

Main groups	Secondary metabolites
Phenols	Flavonoids: kaempferol, quercetin, apigenin, rutin, naringin Phenylpropanoids: rosmarinic acid, chlorogenic acid, 4,5-di-o-caffeoyl quinic acid Tannin: phlobatannin
Terpenoids	Triterpenes: asiaticoside, madecassoside, centelloside, brahmoside, betulic acid, madecassic acid, asiatic acid
Volatile oils and fatty oils	β -caryophyllene, α -pinene, β -pinene Fatty acids: oleic acid, linolenic acid

C. asiatica contains many ursane [asiaticoside (AS), madecassoside (MS), asiatic acid (AA), madecassic acid (MA)], and oleanane types of pentacyclic triterpenoid compounds [terminoloside (isomer of madecassoside), scheffoleoside-A, centelloside-D]. The molecular structures of some important triterpenoid compounds found in *C. asiatica* were shown in Table 3 for ursane subtypes and Table 4 for oleanane subtypes modified from literature (Azerad, 2016).

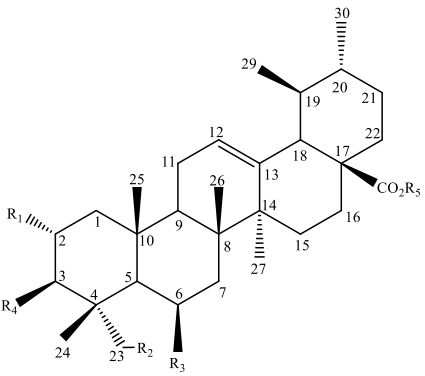
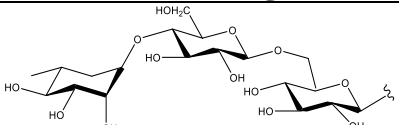
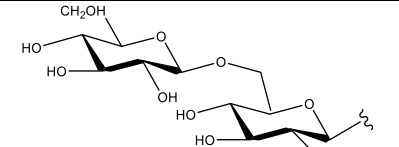
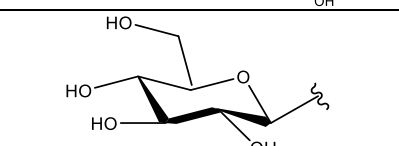
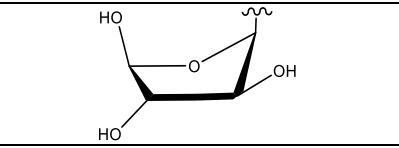
1.3.1. Biological activities of *Centella asiatica*

The biological and pharmacological effects of *C. asiatica* are well known in the literature.

Pharmacological properties possessed by *C. asiatica* are as follows: anti-proliferative (Yoshida et al., 2005), anti-ulcer (Gohil et al., 2010), anti-tumor (Babu et al., 1995), anti-bacterial (Pitinidhipat & Yasurin, 2012), neuroprotective activity (Nasir et al., 2011), cognitive function (Lin et al., 2013),

Table 3. Structure of ursane type pentacyclic triterpenoid compounds found in *Centella asiatica*

(Azerad, 2016)

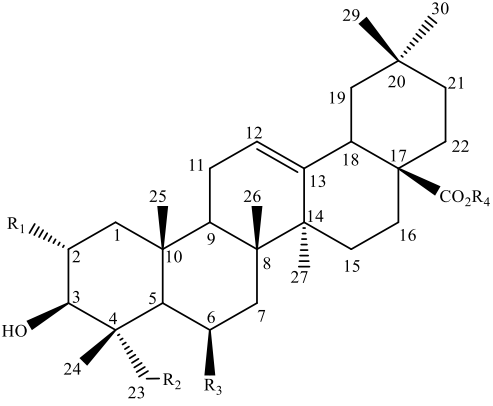
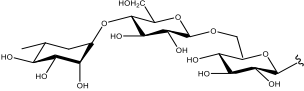
Backbone					Sugar moieties	
						S ₁
						S ₂
						S ₃
						S ₄
R ₁	R ₂	R ₃	R ₄	R ₅	Name	IUPAC name
-OH	-OH	-H	-OH	-S ₁	asiaticoside	2 α ,3 β ,23-trihydroxyurs-12-en-28-oic acid-O- α -L-rhamnopyranosyl-(1-4)-O- β -D-glucopyranosyl-(1-6)-O- β -D-glucopyranosyl ester

(cont. on next page)

-OH	-OH	-OH	-OH	-S ₁	madecassoside	2 α ,3 β ,6 β ,23-tetrahydroyurs-12-en-28-oic acid-O- α -L-rhamnopyranosyl-(1-4)-O- β -D-glucopyranosyl-(1-6)-O- β -D-glucopyranosyl ester
-OH	-OH	-H	-OH	-H	asiatic acid	2 α ,3 β ,23-trihydroxyurs-12-en-28-oic acid
-OH	-OH	-OH	-OH	-H	madecassic acid	2 α ,3 β ,6 β ,23-tetrahydroyurs-12-en-28-oic acid

Table 4. Structure of oleanane type pentacyclic triterpenoid compounds found in *Centella asiatica*

(Azerad, 2016)

Backbone				Sugar moieties	
					
R₁	R₂	R₃	R₄	Name	IUPAC name
-OH	-OH	-OH	-S ₁	asiaticoside B	2 α ,3 β ,6 β ,23-tetrahydroyolean-12-en-28-oic acid O- α -L-rhamnopyranosyl-(1-4)-O- β -D-

(cont. on next page)

					glucopyranosyl-(1-6)- <i>O</i> - β -D-glucopyranosyl ester
-OH	-OH	-OH	-S ₂	centelloside D	2 α ,3 β ,6 β ,23-tetrahydroxolean-12-en-28-oic acid <i>O</i> - β -D-glucopyranosyl-(1-6)- <i>O</i> - β -D-glucopyranosyl ester
-OH	-OH	-OH	-H	terminolic acid	2 α ,3 β ,6 β ,23-tetrahydroxolean-12-en-28-oic acid
-OH	-OH	-H	-S ₁	scheffoleoside A	2 α ,3 β ,23-trihydroxolean-12-en-28-oic acid <i>O</i> - α -L-rhamnopyranosyl-(1-4)- <i>O</i> - β -D-glucopyranosyl-(1-6)- <i>O</i> - β -D-glucopyranosyl ester

cytotoxic activity (Van Loc et al., 2018), immunomodulatory activity (Punturee et al., 2005), cardioprotective (Somchit et al., 2004), memory-enhancing activity (Nalini et al., 1992), anti-viral (Yoosook et al., 2000), anti-allergic (George & Joseph, 2009).

In addition, its healing effects on diseases of endocrine, skin, digestive, respiratory, gynecological, rheumatoid arthritis (B. Sun et al., 2020), leprosy, kidney trouble, blood-circulation, brain, asthma, urinary tract infection, and hypertension (A. J. Das, 2011) have also been reported. Some of these activities were also summarized in Figure 8.

In a study, AA was reported to induce apoptosis in lung cancer cells (A549 and H1299) and also inhibited tumor volume in the mouse lung cancer xenograft model when administered orally (Wu et al., 2017). Additionally, the cytotoxic effect of AA against human melanoma cells (SK-MEL-2) was shown (Park et al., 2005). In another study, ten compounds were isolated from the methanol (MeOH) extract of *C. asiatica* and their anti-proliferative effects on human gastric adenocarcinoma (MK-1), human uterine carcinoma

(HeLa), and murine melanoma (B16F10) cells were investigated. Among them, ursolic acid (GI₅₀: 19 μM for MK-1, 65 μM for HeLa, and 14 μM for B16F10) showed the highest anti-proliferative activity (Yoshida et al., 2005). Ullah et al., 2009 showed in their study that fractions of MeOH extract of *C. asiatica* dissolved in different solvents (n-hexane, carbon tetrachloride, chloroform) exhibit significant cytotoxic effects in the brine shrimp lethality bioassay (Ullah et al., 2009).

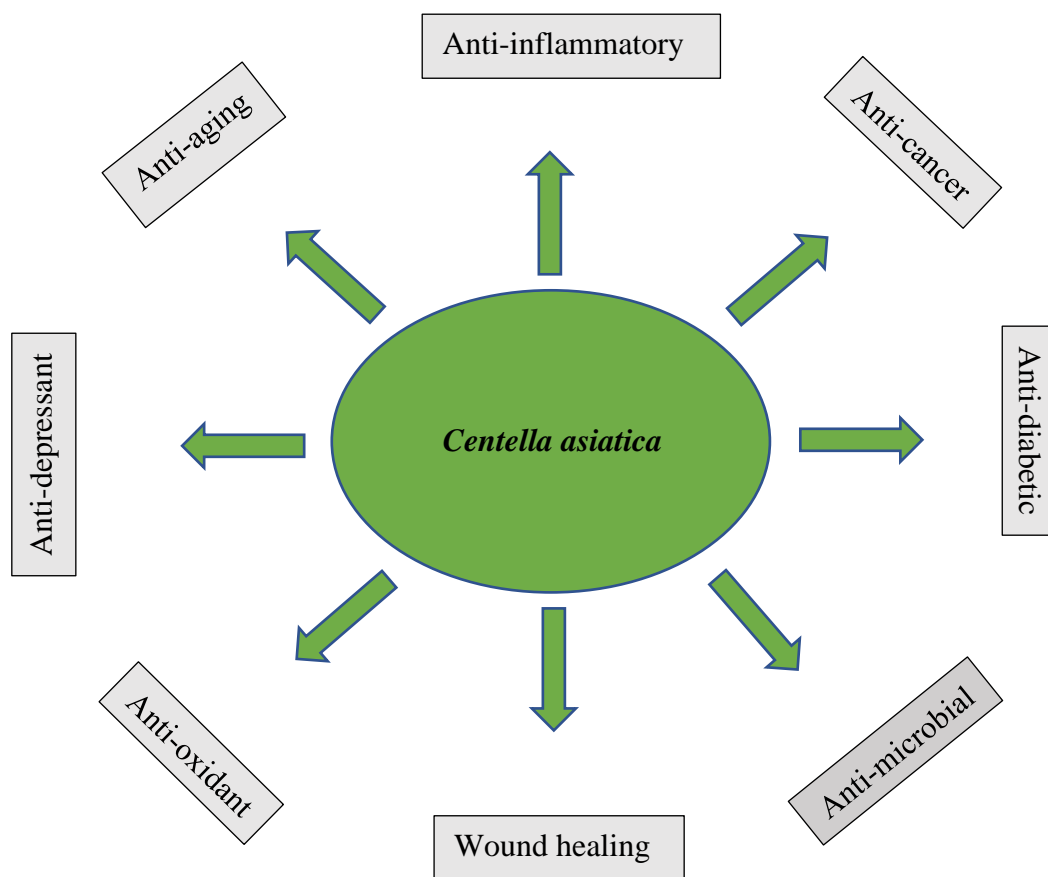


Figure 8. Pharmacological activities of *Centella asiatica*

(Prakash et al., 2017)

In addition to the cytotoxic effect, Zheng & Qin (2007) reported that the volatile extract shows a significant anti-bacterial effect against both Gram-negative and Gram-positive bacteria (Zheng & Qin, 2007). In a study investigating the healing effect of *C. asiatica*, water extract and AS decreased the size of the ulcer on the 3rd and 7th days in acetic acid-induced gastric ulcer model in rats (Cheng et al., 2004).

Nalini et al. (1992) showed that the aqueous extract of *C. asiatica* significantly reduces norepinephrine, dopamine, and 5-HT levels and their metabolites in the brain, and therefore have a memory-enhancing effect (Nalini et al., 1992). According to another study, oral administration of water extract reduces lead-induced oxidative stress and restores suppressed reproductive health in male rats (Sainath et al., 2011). Bradwejn et al., (2000) demonstrated that a single oral dose of 12 g *C. asiatica* reduces the acoustic startle response in humans after 60 minutes (Bradwejn et al., 2000). In another study, oral administration of 200 mg/kg *C. asiatica* extract exhibited a cardioprotective effect against adriamycin-induced cardiac damage in adult male albino Wistar rats (Gnanapragasam et al., 2004). Lee et al., (2006) showed in their study that, AS stimulates the synthesis of type 1 collagen, a skin aging inhibitor, in human dermal fibroblast cells (Lee et al., 2006).

Wound healing is the return of the deterioration in cellular, biochemical and systemic processes that started with trauma to its normal state with the formation of new tissue. There are many different types of wounds with complex structures. Four basic steps are required for wound healing: hemostasis, inflammation, proliferation, and remodeling. Many factors may affect the wound healing process in both ways such as oxygenation, infection, age and sex hormones, stress, diabetes, etc. Along with the technological developments in recent years, the methods used in wound treatment have also been improved and great progress has been made (Guo & DiPietro, 2010).

In a study, the wound healing effect of ten AA derivatives, which were obtained by semi-synthesis, were examined via wound area and tensile strength assay. According to the results, the ethoxymethyl 2-oxo-3,23-isopropylidene-asiatate derivative showed the highest healing activity, and also the scar it left was very small (Jeong, 2006). In another study, AS was used in normal and delayed-type wound healing experiments in guinea pigs and streptozotocin-diabetic rats in which 0.2% and 0.4% AS solution increased hydroxyproline, tensile strength, collagen content, and epithelization in guinea pig punch and rat wounds, respectively (Shukla et al., 1999).

Ruszymah et al. (2012) investigated the migration and proliferation of rabbit corneal epithelial (RCE) cells using *C. asiatica* aqueous extract. While there was a significant increase in the migration rate of RCE at 62.5 ppm, the extract did not show a significant effect at 500 ppm and caused inhibition at 1000 ppm which means that *C. asiatica* aqueous extract provides corneal epithelial wound healing at low concentrations (Ruszymah et al., 2012).

The wound healing effect of MeOH extract of *C. asiatica* on human dermal fibroblast (HDF) and human dermal keratinocyte (HaCaT) cells was evaluated using *in vitro* scratch assay and *in vivo* circular wound excision models. Based on the results, almost no toxicity was observed at concentrations ranging from 0.19 to 100 µg/ml and IC₅₀ could not be determined in that range since there was no cytotoxicity. 3-[4,5-dimethylthiazol-2-yl]-2,5-diphenyltetrazolium bromide (MTT) and scratch assay values exhibited significant stimulation at concentrations of 0.2 and 100 µg/ml on both HDF and HaCaT cell lines (Azis et al., 2017).

Effect of MA, AA, and AS, which are major components of *C. asiatica*, on skin human fibroblast collagen I synthesis were evaluated both separately, in mixture form (all of them together), and the presence or absence of ascorbic acid. It was determined that in the absence of ascorbic acid, all compounds and the combination similarly triggered collagen I synthesis, whereas secretion was higher for all samples in its presence (Bonte et al., 1994).

In an *in vivo* study on rabbits, a polyvinyl alcohol/polyethylene glycol (PVA/PEG) hydrogel formulation, rich in AS, was prepared, and using the incision method healing activity was observed. According to the results, the hydrogel did not cause any damage to the rabbit skin, and the wound healing of the hydrogel was found to be 15% faster than commercial creams. In addition, there was a 40% faster healing rate than untreated wounds (Ahmed et al., 2019).

In addition to wound healing effects, *C. asiatica*, has potential anti-aging activity due to its telomerase activation property. Telomeres are regions composed of specialized DNA repeat sequences (TTAGGG) located on the chromosome ends of eukaryotic organisms which protects chromosome ends from fusion and degradation. Telomerase is a cellular reverse transcriptase (TERT, telomerase reverse transcriptase) enzyme that helps to repair the telomere ends by adding TTAGGG repeats using the complementary RNA components (AAUCCC). It consists of two main components in humans, human telomerase RNA (hTER) and human telomerase reverse transcriptase (hTERT) (Hiyama & Hiyama, 2007). While telomere length shortens with aging, telomerase activity also decreases over time. This phenomenon is associated with many diseases, including cardiovascular diseases, infections, and genetic diseases (Chin & Lansing, 2004; Giardini et al., 2014). In 2019, Tsoukalas et al. examined the effect of natural products (*C. asiatica* extract formulation – 08AGTLF, *Astragalus* extract formulation, TA-65, oleanolic acid, maslinic acid, and three multi-nutrient formulas) on telomerase activity on human

peripheral blood mononuclear cells (PBMCs). 08AGTLF showed an 8.8-fold increase in telomerase activity against untreated cells, while the *Astragalus* formulation showed 4.3-fold and TA-65 only 2.2-fold at concentrations of 0.02, 12.8, and 0.16 $\mu\text{g/ml}$, respectively (Tsoukalas et al., 2019).

CHAPTER 2

MATERIALS AND METHODS

2.1. Materials

The isolation experiments carried out in this thesis were performed on the standardized extract of *C. asiatica* obtained from Kingherbs Limited Company (China). The materials used in this thesis were given in the following sections.

2.1.1. Materials and equipment used in isolation studies

The list of chemicals and solvents were as follows:

- Methanol (MeOH): Sigma-Aldrich, Germany
- Ethanol (EtOH): ISOLAB, Turkey
- *n*-butanol (*n*-BuOH): Carlo Erba, Spain
- *n*-hexane: Sigma-Aldrich, Germany
- tert-butanol: Carlo Erba, Spain
- Chloroform (CHCl₃): VWR Chemicals, U.S.A
- Ethyl Acetate (EtOAc): VWR Chemicals, U.S.A
- Isopropyl alcohol (2-Propanol): ISOLAB, Turkey
- Dimethyl Sulfoxide (DMSO): Carlo Erba, Spain
- Acetonitrile (ACN): ISOLAB, Turkey
- Acetic acid (CH₃COOH): Sigma-Aldrich, Germany
- Acetone (CH₃COCH₃): Carlo Erba, Spain
- Distilled water (dH₂O), Sartorius, Germany
- Pyridine-d₅: Sigma-Aldrich, Germany
- 20% Sulfuric acid (H₂SO₄): Sigma-Aldrich, Germany
- Sodium hydroxide (NaOH): Sigma-Aldrich, Germany
- Sephadex LH-20: GE Healthcare Life Sciences, U.S.A

- RP-18 (Chromabond C18): Macherey-Nagel, Germany
- RP-18 F254s Thin Layer Chromatography (RP-TLC): Merck, Germany
- Kieselgel 60 F254 Thin Layer Chromatography (TLC): Merck, Germany
- Kieselgel 60, 70-230 mesh silica: Merck, Germany

The list of equipment was as follows:

- Nuclear Magnetic Resonance Spectrometry (NMR): Varian AS 400; Bruker 500, U.S.A
- Mass Spectrometry (MS): Agilent 1200/6530 Instrument – HRTOFMS, U.S.A
- SpeedVac Concentrator: Thermo Scientific Savant SPD 121P, U.S.A
- Freeze Dryer: Labconco FreeZone Freeze Dry System, U.S.A
- UV Imaging system: Vilber Lourmat, France
- Autoclave: Nuve OT 90L, Turkey
- Rotavapor: Heidolph, Germany; ISOLAB, Turkey
- Vacuum Pump: Labnet, U.S.A
- Peristaltic Pump: Thermo Scientific, U.S.A
- pH Meter: Mettler Toledo, Even compact S 220, Turkey
- Thermo-shaker: Biosan, TS-100C, Turkey
- Vortex Mixer: Thermo-scientific, U.S.A
- Hotplate with magnetic stirrer Hotplate: ISOLAB, Turkey
- Ultrasonic bath: Bandelin, Germany

2.1.2. Materials for cell proliferation and wound healing studies

The cell line used on cell proliferation and wound healing studies was:

- **MRC-5**: Human lung fibroblast cells

2.1.2.1. Chemicals used on cell proliferation and wound healing studies

- Phosphate buffered saline (PBS): Sigma-Aldrich, Germany
- Fetal Bovine Serum (FBS): Hyclone
- Dimethyl Sulfoxide (DMSO)
- Dulbecco's Modified Eagle Medium (DMEM)
- Trypan Blue Solution: Sigma-Aldrich, Germany
- EDTA-Trypsin: Sigma-Aldrich, Germany
- L-glutamine: Sigma-Aldrich, Germany
- MTT solution: Sigma-Aldrich, Germany

2.1.2.2. Equipment used on cell proliferation and wound healing studies

- CO₂-Incubator: Thermo-scientific, U.S.A
- Light Microscope: Euromex Oxion Inverso, OX.2003-PL, Holland
- Centrifuge: Nuve NF 800R, Turkey
- Laminar Flow Cabinet: Nuve MN 090, Turkey
- Shaking Incubator: Hangzhou Miu, China
- Plate reader: Thermo-scientific Multiskan Sky, U.S.A
- ImageJ software: NIH, Bethesda, MD
- TScratch software: CSElab, Zurich
- GraphPad Prism 8 software: Graphpad Holdings, LLC
- Water Baths: Wisd Laboratory Instruments, Germany
- Neubauer Counting Chamber
- 96-well plate, NUNC, Thermo Scientific, U.S.A

2.1.3. Materials used in immunoblotting studies

2.1.3.1. Cells and antibodies

The cell line used during immunoblotting studies was:

- **HEK_n**: Primary human keratinocyte cells, neonatal (ATCC; PCS-200-010)

Table 5. HEK_n growth medium

Components	Concentrations
Bovine Pituitary Extract (BPE)	0.4%
Rh-TGF- α	0.5 ng/ml
L-Glutamine	6 mM
Hydrocortisone Hemisuccinate	100 ng/ml
Epinephrine	1 mM
Rh Insulin	5 mg/ml
Apo-Transferrin	1 mM

The antibodies used during immunoblotting studies were:

- hTERT: Origene, U.S.A
- GAPDH: Cell Signaling Technology, U.S.A
- Anti- β -Actin: Sigma-Aldrich, Germany

2.1.3.2. Chemicals and equipment used in immunoblotting studies

The list of chemicals was as follows:

- Protease Inhibitor Cocktail (PIC): Promega, U.S.A
- Sodium Dodecyl Sulphate (SDS): Amresco, U.S.A
- Bicinchoninic Acid (BCA) Protein Assay Kit: Thermo Scientific, U.S.A
- β -Mercaptoethanol: Sigma-Aldrich, Germany
- 2-Mercaptoethanol (β ME): Sigma-Aldrich, Germany
- Polyvinylidene Difluoride (PVDF) membrane: EMD Millipore, Thermo Fisher Scientific, U.S.A
- Whatman Filter Papers
- Horseradish Peroxidase (HRP) enzyme
- ECL substrate: Biorad, U.S.A
- Sodium azide: Sigma-Aldrich, Germany
- Isopropyl alcohol (2-Propanol)
- Dimethyl Sulfoxide (DMSO)
- Methanol (MeOH): Sigma-Aldrich, Germany
- Distilled water (dH₂O): Sartorius, Germany

The list of technical devices was as follows:

- CO₂-Incubator: Thermo-scientific, U.S.A
- Centrifuge: Nuve NF 800R, Turkey
- Laminar Flow Cabinet
- Vortex Mixer
- Orbital shaker
- Microplate Reader: VersaMax
- Chemiluminescence Documentation System: Vilber Lourmat FX-7, Thermo Fisher Scientific, U.S.A
- Protein Electrophoresis Equipment

2.1.3.3. Buffers used in immunoblotting studies

- **10x PBS:** 87.5 g sodium chloride, 11.5 g sodium monohydrogen phosphate, and 2.3 g sodium dihydrogen phosphate, were dissolved in 1 L dH₂O. Its pH was 7.4.

- **2x RIPA (Radioimmunoprecipitation Assay) Lysing Buffer:** 40 mg SDS and 200 mg 7-DOC (deoxycholic acid) were dissolved in 0.4 ml NP-40, 4 ml 10x PBS and completed to 20 ml with dH₂O.
- **10% AP (Ammonium persulfate) Solution:** 1 g Ammonium persulfate was dissolved into 10 ml dH₂O, separated into Eppendorf's of 1 ml each one, and stored at -20 °C.
- **10x SDS-PAGE Running Buffer:** 30.2 g Tris Base, 144 g Glycine, and 10 g SDS were dissolved in 1 L dH₂O (For 1x running buffer; 900 ml dH₂O + 100 ml 10x running buffer).
- **4x SDS-PAGE Resolving Buffer:** 1.5 M Tris HCl (90.855 g), 0.4% h/h TEMED (2 ml), and 0.4% a/h SDS (2 g) were dissolved with dH₂O, and the solution was completed to 500 ml.
- **4x SDS-PAGE Stacking Buffer:** 0.5 M Tris HCl (30.285 g), 0.4% h/h TEMED (2 ml) and 0.4% a/h SDS (2 g) were dissolved in 500 ml dH₂O. Its pH was adjusted to 6.8.
- **10x SDS-PAGE Transfer Buffer:** 30.33 g Tris Base and 144 g Glycine were dissolved in 1 L dH₂O (For 1x transfer buffer; 700 ml dH₂O + 100 ml 10x transfer buffer + 200 ml MeOH).
- **1x SDS-PAGE Washing Buffer:** 100 ml 10x PBS and 1 ml Tween-20 were dissolved in 1 L dH₂O. Its pH was adjusted to 7.4.
- **5% Skimmed Milk Blocking Agent:** 5 g skimmed milk powder was dissolved in 100 ml 1x washing buffer. Its pH was adjusted to 7.4.

2.2. Methods

2.2.1. Determination of proper solvent systems to be used in chromatographic separations

The thin-layer chromatography (TLC) method was used to display the phytochemical content of the standardized extract of *C. asiatica*. To determine the mobile phase systems to be used in chromatographic separations, experiments were performed on both silica gel and reverse-phase silica gel (RP-C18) plates.

The standardized powder extract (10 mg) was weighed into a vial and dissolved in 5 ml MeOH, using an ultrasonic bath set to 50 °C. TLC plates were cut into 6-7 cm lengths, and spotting was applied using a glass Pasteur pipette approximately 1.5 cm above the bottom of the plates with intervals of 0.5-0.7 cm. TLC plate was put into tanks saturated with a mobile phase system, as mentioned in detail below, and the solvent was run to 1 cm below the top of the plate. The plate was then removed carefully from the tank, and the mobile phase was evaporated from its surface via air flow. The UV-active molecules were monitored under UV₂₅₄ and UV₃₆₅ lights (UV-active molecules were not detected). To visualize spots, the dried TLC plates were sprayed with 20% sulfuric acid in a fume hood and then heated on a hotplate which was set to approximately 110 °C, until the spots became visible. The spots that emerged were monitored under daylight and UV₃₆₅ light.

Mobile phase systems used on silica gel plates were as follows:

1. CHCl₃:MeOH → 90:10
2. CHCl₃:MeOH:H₂O → 80:20:2
3. CHCl₃:MeOH:H₂O → 61:32:7
4. EtOAc:MeOH:H₂O → 80:25:20
5. EtOAc:MeOH:H₂O → 100:25:20
6. EtOAc:2-propanol:H₂O → 8:4:2

Mobile phase systems used on reverse phase silica (RP-C18) plates were as follows:

1. ACN:H₂O → 40:60
2. MeOH:H₂O → 70:30
3. MeOH:H₂O → 40:60

Mobile phase systems used for silica gel plates after alkaline hydrolysis were as follows:

1. CHCl₃:MeOH:H₂O → 80:20:2
2. n-Hexane:EtOAc:MeOH → 10:10:3
3. EtOAc:MeOH:H₂O → 110:10:5

At the end of the mobile phases system trials, it was decided to use MeOH:H₂O (40:60) mobile phase system for RP-C18 column system and CHCl₃:MeOH:H₂O (61:32:7) mobile phase system for TLC screenings of the fractions during the purification steps. In addition, n-Hexane:EtOAc:H₂O (10:10:3) and CHCl₃:MeOH:H₂O (95:5:0.1) were decided to be used as mobile phase systems in column chromatography for alkaline hydrolysis products. Additionally, it was decided to use n-Hexane:EtOAc:H₂O (10:10:3) and CHCl₃:MeOH:H₂O (85:15:1) as mobile phase systems in TLC screenings of fractions during the purification process for alkaline hydrolysis products.

2.2.2. Alkaline hydrolysis and isolation studies

2.2.2.1. Alkaline hydrolysis step

In an ultrasonic bath, 200 mg the standardized powder extract of *C. asiatica* was dissolved in 20 ml of NaOH-H₂O (1 M) alkaline solution [18 ml dH₂O and 2 ml NaOH (10 M)]. Subsequently, the dissolved extract was divided into two separate reaction vials. The alkaline hydrolysis reaction was initiated on a hotplate that has a magnetic stirrer at 700 rpm at 150-200 °C (Figure 9). When the reaction reached the reflux state, it was halted and allowed to cool. A pH meter was used to measure the pH value of the alkaline hydrolysis reaction solution. The pH value of the alkaline hydrolysis reaction solution had found to be around 13-14. After cooling, neutralization of the pH was done by adding a few drops of acetic acid in each vial. Solutions were then taken from both vials and transferred to four separate Eppendorf tubes (1 ml each). The samples were partitioned separately with n-BuOH or EtOAc. After separation of solvents using a separation funnel, both solvents were run on silica gel plates in different mobile phase systems (as mentioned in section 2.2.1.) resulting selection of the most suitable mobile phase system. It was decided to perform EtOAc partition, after alkaline hydrolysis.

2.2.2.2. The EtOAc partition of alkaline hydrolysis solution

After the neutralization of the alkaline hydrolysis solution, it was poured into a separatory funnel (the vials were washed three times with dH₂O) and the final volume was adjusted to 50 ml by adding dH₂O. For partition, an equal volume (50 ml) of EtOAc

was added to the solution in the separatory funnel. The separatory funnel was shaken gently to make sure that the solvents were well mixed without emulsifying them (Figure 10). Due to the difference in density, the water phase (higher density than solvent) remained at the bottom and was poured directly from the bottom tap into an Erlenmeyer flask.



Figure 9. Alkaline hydrolysis of the standardized extract of *C. asiatica*

EtOAc phase was transferred from the funnel's upper chamber to a volumetric flask. This partitioning procedure was carried out three times. The EtOAc phase in the volumetric flask (250 ml) was evaporated at 45-50 °C in the rotavapor. Following that, the volumetric flask was washed three times with MeOH, and the MeOH solution was transferred to a previously tared vial. The vial was placed in a vacuum-free Speedvac and centrifuged (1500 rpm, 4 h, 35 °C) until no change in the weight was observed. The dry matter content in the vial was determined by precision balance.

- Vial tare = 14.4483 g
- The amount of substance = 121 mg

2.2.2.3. Purification of the EtOAc phase obtained from alkaline hydrolysis

121 mg of the substance was dissolved with MeOH in a vial to purify the EtOAc phase, a small amount of silica gel was added and the mixture was reintroduced into the Speedvac for centrifugation. n-Hexane:EtOAc:MeOH (10:10:0.5) was used as the mobile phase. 37 g of silica gel was suspended with starting mobile phase system, loaded onto a glass column, and then the column was conditioned by passing about 500 ml of the mobile phase. The substance dried into the Speedvac was subjected to the column, and fractions were collected in test tubes that passed the mobile phase.

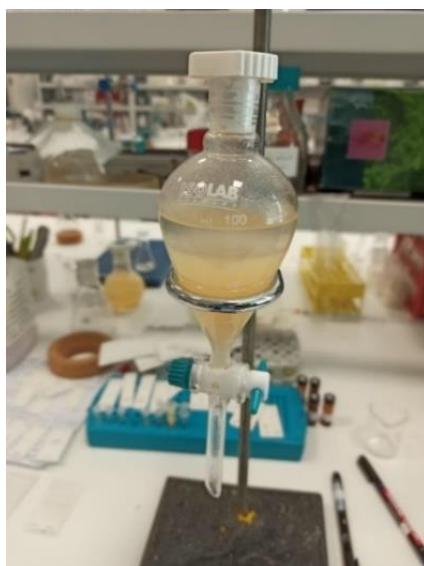


Figure 10. EtOAc partition of the alkaline hydrolysis reaction

n-Hexane:EtOAc:MeOH (10:10:3) system was used as mobile phase for all fractions for TLC screenings, and the samples were spotted 15 times, whereas the standard sample was spotted only once, due to its high concentration. The major bands began to be visible after Fr. 85 fraction. Therefore, the solvent system was polarized to n-Hexane:EtOAc:MeOH (10:10:1.5) as from Fr. 90. The column was halted at Fr. 168.

The fractions having similar TLC profiles were combined and evaporated under vacuum at 50 °C by the rotavapor. The evaporated fractions were dissolved with MeOH and transferred to the previously tared vials and centrifuged into Speedvac at 40 °C. The purity of all fractions was screened by the TLC method (four spots for the samples and

one spot for the standard). The combined fractions and their amounts were given in Table 6.

According to the TLC images, four fractions from Fr.74-84 to Fr. 131-168 (47.2 mg) were combined for further purification and evaporated under vacuum at 50 °C. Evaporated samples were subjected to 13 g silica gel which was conditioned with 200 ml CHCl₃:MeOH:H₂O (95:5:0.1) starting mobile phase system. The mobile phase system was polarized (92:8:0.5) after Fr. 6 according to the TLC chromatogram of the fractions. It was figured out that the first substance started to show up at Fr. 12. The column was halted at Fr. 57 and washed with acetone.

Table 6. The amounts of fractions

Fractions	Amount (mg)
Fr. 1-19	5.5
Fr. 20-22	0.5
Fr. 23-24	0.1
Fr. 25-47	5.3
Fr. 48-63	6.2
Fr. 64-73	2.5
Fr. 74-84	7.1
Fr. 85-104	16.3
Fr. 105-130	18.1
Fr. 131-168	5.7

Overall TLC monitoring was performed for all fractions (shown in Figure 20). Fr. 28-45 were combined and evaporated in rotavapor at 50 °C. After evaporation, flasks were washed with MeOH (three times), the solution was then transferred to a pre-tared vial and coded as **DD-GK-S(74-168)-S(28-45)** since it was considered to be a pure compound. Precision balance was used to determine the amount of DD-GK-S(74-168)-S(28-45) that was centrifuged into Speedvac in a vacuum-free environment. The isolation scheme of DD-GK-S(74-168)-S(28-45) was shown in Figure 12.

- Vial tare = 14.4907 g
- The amount of **DD-GK-S(74-168)-S(28-45)** = 22 mg

2.2.2.4. Isolation and purification of four major compounds from the standardized extract

Medium pressure liquid chromatography (MPLC) column was prepared for the isolation process of the standardized extract of *C. asiatica* (Figure 11). 100 g of RP-C18 silica gel was conditioned to the column after suspending it with approximately 250 ml MeOH:H₂O (40:60). 3 g of the standardized extract of *C. asiatica* was dissolved in starting mobile phase system and was subjected to the column. The peristaltic pump was run at 15 rpm. TLC analysis was performed with CHCl₃:MeOH:H₂O (61:32:7) for each of the fractions that were collected. While non-polar bands were observed first 37 fractions, more polar bands were observed after Fr. 38. The system was polarized after Fr. 38 with 45:55 (MeOH:H₂O) mobile phase system. The column was halted at Fr. 225 and washed with dimethyl sulfoxide (DMSO).



Figure 11. Image of MPLC column system

Combined fractions were given in Table 7. Combined fractions were dried under vacuum at 50 °C by the rotavapor. Evaporated fractions were then dissolved in 65% tert-BuOH:H₂O mixture in an ultrasonic bath and were then transferred to pre-tared vials.

Samples were frozen at -80 °C. Furthermore, the frozen samples were placed into the freeze dryer for lyophilization (-59 °C, 0.33 mbar).

70 mg specimens from saponin-rich lyophilized fractions (Fr. 64-74 and Fr. 151-169 were encoded as **DD-GK-01** and **DD-GK-02**, respectively) were taken to reaction vials and then dissolved with 5 ml NaOH-H₂O (1 M) alkaline solution [4.5 ml dH₂O and 0.5 ml NaOH (10 M)] in an ultrasonic bath. The reaction was performed according to the alkaline hydrolysis procedure described in Section 2.2.2.1. TLC screenings were used to examine n-BuOH and EtOAc partitions. It was decided that partition would be carried out for both fractions using EtOAc. The hydrolysis residue of Fr. 64-74 was found to have sufficient purity and was coded as **DD-GK-03**.

Table 7. The amounts of MPLC column fractions

Fractions	Amounts (mg)
1) Fr. 0-2	35.3
2) Fr. 3-5	18.7
3) Fr. 6-14	55.1
4) Fr. 15-28	42.2
5) Fr. 29-35	19.7
6) Fr. 36-41	55.4
7) Fr. 42-43	42.1
8) Fr. 44-52	296
9) Fr. 53-63	572.7
10) Fr. 64-74	452.4
11) Fr. 75-89	314.2
12) Fr. 90-126	307.3
13) Fr. 127-143	76.8
14) Fr. 144-150	154.3
15) Fr. 151-169	147.6
16) Fr. 170-188	99.8
17) Fr. 189-206	33.5
18) Fr. 207-224	12.5

Vacuum liquid chromatography (VLC) was set up to remove hydrolysis residues of Fr. 151-169 with RP-C18 silica gel (Figure 13). 20 g of RP-C18 silica gel was suspended in MeOH and approximately 200 ml of MeOH was used to condition the column. The initial mobile phase system of the column was MeOH:H₂O (60:40).

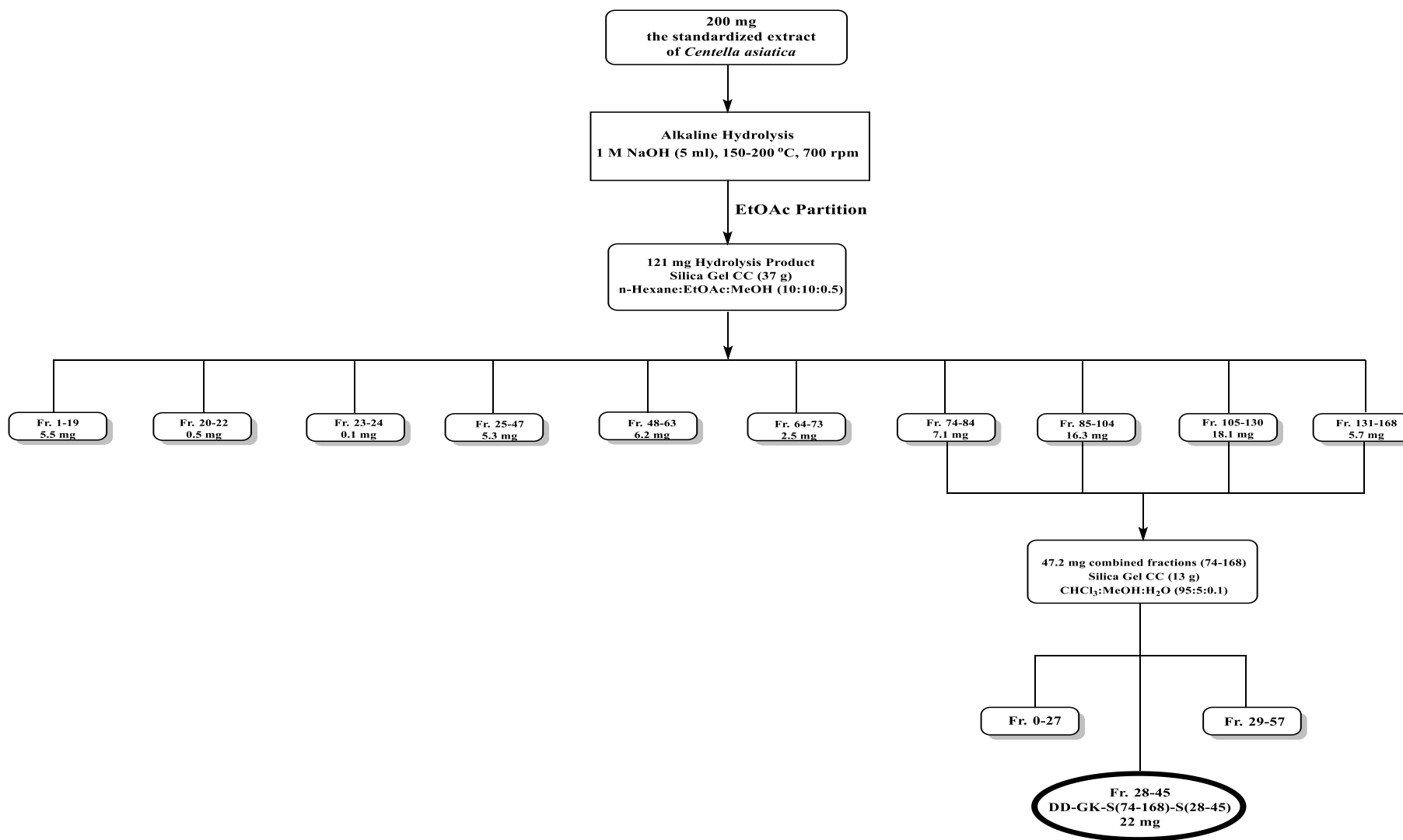


Figure 12. The isolation scheme of DD-GK-S(74-168)-S(28-45)

Fr. 151-169 was dissolved with MeOH, mixed with RP-C18 silica gel, and centrifuged in Speedvac under vacuum. The dried sample was subjected to column and the fraction profiles were monitored on TLC using $\text{CHCl}_3:\text{MeOH}:\text{H}_2\text{O}$ (80:20:2) mobile phase system. Bands had become more visible since the first fraction where there was no separation. For this reason, the column was washed with MeOH, fractions were recombined and evaporated in rotavapor.

Recombined fractions (Fr. 151-169) were subjected to silica gel (35 g) column using $\text{CHCl}_3:\text{MeOH}:\text{H}_2\text{O}$ (95:5:0.5) mobile phase system and $\text{CHCl}_3:\text{MeOH}:\text{H}_2\text{O}$ (85:15:1) mobile phase system was used for TLC. Bands were visible as from Fr. 10, Fr. 11-25 were combined, and fractions $\text{RP}(151-169)_{\text{Hydrolysis}}\text{-S}(11-25)$ were coded as **DD-GK-04**.

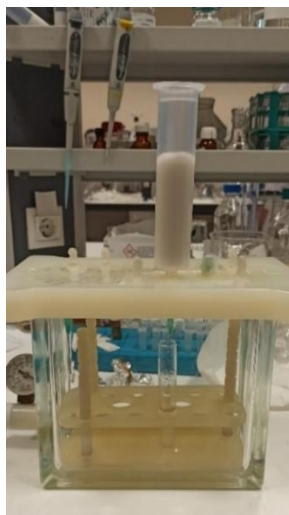


Figure 13. Image of VLC column system

Since DD-GK-01, DD-GK-02, DD-GK-03, and DD-GK-04 had impurities, they were weighed in vials separately 40, 40, 58.4, and 53.8 mg, respectively and dissolved with MeOH. The samples were subjected to Sephadex LH-20 (20 g) column using MeOH as mobile phase to get rid of the present impurities (Table 8). All fractions that were collected from columns were lyophilized [samples were frozen at $-80\text{ }^\circ\text{C}$, then frozen samples were placed into freeze dryer for lyophilization ($-59\text{ }^\circ\text{C}$, 0.33 mbar)]. The structures of four purified compounds (DD-GK-01, DD-GK-02, DD-GK-03, and DD-GK-04) were elucidated by spectral methods (1D-, 2D-NMR, and HR-ESI-MS). The isolation scheme of the metabolites was given in Figure 14.

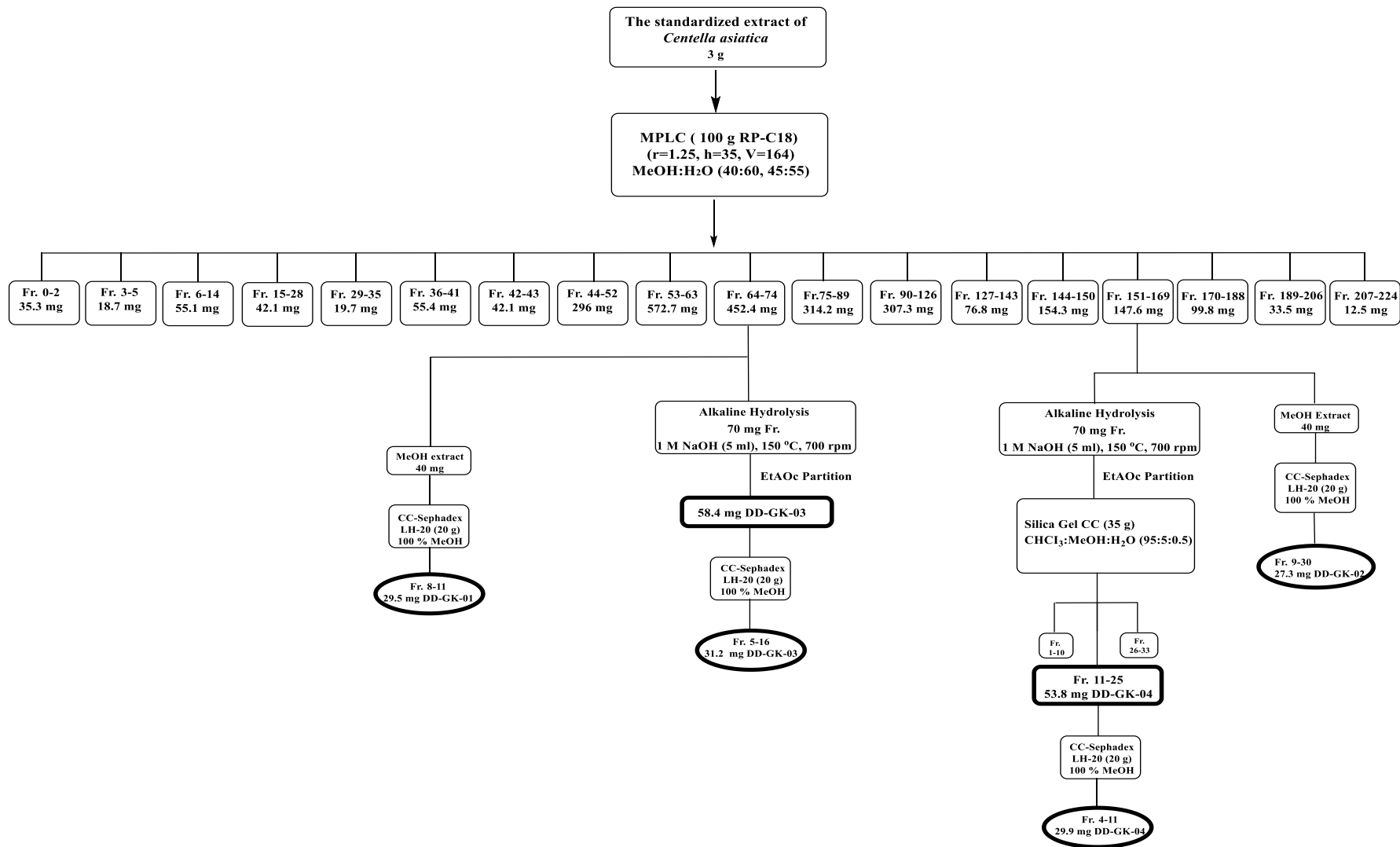


Figure 14. The isolation scheme of DD-GK-01, DD-GK-02, DD-GK-03, and DD-GK-04

Table 8. Fractions of metabolites collected from Sephadex LH-20 column and amounts of lyophilized substances

Metabolites	Combined fractions	Amounts (mg)
DD-GK-01	Fr. 8-11	29.5
DD-GK-02	Fr. 9-30	27.3
DD-GK-03	Fr. 5-16	31.2
DD-GK-04	Fr. 4-11	29.9

2.2.3. Bioactivity Studies

The bioactivity studies in this thesis were explained briefly in this section.

2.2.3.1. Cell culture studies

Cell viability of MRC-5 (Human lung fibroblast cell line) cells were investigated. Certain concentrations of compounds were applied to the cells under standard culture and oxidative stress (H₂O₂) conditions. Briefly, cells were grown in a 100 mm tissue culture petri dish with DMEM (supplemented with 10% FBS and 1% L-glutamine, without antibiotics) at 37 °C in a humidified incubator with 5% CO₂. When the cells reached 80-90% confluency, they were detached from the surface using trypsin-EDTA solution (0.25% trypsin, 0.02% EDTA), counted using a hemocytometer (Neubauer) and seeded 6 x 10³ cells/well in 96-well plates, and incubated at 37 °C in a humidified incubator with 5% CO₂ for 24 h.

HEK293 cells were cultured in a nutrient medium that contained the components mentioned in Table 5 and was incubated overnight at 37 °C in an atmosphere of 5% CO₂ in a humidified incubator. Cells were seeded at 2.5-5 x 10³ cell/cm² and the medium was changed after 24 h. The next day metabolites dissolved in DMSO were subjected to cells and incubated for 24 h at 37 °C in an atmosphere of 5% CO₂ in a humidified incubator.

2.2.3.2. Cell proliferation studies (MTT assay)

Stock solutions were prepared in DMSO (5 mg/ml or 5 mM) and stored at -20 °C until use. Cells were subjected to metabolites with different concentrations in triplicates and incubated for 72 h in a humidified incubator at 37 °C with 5% CO₂. The final concentration of DMSO in media was 0.2%. Cell viability was determined by the 3-(4,5-dimethylthiazol-2-yl)-2,5-diphenyltetrazolium bromide (MTT) assay at the end of each day (24, 48, and 72 h) according to the manufacturer's instructions. Briefly, the existing media was replaced with 100 µl of fresh media including 10% MTT (5 µg/ml final concentration). After 3 h incubation time, MTT solution was removed and formazan crystals were dissolved with 100 µl DMSO for 15 minutes in a rotary shaker incubator at room temperature. Then, absorbance was measured at 570 nm via a micro-plate reader. The results were normalized to DMSO control (0.2%) and were represented as percentages.

To evaluate the effects of compounds and the extract under oxidative stress, two methods were applied. Firstly, MRC-5 cells were exposed to H₂O₂ (50µM) for 2 h and H₂O₂ was removed and wells were washed with 1x PBS twice. After washing, media containing different concentrations of compounds were added to the wells and incubated for 24 h. Secondly, cells were treated with different concentrations of compounds for 4 h. After incubation, existing media was removed and cells were exposed to H₂O₂ (50µM) for 2 h, then wells were washed with 1x PBS twice and different concentrations of the compounds were added to the wells again as described previously in the first condition. Finally, the MTT analysis was performed.

2.2.3.3. Wound healing studies (Scratch assay)

Wound closure effects of the extract and aglycone derivatives (DD-GK-03 and DD-GK-04) on MRC-5 cells were investigated via *in vitro* scratch assay. Briefly, MRC-5 cells were cultivated with standard culture conditions and seeded on 48-well plates (5 x 10⁴ cells/well) and incubated at 37 °C in a humidified incubator with 5% CO₂ for 24 h. A linear scratch was created in the confluent monolayer by gently scraping with sterile 200 µl pipette tips. Afterwards, the medium was removed and the surface was washed with PBS to remove cellular debris. After the washing step, compounds were added to

the wells at concentrations ranging from 2 to 300 nM and ng/ml (2, 10, 30, 100, 300 nM; and 2, 10, 30, 100, 300 ng/ml for the extract). DMSO (0.2%) was used as a control group. Promotion of the wound closures was observed by capturing micrographs (4x objective) with an inverted light microscope at 0, 24, and 36 h, respectively. The wound closure at each time point was analyzed by using the ImageJ and TScratch softwares and results were quantified by normalization to DMSO control and were represented as percentages.

2.2.3.4. Immunoblotting studies

The effects of the standardized extract of *C. asiatica* and major compounds to the hTERT protein level on the HEK293 cell line were investigated by *in vitro* immunoblotting assay.

2.2.3.4.1. Protein isolation

After the treatment period, the cells were detached by trypsinization and were transferred to Eppendorf tubes with cold 1x PBS and were centrifugated at 10000 g at 4 °C for 3 minutes (three times) and the supernatant was discarded after centrifugation. Depending on the amount of cell pellet in isolation, the PBS+PIC mixture was added to the Eppendorf and vortexed for 15 seconds. Afterward, a volume of 2x RIPA+PIC mixture equal to PBS+PIC was added and vortexed for another 15 seconds. The aim here was to expose the cell contents by crashing the cell membrane with the detergent effect of RIPA and the physical effect of a vortex. The vortexing process was repeated every 5 minutes five times. After centrifugation at 15000 g at 4 °C for 15 minutes, the supernatant (cell residues considered to pass into solution since the membrane integrity was disrupted) was carefully taken and transferred to new Eppendorf tubes.

2.2.3.4.2. Determination of protein amount

The amount of protein in the cell contents (lysate) released as a result of crashing the cell membrane was determined using the BCA protein assay kit. The BCA protein assay is a test to determine the total amount of protein in a solution. The total protein concentration is determined by measuring the color change from green to purple in the

sample solution. For this purpose, 8 μl dH_2O and 2 μl samples were added to each well of the 96 well-plate with three replicates. 200 μl of BCA solution (reagent A and B in a 50:1 ratio) was added to the wells and the plate was mixed in an orbital shaker for 1 minute. The plate was wrapped with aluminum foil and incubated for 30 minutes so that it was not affected by light as it is a light-sensitive experiment. After incubation, absorbance was measured at 562 nm wavelength against the blank (1x PBS+2x RIPA). The average of the absorbance values was calculated and the protein concentrations were determined by entering the absorbances into the line equation drawn with the standard solution (bovine serum albumin).

2.2.3.4.3. Separation of proteins by SDS-PAGE

SDS-PAGE gel pouring apparatus and a separation gel with a 10% concentration were prepared. A strong oxidizing agent, Ammonium Persulfate, was added to gel solutions to initiate the polymerization process. As air contact prevents polymerization, the gel was covered with isopropyl alcohol as soon as it was poured. After polymerization, the supernatant was decanted and washed with dH_2O (four times). Then the prepared stacking gel was poured onto the separation gel. A comb was placed on the gel, forming the wells and the gel was allowed to solidify for 45 minutes. The gel was separated from the apparatus and placed into the electrophoresis tank. The tank was filled with 1x running buffer. Before use, 10% β -Mercaptoethanol was added to the required volume of 4x loading buffer and centrifuged short time.

The total volume of the samples to be loaded was completed to 30 μl by adding dH_2O (22.5 μl) and 4x loading buffer (7.5 μl) on top of the volume corresponding to 50-100 μg of protein lysates. Prepared protein samples were denatured at 95 $^\circ\text{C}$ for 5 minutes and centrifuged for a short time before loading onto the gel. The compositions of the stacking and resolving gels were shown in Table 9. Samples were carefully applied to the wells and electrophoresis was performed at 60 V for stacking gel and 120 V for separating gel for approximately 120 minutes.

Table 9. Preparation of stacking and resolving gels

Resolving gel	
Gel percentage	10%
Acrylamide (30%)	3.33 ml
4x Resolving Buffer	2.5 ml
Distilled water	4.1 ml
AP (10%)	75 μ l

Stacking Gel	
Acrylamide (30%)	0.35 ml
4x Stacking Buffer	0.75 ml
Distilled water	1.9 ml
AP (10%)	25 μ l

2.2.3.4.4. Transfer to Polyvinylidene Difluoride (PVDF) membrane

Western Blot sandwich apparatus includes a sponge, two Whatman filter papers, gel on which proteins walk, and a PVDF membrane, respectively, were placed in the cassette for transfer. 1x transfer buffer was poured into the cassette, transfer of proteins onto the PVDF membrane was achieved by applying a current of 300 mA for 90 minutes on ice or at 20-40 mA overnight at room temperature.

2.2.3.4.5. Blocking, primary and secondary antibodies labeling

Non-protein binding sites were blocked after transfer to the PVDF membrane to prevent non-specific linkages between protein and antibodies. For this purpose, the membrane was incubated on an orbital shaker for 40 minutes at room temperature with 5% milk solution prepared and 1x washing buffer. After blocking, the membrane was washed with 1x washing buffer for 5 minutes and incubated with a primary antibody for

1 h at room temperature or overnight in a cold room (+4 °C). After the primary antibody treatment, the membrane was washed 5 times for 5 minutes with 1x washing buffer. Then, it was incubated with an HRP enzyme-linked mouse secondary antibody for 1 h at room temperature on an orbital shaker. After the last washing step for 30 minutes, chemiluminescence images were taken using an ECL substrate with a Vilber Lourmat Fx-7 imaging system.

2.2.4. Statistical analyses

The data was represented as mean \pm standard deviation (SD). The statistical significance was determined by One-way analysis of variance (ANOVA) with Dunnettpost-hoc correction (GraphPad Prism version 8). $P < 0.05$ was considered statistically significant (* $p < 0.05$, ** $p < 0.01$, *** $p < 0.001$, **** $p < 0.0001$).

CHAPTER 3

RESULTS AND DISCUSSION

In this section, results of isolation studies performed on the standardized extract of *C. asiatica*, spectral elucidation of the isolates, and biological activities were described and discussed in comparison with previous reports.

3.1. Isolation and purification studies

The isolation and purification studies of pure major compounds were explained briefly in this section.

3.1.1. Determination of proper solvent systems to be used in chromatographic separations

The sample was prepared by dissolving the standardized extract of *C. asiatica* with MeOH. TLC screenings were performed in various mobile phase systems along with different ratios. According to the product sheet of the standardized powder extract of *C. asiatica* [Kingherbs Limited Company (China)], the phytochemicals composition of the extract contains more than %80 triterpenoid saponins which are AS (23.91%), MS (31.75%) and terminoloside (25.41%). As terminoloside (oleanane) and MS (ursane) molecules are structural isomers. Because the bands of these two molecules overlap, only two major bands were observed on TLC profiles in Figures 15 and 16. The lack of polarity difference between the molecules prevents them to be differentiated in TLC screenings. Isolation of the metabolites studies mainly focused on the purification of major compounds which were not isomers (MS and AS). In a study, an HPLC system was developed to separate the isomers. Beta-cyclodextrin (β -CD) was added to the mobile phase as an additive, achieving separation providing a high resolution. The differences in molecular structures between isomers produce different inclusion forces, leading to different chromatographic behaviors. It was hypothesized that the separation of the isomers might be due to the different inclusion forces of complexes with β -CD (Kai et

al., 2008; J. Pan et al., 2007). This distinction was not achieved via liquid chromatography experiments that we performed throughout the thesis.

CHCl_3 :MeOH:H₂O system was chosen as a TLC mobile phase system with a ratio of 61:32:7 to separate glycosides from each other. (Figure 15).

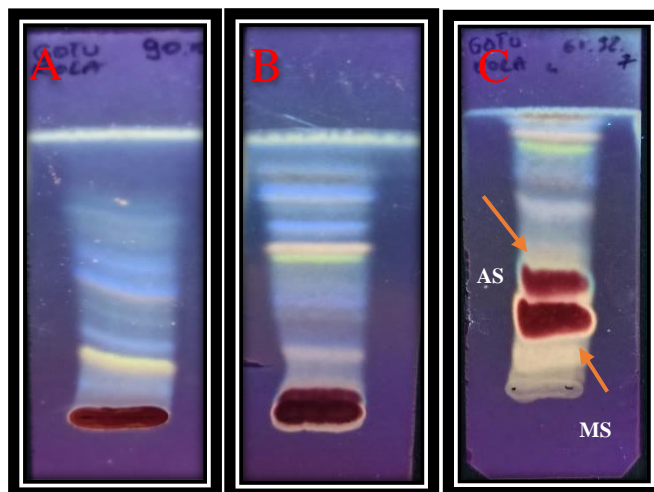


Figure 15. TLC chromatograms of the general phytochemical profiles of the extract dissolved in MeOH under UV₃₆₅, using silica gel plate, mobile phases; 90:10; CHCl_3 :MeOH (A), 80:20:2; CHCl_3 :MeOH:H₂O (B), 61:32:7; CHCl_3 :MeOH:H₂O (C)

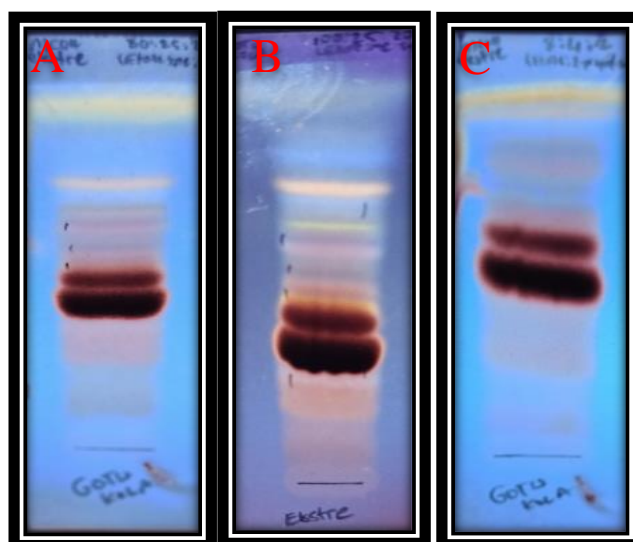


Figure 16. TLC chromatograms of the general phytochemical profiles of the extract dissolved in MeOH under UV₃₆₅, using silica gel plate, mobile phases; 80:25:20;

EtOAc:MeOH:H₂O (A), 100:25:20; EtOAc:MeOH:H₂O (B), 8:4:2; EtOAc:2-propanol:H₂O (C)

Phytochemical profiles were also screened on an RP-C18 silica gel plate to decide the column system which will use for isolation (Figure 17). According to the TLC images, MeOH:H₂O system (40:60) was chosen to be the mobile phase for the RP-C18 silica gel columns.

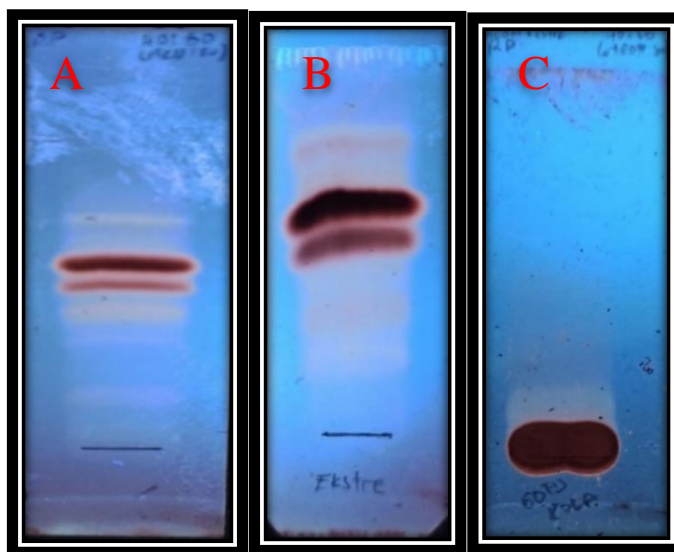


Figure 17. TLC chromatograms of the general phytochemical profiles of the extract dissolved in MeOH under UV₃₆₅, using reverse phase (RP-C18) silica gel plate, mobile phases; 40:60; ACN:H₂O (A), 70:30; MeOH:H₂O (B), 40:60; MeOH:H₂O (C)

RP-C18 columns were used to separate major glycosides. Alkaline hydrolysis was performed to obtain aglycones derivatives by hydrolyzing sugar moieties. TLC chromatogram for the products obtained using the alkaline hydrolysis method, mentioned in 2.2.2.1, was shown in Figure 18.

3.1.2. Alkaline hydrolysis of the standardized extract of *C. asiatica*

Two major saponin glycosides of the standardized extract of *C. asiatica* (MS and AS) contain an ester bond at C-28 position and three sugar moieties (glucose-glucose-rhamnose) attached to this bond (Shao et al., 2017). Ester bonds are commonly found in

several secondary metabolites. An ester bond is defined as a chemical bond between an alcohol group (-OH) and a carboxylic acid group (-COOH).

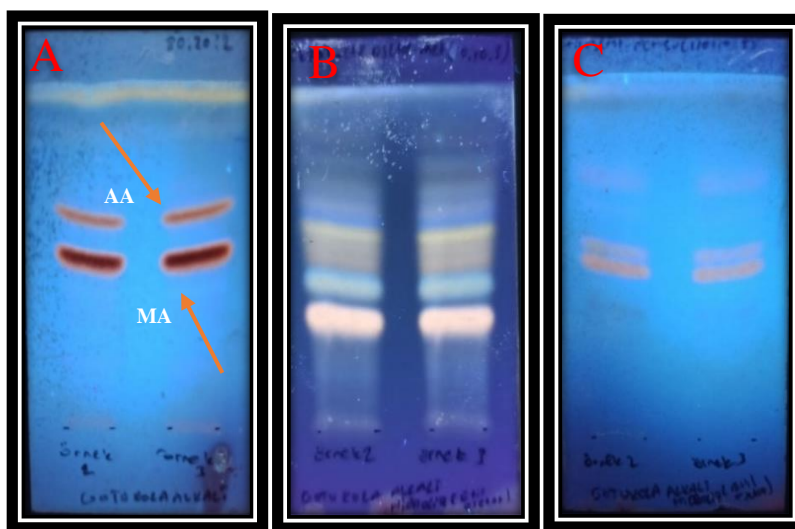


Figure 18. TLC chromatograms of the extract for alkaline hydrolysis residues after n-BuOH and EtOAc partitions under UV₃₆₅, using silica gel plate, mobile phases; 80:20:2; CHCl₃:MeOH:H₂O (A), 10:10:3; n-Hexane:EtOAc:MeOH (B), 110:10:5; EtOAc:MeOH:H₂O (C)

Ester bonds are relatively weak and can be easily hydrolyzed in acidic/alkaline environments. In an alkaline medium, hydroxides form a carboxylic acid at the C-28 position by cleaving the ester bonds and thus creating an aglycone structure (Theodorou et al., 2007).

In alkaline hydrolysis reaction, ester bonds in saponin glycosides of the standardized extract of *C. asiatica* were cleaved by NaOH (10 M) with a pH of about 13-14, and aglycones were separated from the by-products using EtOAc partition.

3.1.3. Isolation of DD-GK-S(74-168)-S(28-45)

Sugar moieties of the standardized extract of *C. asiatica* were removed by alkaline hydrolysis followed by EtOAc partitioning. The EtOAc fraction was subjected to a silica gel column as mentioned in Section 2.2.2.2. The TLC chromatogram showing the combined fractions were described in Figure 19.

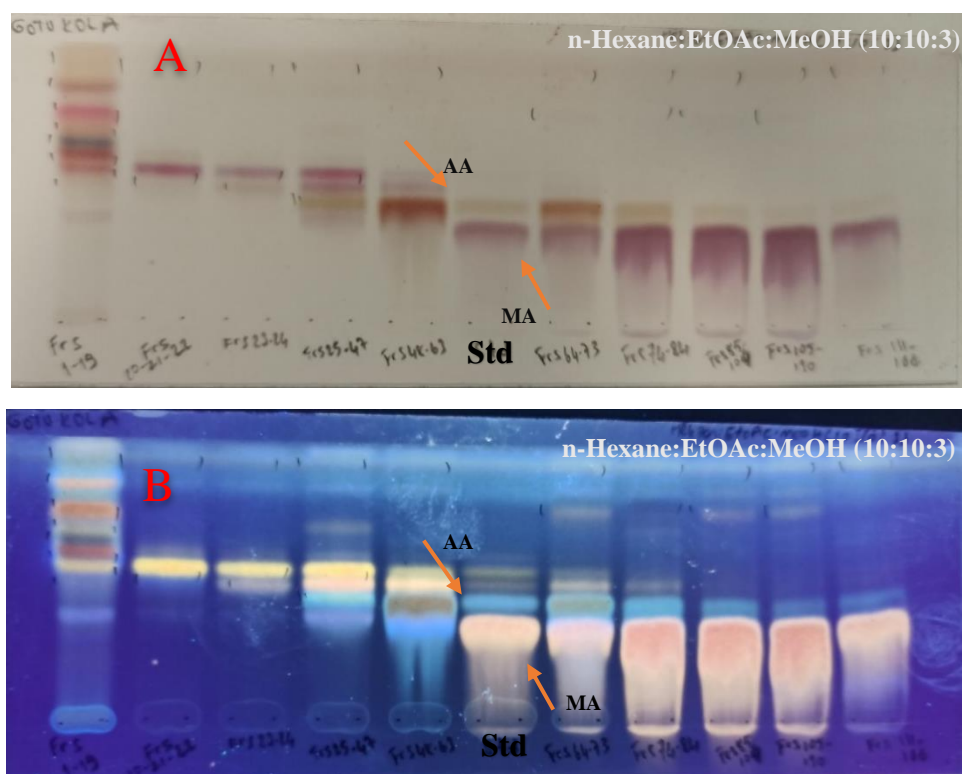


Figure 19. TLC chromatograms of combined fractions; view under daylight and UV₃₆₅ (A), after spraying (B), silica gel plate, mobile phase; 10:10:3; n-Hexane:EtOAc:MeOH

One of the major saponin glycosides that were isolated (thick band indicated by an arrow on the TLC plate) did not appear to be pure enough. For this reason, fractions between Fr.74-168 that were thought the thick band is relatively pure were collected and subjected to a silica gel column to remove potential impurities. CHCl₃:MeOH:H₂O mobile phase system was used that provided substantially cleaning of the minor substances. TLC spotting for the collected fractions was shown in Figure 20. Purified fractions were combined and dried under a vacuum. 22 mg of DD-GK-S(74-168)-S(28-45), predicted to be MA, was obtained.

3.1.4. Major compounds isolated by reverse phase silica gel (RP-C18) column system

MPLC is a preparative column system that allows separation under pressure, the use of smaller particle size supports and increases the variety of stationary phases.

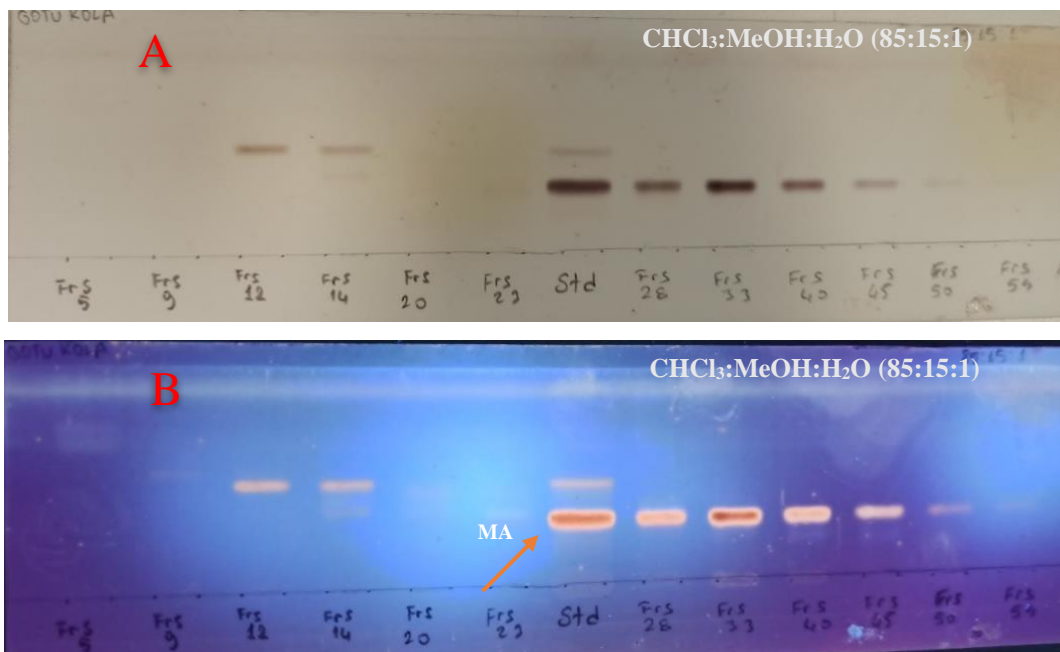


Figure 20. TLC chromatograms of S(74-168) combined fractions; view under daylight (**A**) and UV₃₆₅ (**B**), after spraying using silica gel plate, mobile phases; 85:15:1; CHCl₃:MeOH:H₂O

Unlike open column chromatography, it allows for more advanced separations. Also, the solid phase can be reused in the MPLC column system (Hostettmann & Terreaux, 2000). This system was used to isolate major compounds as a more pure state.

To reduce the retention time of the analytes in the column, the polarity of the mobile phase was reduced as of Fr. 38 which was seen as the major bands. TLC chromatograms where the minor bands were observed (between Fr. 0-35) were given in Figure 21. Furthermore, the TLC chromatogram where the fractions were numbered in Table 7 was given in Figure 22.

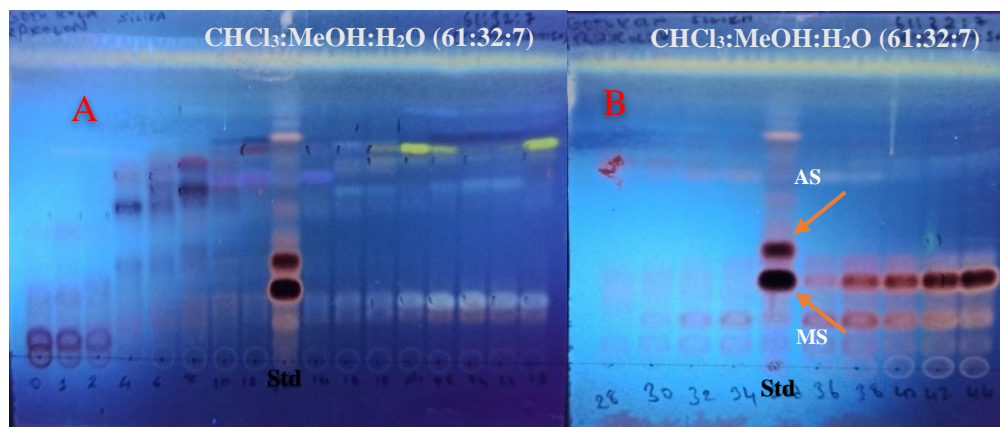


Figure 21. TLC chromatograms of minor bands under UV₃₆₅ after spraying, using silica gel plate, mobile phases; 61:32:7; CHCl₃:MeOH:H₂O

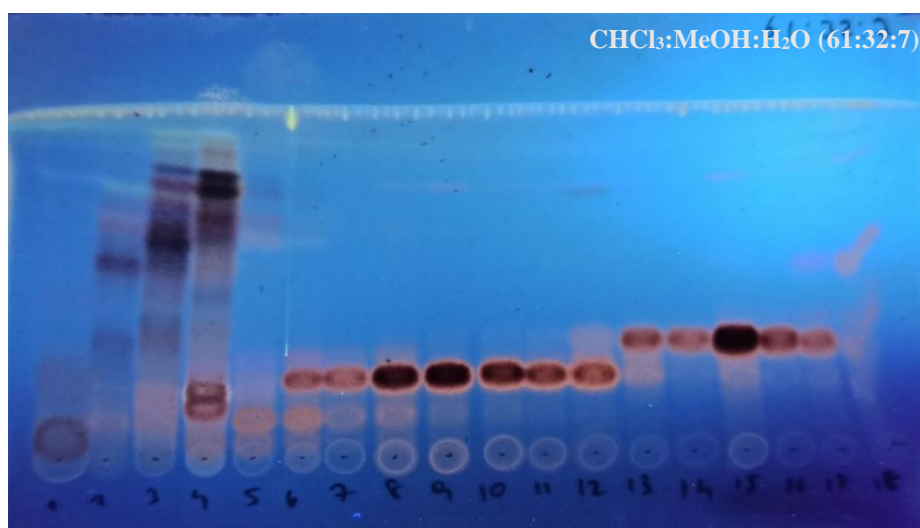


Figure 22. TLC chromatogram of all fractions numbered under UV₃₆₅ after spraying, using silica gel plate, mobile phases; 61:32:7; CHCl₃:MeOH:H₂O

In figure 22, the major compounds were observed to be quite pure. As it could be seen on the TLC plate, there were saponin-rich fractions between numbers 6-18. It was estimated that Fr. 6-12 represents MS and Fr. 13-18 represents AS. All collected fractions were frozen at -80 °C with 65% tert-BuOH and were subjected to lyophilization. Powder forms (lyophilized) of Fr. 64-74, Fr. 75-89 (MS), and Fr. 144-150 (AS) were subsequently shown in Figure 23.

MS and AS, ursane-type triterpenoid saponin glycosides, are major components of *C. asiatica*. The only difference between the molecular structure of two major compounds is MS has an -OH functional group at the C-6 position (Figure 26), conversely, AS does not contain (Figure 27) (Inamdar et al., 1996). Purified MS was in a salt-like form. On the other hand, AS was in a more cotton form (Figure 23). MS readily dissolved in dH₂O and MeOH. However, AS was insoluble in water, it only dissolved in MeOH under the influence of temperature.



Figure 23. Image of lyophilized fractions (Fr. 64-74, Fr. 75-89, and Fr. 144-150)

The presence of an -OH functional group increases the polarity of the compounds. Accordingly, the fact that AS which is less polar than MS did not dissolve with a highly polar solvent like water is consistent with our observed findings. In an intravenous administration to rats, the apparent volume of distribution of AS (2.30 L/kg) was higher compared to MS (1.28 L/kg). This was due to the superior lipophilic properties of AS. AS diffuses better in lipophilic tissues and internal organs. A study in mice using a water-soluble titrated extract of *C. asiatica* (TECA) showed that the oral bioavailability of MS and AS was very low (approximately 6%) when TECA (41.6% MS, 46.3% AS, 3.0% MA and 1.7% AA) were administered orally. Precursor compounds with poor oral bioavailability can be further developed as therapeutic agents (Hengjumrut et al., 2018).

Furthermore, an alkaline hydrolysis reaction was applied to 70 mg of Fr. 64-74 and Fr. 151-169 as mentioned in Section 2.2.2.2. to obtain aglycone derivatives by

cleaving sugar moieties of the glycosides. NaOH directly attacked the ester bond at the C-28 position, cleaving the bond and forming a carboxylic acid at the C-28 position. Sugar moieties that were separated from the aglycone structure were removed from the reaction solution by the partition method. TLC chromatograms of EtOAc and n-BuOH partitions which were applied to remove alkaline hydrolysis residues were shown in Figure 24. TLC chromatogram which is related to EtOAc partition of RP(64-74)_{Hydrolysis} and RP(151-169)_{Hydrolysis} were shown in Figure 25.

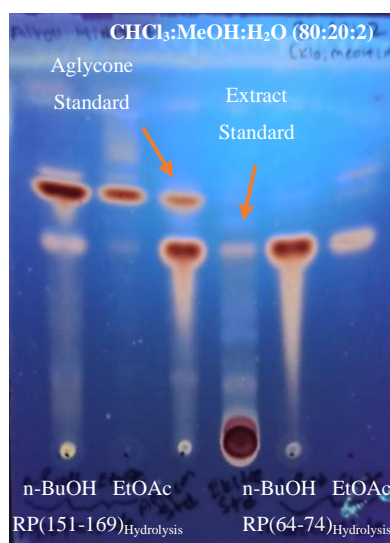


Figure 24. TLC chromatogram of alkaline hydrolysis residues under UV₃₆₅ after spraying, using silica gel plate, mobile phases; 80:20:2; CHCl₃:MeOH:H₂O

Sugar moieties of the glycosides linked by an ester bond at C-28 position were cleaved by alkaline hydrolysis, subsequently, aglycone derivatives (MA and AA) were obtained. Since aglycone derivatives did not contain any sugar moieties, they had more hydrophobic properties than glycosides. Hydrophobic molecules are generally non-polar. It was clear that these properties influenced the activities of the compounds in biological activity studies. The standardized extract of *C. asiatica* always had a higher solubility compared to pure major compounds.

As RP(64-74)_{Hydrolysis} turned out to be quite pure, was lyophilized without the need for further processing. As for RP(151-169)_{Hydrolysis}, it was figured out that there were impurities. To remove impurities, RP(151-169)_{Hydrolysis} was once again passed through the silica gel column and then lyophilized.

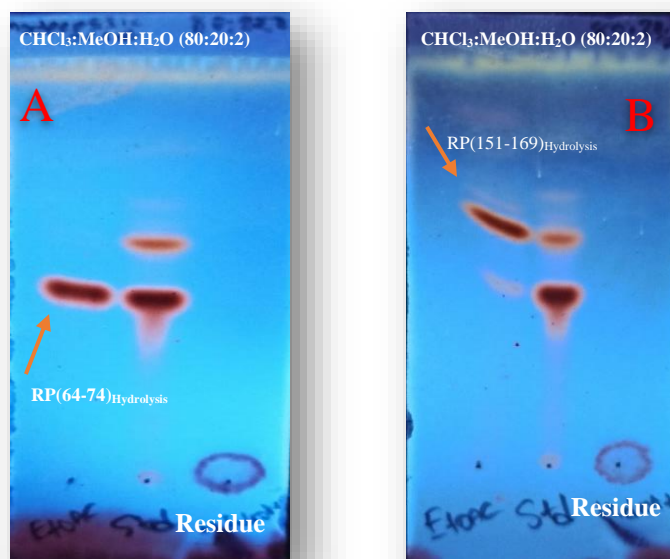


Figure 25. TLC chromatograms of EtOAc partition; RP(64-74)_{Hydrolysis} (A), and RP(151-169)_{Hydrolysis} (B), under UV₃₆₅ after spraying, using silica gel plate, mobile phases; 80:20:2; CHCl₃:MeOH:H₂O

Finally, Fr. 64-74, Fr. 151-169, RP(64-74)_{Hydrolysis}, and RP(151-169)_{Hydrolysis}-S(11-25) were passed through the Sephadex LH-20 column that was encoded as **DD-GK-01**, **DD-GK-02**, **DD-GK-03**, and **DD-GK-04**, respectively. Structure identification of coded pure compounds was elucidated by spectral methods (1D-, 2D-NMR and HR-ESI-MS).

3.2. Structure elucidation studies

Two known saponins and two known sapogenins were obtained by a combination of chromatographic steps from the standardized extract of *C asiatica*. These molecules were elucidated based on spectroscopic methods (1D-NMR, 2D-NMR, and HR-ESI-MS).

3.2.1. Structure elucidation of DD-GK-01

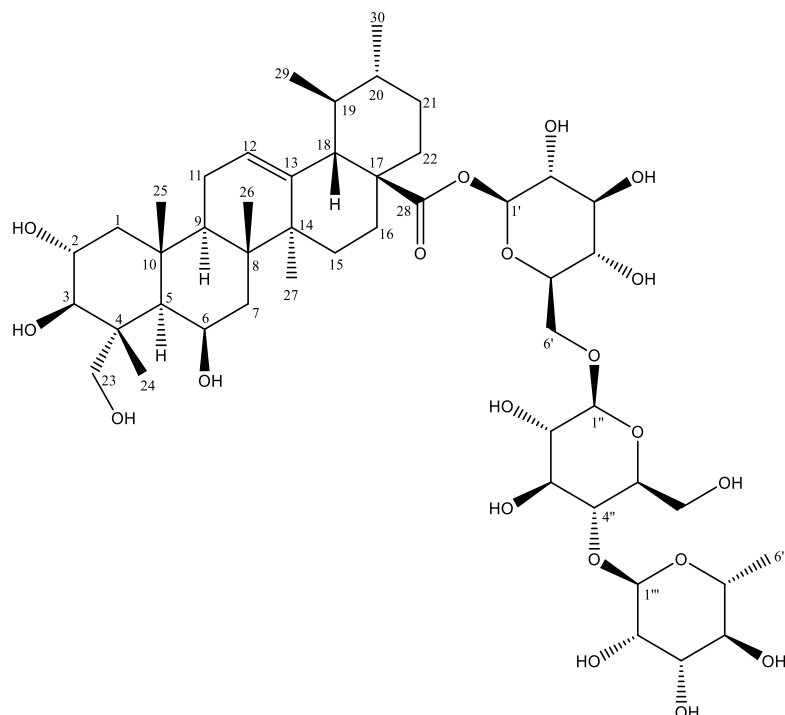


Figure 26. Chemical structure of DD-GK-01

The spectroscopic data of DD-GK-01 was presented in Table 10. In the HR-ESI-MS spectrum of DD-GK-01, a major ion peak was observed at m/z 997.4965 $[M+Na]^+$ indicating the molecular formula as $C_{48}H_{78}O_{20}$ (calc. 997.4984 for $C_{48}H_{78}O_{20}Na$).

The 1H -NMR spectrum of DD-GK-01 demonstrated signals of primary alcohol protons δ 4.36 and δ 4.02 (each d, $J = 10.6$ Hz, H_{2-23}) in the down-field region, four tertiary methyl groups at δ 1.06, 1.69, 1.70 and 1.77 and two secondary methyl groups at δ 0.84 (d, $J = 6$ Hz, H_{3-30}) and δ 0.90 (d, $J = 6$ Hz, H_{3-29}) in the up-field region, which were attributed to characteristic resonances of a ursane-type triterpene aglycone, which was common in *C. asiatica* chemistry. Besides, a secondary methyl group at δ 1.66 (d, $J = 6.4$ Hz) was readily assigned to $H_{3-6''}$ of the L-rhamnose moiety. Moreover, the 1H NMR spectrum of DD-GK-01 displayed three anomeric protons at δ 4.94 (d, $J=7.9$ Hz, $H-1''$), 5.82 (s, $H-1'''$) and 6.10 (d, $J=8.1$ Hz, $H-1'$) in the down-field region, indicative of two β -linked and one α -linked sugar units. These protons were correlated to carbons at δ 105.1, 102.8, and 95.9, respectively, in the HSQC spectrum (see Spectrum 10). Also, a trisubstituted double bond system was evident in the 1H -, ^{13}C -NMR and DEPT-135

spectra (δ_{C-12} 126.6, d; δ_{C-13} 138.0, s; δ_{H-12} 5.52, d). The position of the double bond was justified via the 2D-NMR spectra of DD-GK-01. When the spectral data of DD-GK-01 was compared with those of *C. asiatica* saponins, the structure was unambiguously determined as madecassoside (Du et al., 2004).

Table 10. ^1H - and ^{13}C -NMR spectroscopic data of DD-GK-01, ^{a)} (in $\text{C}_5\text{D}_5\text{N}$, δ ppm, ^1H : 500 MHz, ^{13}C : 125 MHz)

H/C	δ_{C} (ppm)	δ_{H} (ppm), (J in Hz)
1	50.7 t	2.34 ^{b)} ; 1.45 ^{b)}
2	69.3 d	4.41 ^{b)}
3	78.2 d	4.23 ^{b)}
4	44.8 s	-
5	48.6 d	1.96 ^{b)}
6	67.7 d	5.05 ^{b)}
7	41.5 t	1.97 ^{b)} ; 1.85 ^{b)}
8	39.8 s	-
9	48.8 d	1.96 ^{b)}
10	38.3 s	-
11	24.1 t	2.23 ^{b)} ; 2.11 ^{b)}
12	126.6 d	5.46 d (9.1)
13	138.0 s	-
14	43.3 s	-
15	28.9 t	2.48 ^{b)} ; 1.12 ^{b)}
16	24.9 t	1.99 ^{b)} ; 1.91 ^{b)}
17	48.7 s	-
18	53.5 d	2.47 ^{b)}
19	39.6 d	1.33 ^{b)}
20	39.3 d	0.81 ^{b)}
21	31.0 t	1.32 ^{b)} ; 1.18 ^{b)}
22	37.0 t	1.86 ^{b)} ; 1.69 ^{b)}
23	66.1 t	4.36 ^{b)} ; 4.02 ^{b)}
24	16.3 q	1.70 s
25	19.5 q	1.77 s
26	19.5 q	1.69 s
27	24.0 q	1.06 s
28	176.5 s	-
29	17.6 q	0.90 d (6.0)
30	21.5 q	0.84 d (6.0)
1'	95.9 d	6.10 d (8.1)
2'	73.9 d	4.11 ^{b)}
3'	78.7 d	4.17 ^{b)}
4'	71.0 d	4.31 ^{b)}
5'	78.0 d	4.04 ^{b)}
6'	69.5 t	4.62 ^{b)} ; 4.25 ^{b)}

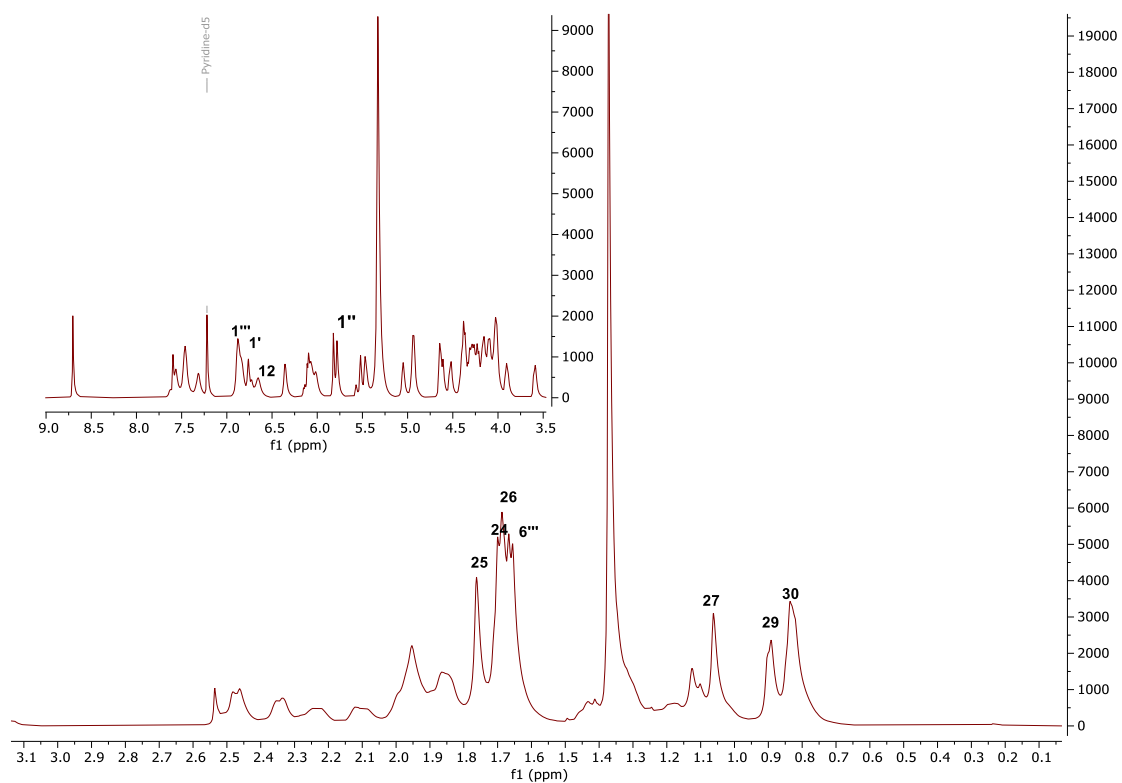
(cont. on next page)

Table 10 (cont.)

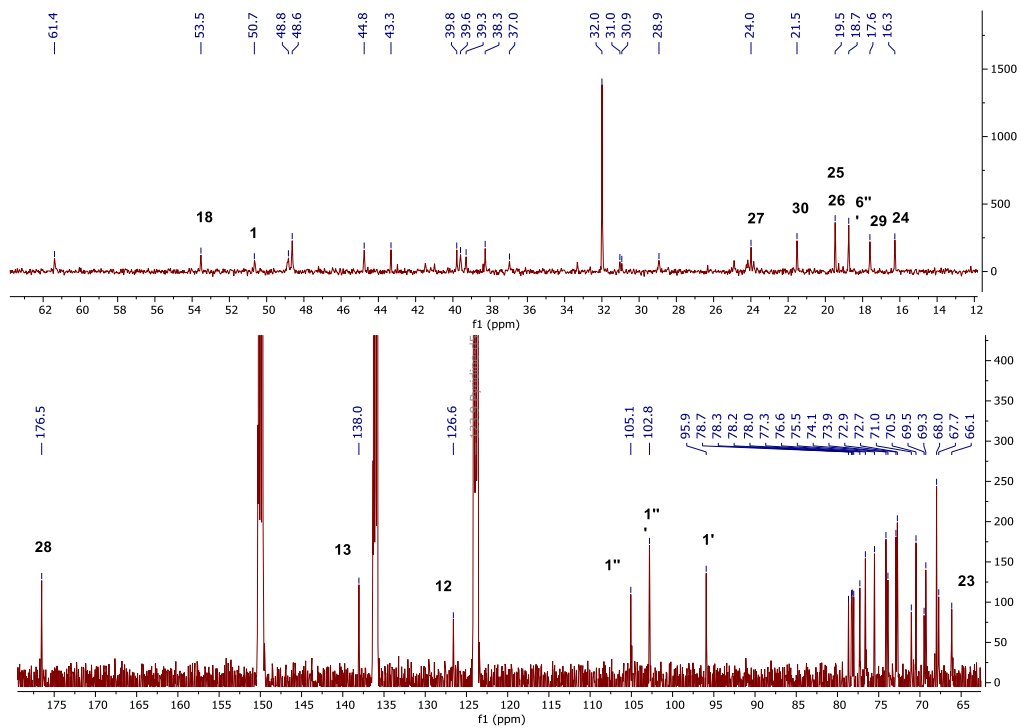
H/C	δ_C (ppm)	δ_H (ppm), (J in Hz)
1''	105.1 d	4.94 d (7.9)
2''	75.5 d	3.91 ^{b)}
3''	76.6 d	4.11 ^{b)}
4''	78.3 d	4.36 ^{b)}
5''	77.3 d	3.60 ^{b)}
6''	61.4 t	4.17 ^{b)} ; 4.04 ^{b)}
1'''	102.8 d	5.82 s
2'''	72.7 d	4.64 ^{b)}
3'''	72.9 d	4.53 ^{b)}
4'''	74.1 d	4.31 ^{b)}
5'''	70.5 d	4.94 ^{b)}
6'''	18.7 q	1.66 d (6.4)

a) Assignments are confirmed by 2D-COSY, HSQC, HMBC, and NOESY experiments.

b) Signal pattern was unclear due to overlapping



Spectrum 1. ¹H-NMR spectrum of DD-GK-01



Spectrum 2. ^{13}C -NMR spectrum of DD-GK-01

3.2.2. Structure elucidation of DD-GK-02

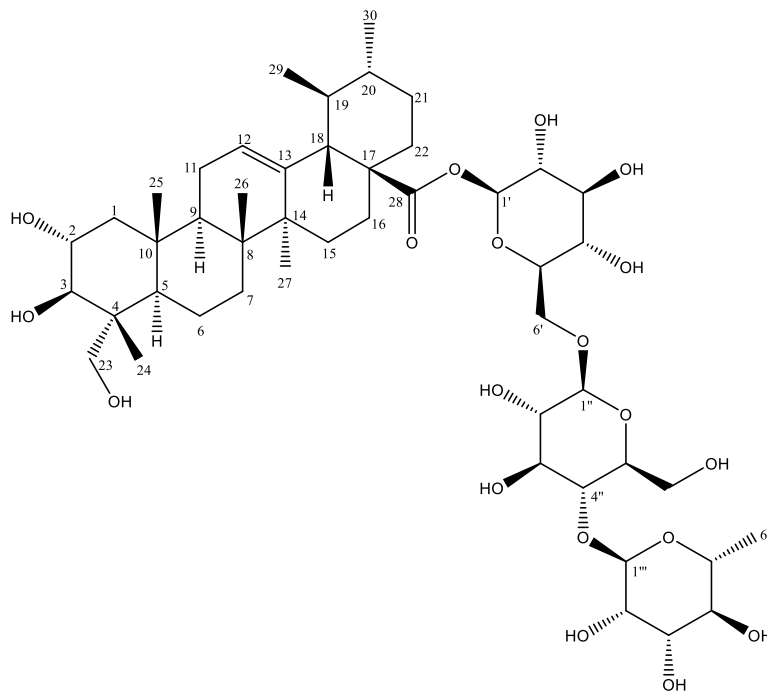


Figure 27. Chemical structure of DD-GK-02

DD-GK-02 is another saponin that was isolated from the standardized extract of *C. asiatica*. The spectroscopic data of DD-GK-02 was presented in Table 11. In the positive mode of HR-ESI-MS spectrum of DD-GK-02, the base ion peak was seen at m/z 981.5024 $[M+Na]^+$ suggesting the molecular formula as $C_{48}H_{78}O_{19}$ (calc. 981.5035 for $C_{48}H_{78}O_{19}Na$). When the MS data of DD-GK-02 was compared to that of DD-GK-01, a 16 atomic mass unit difference was seen indicating the removal of one oxygen atom. Also, the lack of peaks ($C_6:67.7$ d, $H_6:5.05$ m) suggested that one hydroxyl group was lacking at C-6 position of the skeleton, which was further confirmed by 2D-NMR spectral data.

The 1H -NMR spectrum of DD-GK-02 revealed primary alcohol signals at 4.20 and δ 3.70 (each d, $J = 8.4$ Hz, H_{2-23}) in the down-field region, four tertiary methyl groups at δ 1.06, 1.07, 1.10 and 1.17 and two secondary methyl groups at δ 0.87 (d, $J = 6$ Hz, H_{3-30}) and δ 0.90 (d, $J = 6.3$ Hz, H_{3-29}) in the up-field region which were ascribed to typical signals of a ursane-type triterpenic aglycone. Also, one secondary methyl group at δ 1.70 (d, $J = 6.2$ Hz) belonging to $H_{3-6''}$ of L-rhamnose moiety was apparent. Additionally, the down-field region of the 1H -NMR spectrum of DD-GK-02 demonstrated three anomeric protons at δ 4.99 (d, $J=7.7$ Hz, $H-1''$), 5.86 (s, $H-1'''$) and 6.18 (d, $J=8.2$ Hz, $H-1'$). In the HSQC spectrum, these protons were correlated to carbons at δ 105.5, 103.2, and 96.2, respectively (see Spectrum 15). Also, the presence of a trisubstituted double bond system was apparent in the 1H -, ^{13}C -NMR and DEPT-135 spectra (δ_{C-12} 126.5, d; δ_{C-13} 139.1, s; δ_{H-12} 5.37). The position of the olefinic bond was confirmed based on the 2D-NMR spectra of DD-GK-02. When the spectral data of DD-GK-02 was compared with those of *C. asiatica* saponins, the structure was clearly determined to be asiaticoside (Du et al., 2004).

Table 11. 1H - and ^{13}C -NMR spectroscopic data of DD-GK-02, ^{a)} (in C_5D_5N , $^1H:500$ MHz, $^{13}C:125$ MHz)

H/C	δ_C (ppm)	δ_H (ppm), (J in Hz)
1	48.2 t	2.28 ^{b)} ; 1.35 ^{b)}
2	69.1 d	4.25 ^{b)}
3	78.2 d	4.22 ^{b)}
4	43.9 s	-
5	47.9 d	1.78 ^{b)}
6	18.7 t	1.40 ^{b)}

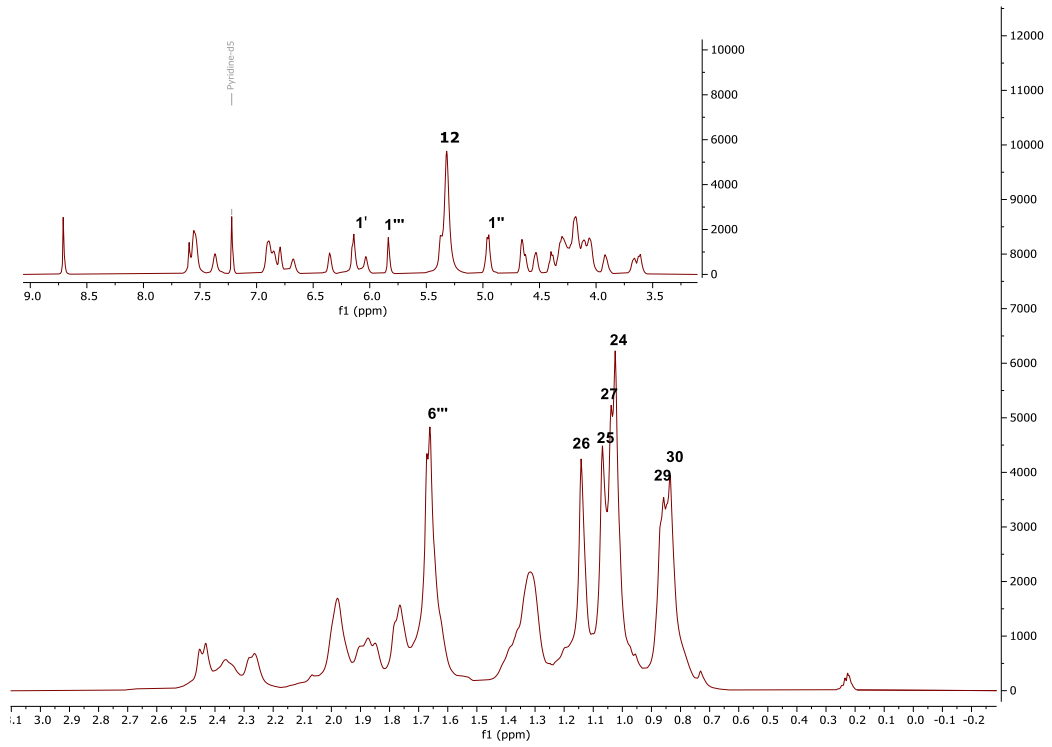
(cont. on next page)

Table 11 (cont.)

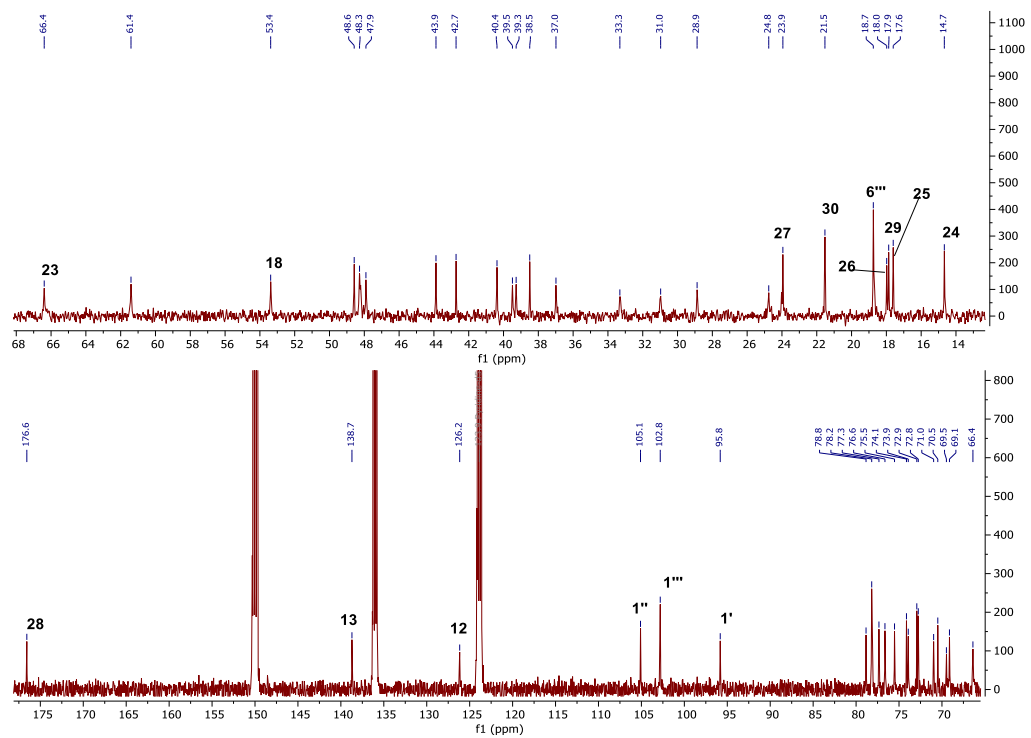
H/C	δ_C (ppm)	δ_H (ppm), (J in Hz)
7	33.3 t	1.64 ^b ; 1.32 ^b
8	40.3 s	-
9	47.6 d	1.78 ^b
10	38.5 s	-
11	23.9 t	1.98 ^b
12	126.2 d	5.37 ^b
13	138.7 s	-
14	42.7 s	-
15	28.9 t	2.37 ^b ; 1.07 ^b
16	24.7 t	2.98 ^b ; 1.90 ^b
17	48.3 s	-
18	53.4 d	2.44 d (11.0)
19	39.5 d	1.32 ^b
20	39.2 d	0.80 ^b
21	31.0 t	1.32 ^b ; 1.19 ^b
22	37.0 t	1.87 ^b ; 1.72 ^b
23	66.4 t	4.18 d (8.4), 3.67 d (8.4)
24	14.7 q	1.03 s
25	17.9 q	1.07 s
26	18.0 q	1.14 s
27	23.9 q	1.04 s
28	176.5 s	-
29	17.6 q	0.87 d (6.3)
30	21.5 q	0.84 d (6.0)
1'	95.8 d	6.15 d (8.2)
2'	73.9 d	4.11 ^b
3'	78.8 d	4.20 ^b
4'	71.0 d	4.30 ^b
5'	78.1 d	4.06 ^b
6'	69.5 t	4.64 ^b ; 4.27 ^b
1''	105.1 d	4.96 d (7.7)
2''	75.4 d	3.91 d (9.0)
3''	76.6 d	4.11 ^b
4''	78.2 d	4.39 d (8.9)
5''	77.3 d	3.61 ^b
6''	61.4 t	4.18 ^b ; 4.06 ^b
1'''	102.8 d	5.82 s
2'''	72.7 d	4.66 ^b
3'''	72.9 d	4.54 d (9.0)
4'''	74.1 d	4.33 ^b
5'''	70.5 d	4.96 ^b
6'''	18.7 q	1.67 d (6.2)

a) Assignments are confirmed by 2D-COSY, HSQC, HMBC, and NOESY experiments.

b) Signal pattern was unclear due to overlapping.



Spectrum 3. ^1H -NMR spectrum of DD-GK-02



Spectrum 4. ^{13}C -NMR spectrum of DD-GK-02

3.2.3. Structure elucidation of DD-GK-03

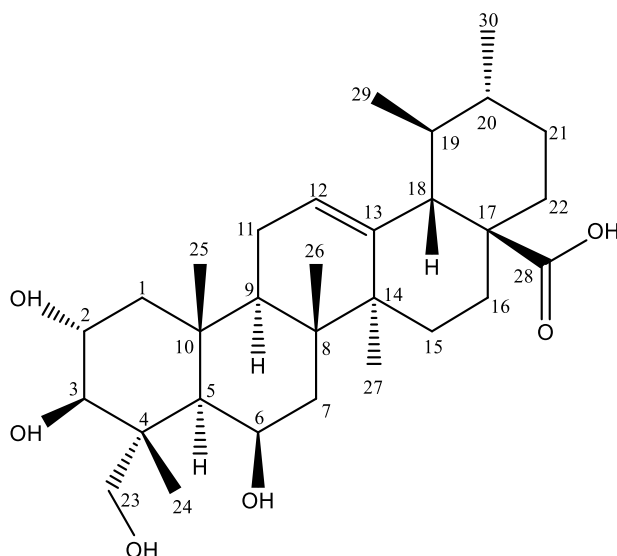


Figure 28. Chemical structure of DD-GK-03

The spectroscopic data of DD-GK-03 was given in Table 12. The HR-ESI-MS spectrum observing a major peak at m/z 527.3337 $[M+Na]^+$ infers the molecular formula as $C_{30}H_{48}O_6$ (calc. 527.3349 for $C_{30}H_{48}O_6Na$).

The 1H -NMR spectrum of DD-GK-03 displayed characteristic signals of primary alcohol protons δ 4.38 and δ 4.03 (each d, $J = 10.6$ Hz, H_2 -23) in the down-field region, four tertiary methyl groups at δ 1.18, 1.63, 1.71 and 1.76 and two secondary methyl groups at δ 0.92 (d, $J = 5.8$ Hz, H_3 -30) and δ 1.01 (d, $J = 5.6$ Hz, H_3 -29) in the up-field region, which were attributed to characteristic signals of a ursane-type triterpene structure. Besides, deglycosylation from the C-28 position of the triterpene skeleton was deduced since the resonances of sugar moiety were not observed in the 1H -NMR spectrum. This argument was justified via 1D- and 2D- NMR spectra. Furthermore, an oxo-bearing carbon atom at 67.8 ppm was apparent in the down-field region. This carbon was located onto the C-6 based on the COSY correlations from δ 2.00 (H-5) to δ 5.08 (H-6) and subsequent δ 2.04 (H-7a), δ 1.83 (H-7b). Additionally, a trisubstituted double bond system was seen in the 1H -, ^{13}C -NMR and DEPT-135 spectra (δ_{C-12} 125.9, d; δ_{C-13} 139.3, s; δ_{H-12} 5.56). The position of the double bond was determined based on the 2D-NMR spectra of DD-GK-03. When the spectral data of DD-GK-03 was compared with

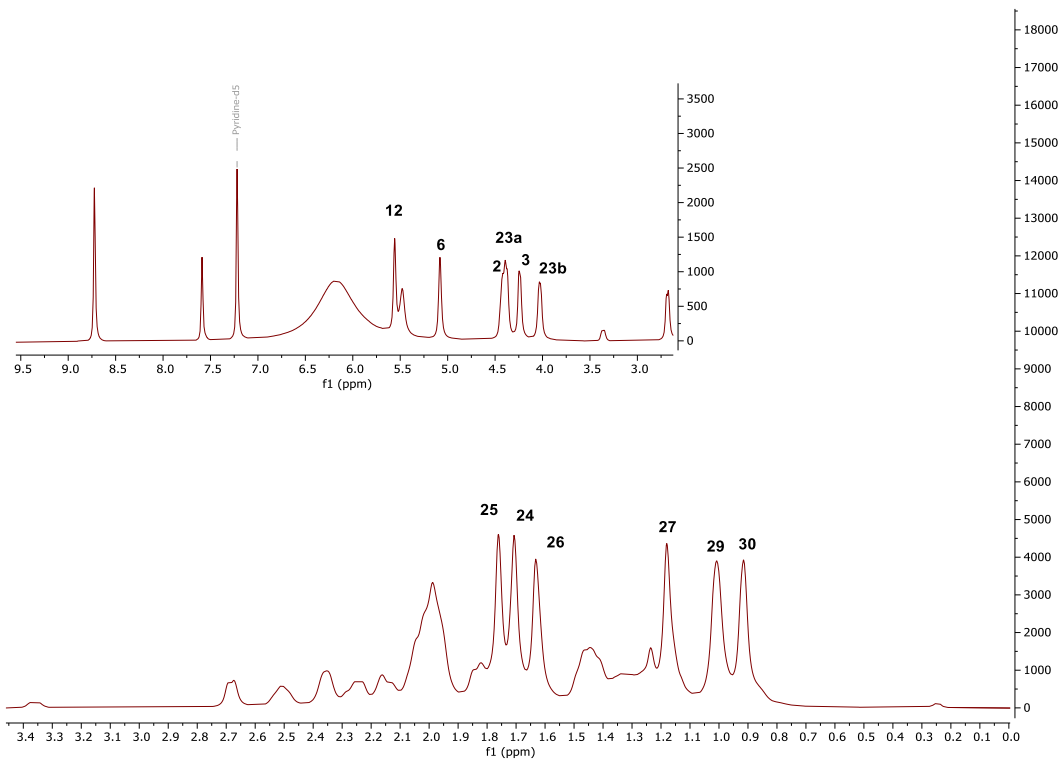
those of *C. asiatica* sapogenins, the structure was unambiguously determined as madecassic acid (Du et al., 2004).

Table 12. ^1H - and ^{13}C -NMR spectroscopic data of DD-GK-03, ^{a)} (in $\text{C}_5\text{D}_5\text{N}$, ^1H : 500 MHz, ^{13}C : 125 MHz)

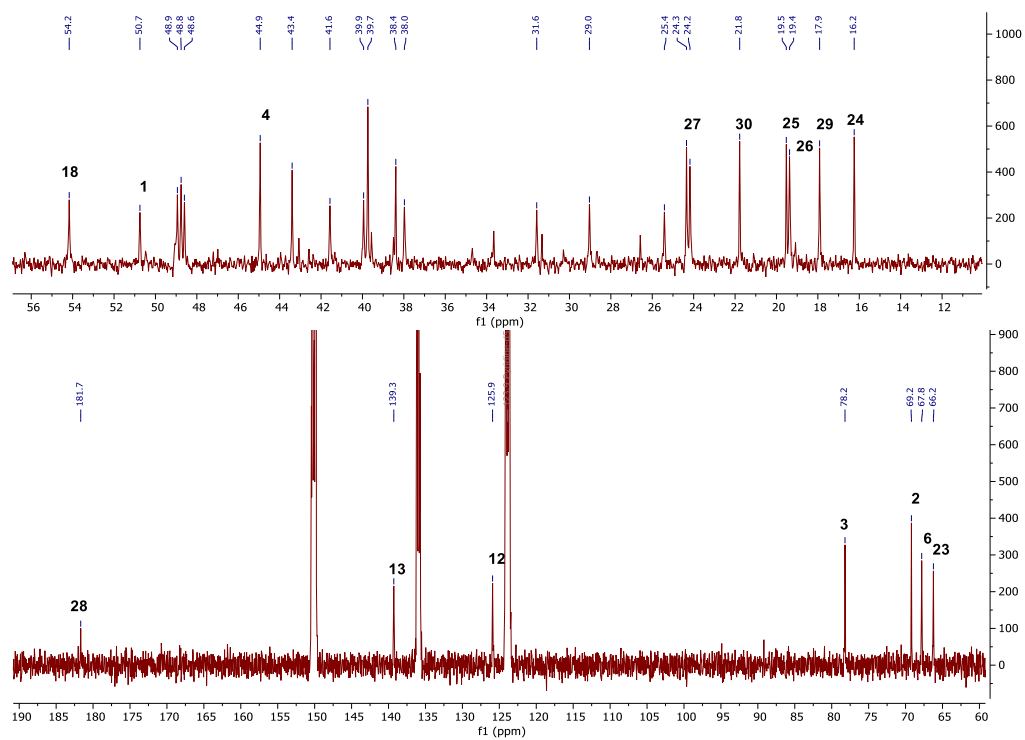
Position	δ_{C} (ppm)	δ_{H} (ppm), (J in Hz)
1	50.8 t	2.37 ^{b)} ; 1.49 ^{b)}
2	69.2 d	4.43 ^{b)}
3	78.2 d	4.24 d (9.2)
4	44.9 s	-
5	48.8 d	2.00 ^{b)}
6	67.8 d	5.08 ^{b)}
7	41.6 t	2.04 ^{b)} ; 1.83 ^{b)}
8	39.7 s	-
9	48.9 d	2.00 ^{b)}
10	38.4 s	-
11	24.2 t	2.24 ^{b)} ; 2.15 ^{b)}
12	125.9 d	5.56 s
13	139.3 s	-
14	43.4 s	-
15	29.0 t	2.50 ^{b)} ; 1.18 ^{b)}
16	25.4 t	2.02 ^{b)}
17	48.6 s	-
18	54.2 d	2.68 d (11.0)
19	39.9 d	1.47 ^{b)}
20	39.7 d	1.01 ^{b)}
21	31.6 t	1.41 ^{b)}
22	38.0 t	1.98 ^{b)}
23	66.2 t	4.38 d (10.6); 4.03 d (10.6)
24	16.2 q	1.71 s
25	19.5 q	1.76 s
26	19.4 q	1.63 s
27	24.4 q	1.18 s
28	181.7 s	-
29	17.9 q	1.01 d (5.6)
30	21.8 q	0.92 d (5.8)
6-OH	-	5.49 s

a) Assignments are confirmed by 2D-COSY, HSQC, HMBC, and NOESY experiments.

b) Signal pattern was unclear due to overlapping.



Spectrum 5. ¹H-NMR spectrum of DD-GK-03



Spectrum 6. ¹³C-NMR spectrum of DD-GK-03

3.2.4. Structure elucidation of DD-GK-04

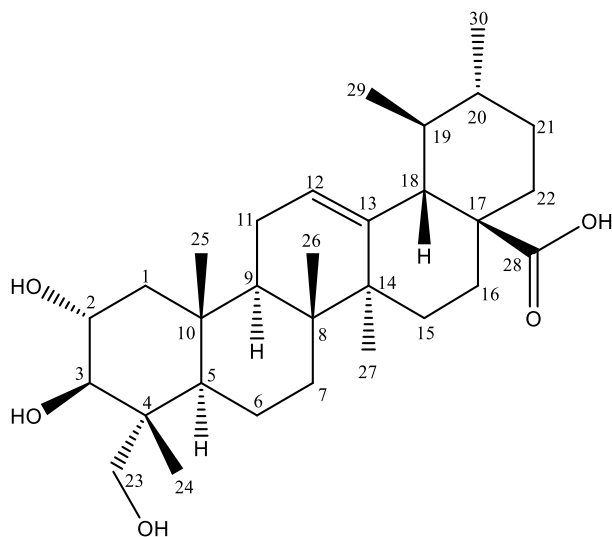


Figure 29. Chemical structure of DD-GK-04

DD-GK-04 is another sapogenin isolated from the standardized extract of *C. asiatica*. The spectroscopic data of DD-GK-04 was shown in Table 13. HR-ESI-MS spectrum demonstrating major peak at m/z 511.3387 $[M+Na]^+$ implied the molecular formula as $C_{30}H_{48}O_5$ (calc. 511.3399 for $C_{30}H_{48}O_6Na$). When the MS data of DD-GK-04 was compared with DD-GK-03, a 16 atomic mass unit difference indicated the removal of one oxygen atom. Also, the lack of peaks ($C_6:67.8$ d, $H_6:5.08$ m) suggests that one hydroxyl group was lacking at C-6 position of the skeleton, which was further confirmed by 2D-NMR spectral data.

The 1H NMR spectrum of DD-GK-04 showed the signals of primary alcohol protons δ 4.21 and δ 3.72 (each d, $J = 10.1$ Hz, H_{2-23}) in the down-field regions, four tertiary methyl groups at δ 1.05, 1.05, 1.05 and 1.13 and two secondary methyl groups at δ 0.92 (d, $J = 6.2$ Hz, H_{3-30}) and δ 0.96 (d, $J = 6.4$ Hz, H_{3-29}) in the up-field region, which were attributed to particular resonances of a ursane-type triterpene framework. Besides, deglycosylation from the C-28 position of the triterpene skeleton was inferred since the resonances of sugar moiety were not seen in the 1H -NMR spectrum. This inference was confirmed via 1D- and 2D-NMR spectra. Moreover, a trisubstituted double bond system was evident in the 1H -, ^{13}C -NMR and DEPT-135 spectra (δ_{C-12} 125.9, d; δ_{C-13} 139.6, s;

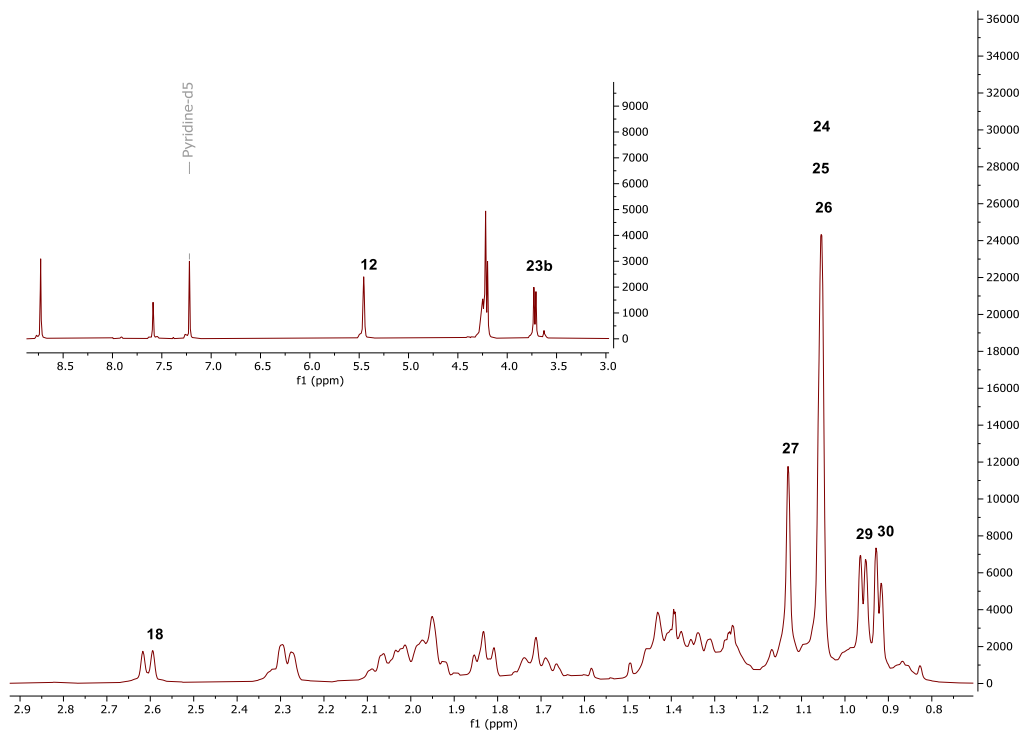
$\delta_{\text{H-12}}$ 5.45). The location of the double bond was established based on the 2D-NMR spectra of DD-GK-04. When the spectral data of DD-GK-04 was compared with those of *C. asiatica* sapogenins, the structure was clearly determined as asiatic acid (Du et al., 2004).

Table 13. ^1H and ^{13}C NMR spectroscopic data of DD-GK-04, ^{a)} (in $\text{C}_5\text{D}_5\text{N}$, ^1H : 500 MHz, ^{13}C : 125 MHz)

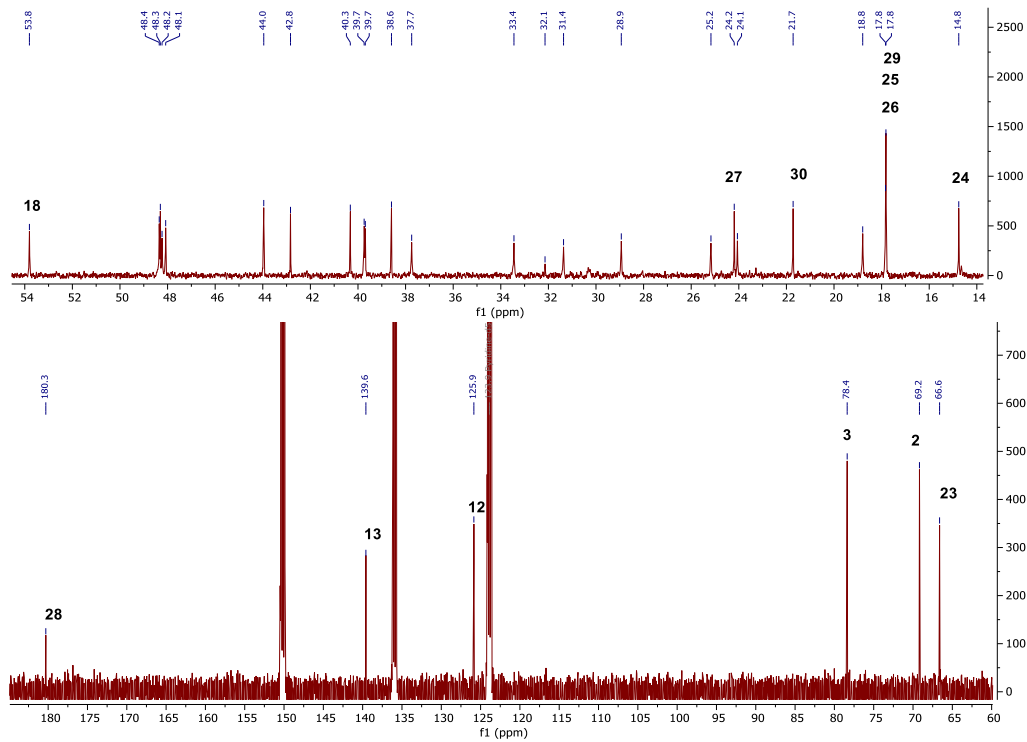
Position	δ_{C} (ppm)	δ_{H} (ppm), (J in Hz)
1	48.2 t	2.28 ^{b)} ; 1.35 ^{b)}
2	69.2 d	4.26 ddd (9.9, 8.2, 4.1)
3	78.4 d	4.23 d (8.2)
4	44.0 s	-
5	48.1 d	1.82 ^{b)}
6	18.8 t	1.71 ^{b)} ; 1.41 ^{b)}
7	33.4 t	1.68 ^{b)} ; 1.33 ^{b)}
8	40.3 s	-
9	48.4 d	1.82 ^{b)}
10	38.6 s	-
11	24.1 t	2.00 ^{b)}
12	125.9 d	5.45 dd (5.8; 3.6)
13	139.6 s	-
14	42.8 s	-
15	28.9 t	2.29 ^{b)} ; 1.15 ^{b)}
16	25.2 t	2.05 ^{b)} ; 1.94 ^{b)}
17	48.3 s	-
18	53.8 d	2.61 d (11.3)
19	39.7 d	1.41 ^{b)}
20	39.7 d	0.98 ^{b)}
21	31.4 t	1.43 ^{b)} ; 1.34 ^{b)}
22	37.7 t	1.95 ^{b)}
23	66.6 t	4.21 d (10.1); 3.72 d (10.1)
24	14.8 q	1.05 s
25	17.8 q	1.05 s
26	17.8 q	1.05 s
27	24.2 q	1.13 s
28	180.3 s	-
29	17.8 q	0.96 d (6.4)
30	21.7 q	0.92 d (6.2)

a) Assignments are confirmed by 2D-COSY, HSQC, HMBC, and NOESY experiments.

b) Signal pattern was unclear due to overlapping.



Spectrum 7. ^1H -NMR spectrum of DD-GK-04



Spectrum 8. ^{13}C -NMR spectrum of DD-GK-04

3.3. Results of biological activity studies

3.3.1. Proliferative effects of DD-GK-S(74-168)-S(28-45) and the standardized extract of *C. asiatica* on MRC-5 cell line via MTT assay

The effects of DD-GK-S(74-168)-S(28-45), i.e. MA, and the standardized extract of *C. asiatica* on the proliferation of MRC-5 cell line were investigated by the MTT assay. Cells were treated with different concentrations (1, 5, 12.5, 25, 50, 100, 125, 150, 300, 1000 $\mu\text{g/ml}$) for 48 h and DMSO (0.2%) was used as control. Cell viability was calculated by reading absorbances at 570 nm using a plate reader. Cell viability (%) versus concentration graphs were drawn using the GraphPad Prism 8 software and were shown in Figures 30 and 31, respectively.

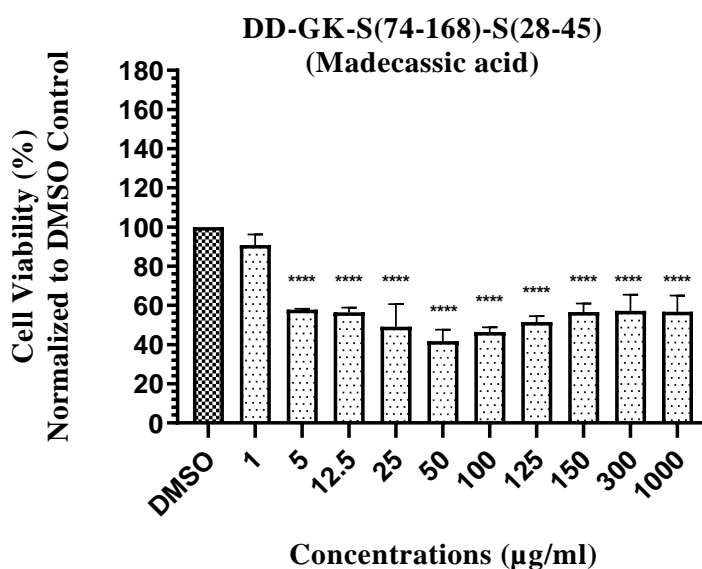


Figure 30. Proliferative effects of DD-GK-S(74-168)-S(28-45) on MRC-5 cell line at 48 h. Each concentration was repeated as a triplicate. DMSO was used as a solvent control. The significant differences of all concentrations versus DMSO were defined: * $p < 0.05$, ** $p < 0.01$, *** $p < 0.001$, **** $p < 0.0001$

It was observed that all of the tested concentrations caused a decrease in cell viability except (1 $\mu\text{g/ml}$) according to the obtained MTT assay results represented in

Figure 30. This might be due to the toxic effects of aglycone at relatively high concentrations ($\mu\text{g/ml}$), since the solubility problems may occur in pure compounds via the self-assembly nanoparticle formation. It can be concluded that most importantly cell damage occurred as a result of this aggregation. If there is any doubt about aggregation in solution, pure molecules could be applied with surfactants that will not affect the tests to avoid this.

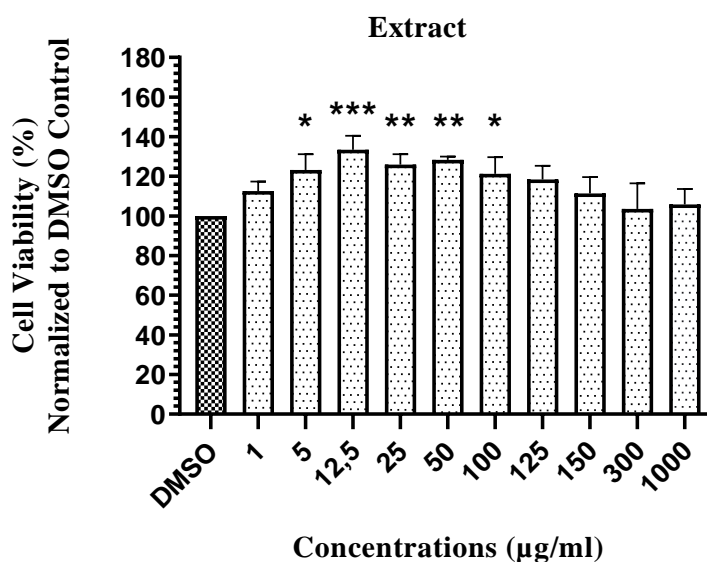


Figure 31. Proliferative effects of the standardized extract of *C. asiatica* on MRC-5 cell line at 48 h. Each concentration was repeated as a triplicate. DMSO was used as the solvent control. The significant differences of all concentrations versus DMSO were defined: * $p < 0.05$, ** $p < 0.01$, *** $p < 0.001$, **** $p < 0.0001$

The graphic results showed that the extract has a proliferative effect on cell viability at $\mu\text{g/ml}$ levels. In particular, significant increases were observed at concentrations of 5, 12.5, 25, 50, and 100 $\mu\text{g/ml}$. The viability of MRC-5 cells increased approximately by 40% at a concentration of 12.5 $\mu\text{g/ml}$, where the highest effect was reached. After carefully examining the graph, it was concluded that the viability rates started to decrease after the concentration of 12.5 $\mu\text{g/ml}$. Considering these data, it can be deduced that 12.5 $\mu\text{g/ml}$ concentration is an optimum concentration for the extract. One of the most important reasons for the proliferative effect of the extract at high concentrations may be due to the synergetic effects of the compounds. It was also thought that the extract did not have any dissolution problems because of the presence of surface-active agents such as saponin glycosides.

3.3.2. Proliferative effects of DD-GK-S(74-168)-S(28-45) and the standardized extract of *C. asiatica* on MRC-5 cell line via MTT assay under oxidative stress conditions

The proliferation effect of DD-GK-S(74-168)-S(28-45) and the standardized extract of *C. asiatica* on the MRC-5 cell line under oxidative stress induced by H₂O₂ were investigated by the MTT assay. Cells were treated at desired concentrations of aglycone (10, 30, 100 and 300 nM) and the extract (10, 30, 100, 300, 500 and 1000 ng/ml) for 24 h. DMSO (0.2%) and H₂O₂ were used as controls. Cell viability was calculated by reading absorbances at 570 nm using a plate reader. Cell viability (%) versus concentration graphs were drawn using the GraphPad Prism 8 software and were shown in Figures 32 and 33, respectively.

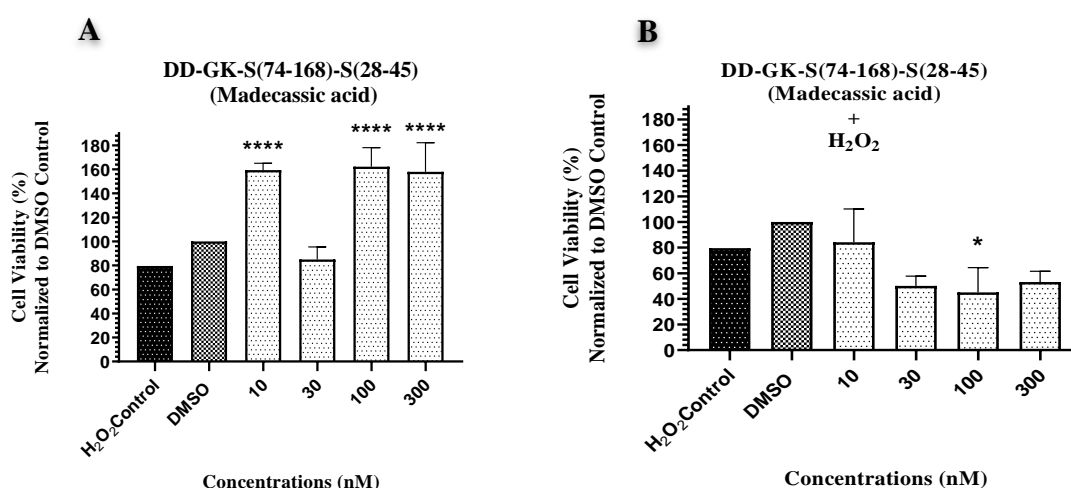


Figure 32. Proliferative effects of DD-GK-S(74-168)-S(28-45) on the MRC-5 cell line under oxidative stress conditions at 24 h. Pre-treatment before exposure to H₂O₂ **A**), Treatment after exposure to H₂O₂ **B**) Each concentration was repeated as a triplicate. DMSO and H₂O₂ were used as control. The significant differences of all concentrations versus H₂O₂ control were defined: *p < 0.05, **p < 0.01, ***p < 0.001, ****p < 0.0001

Oxidative stress induced by H₂O₂ reduced cell viability by 20% compared to those of the DMSO control. Based on the results from previous studies, it was determined that aglycone causes cell death due to toxic effects at $\mu\text{g/ml}$ concentration levels (Figure 30),

but it had a significant proliferative effect at nM concentration levels (Figure 32.A). Accordingly, it was understood that the pure molecules exhibited higher proliferative effects at low concentration ranges and did not cause cytotoxicity. The decrease in viability at 30 nM concentration may be due to an experimental error and/or the presence of colloidal structures formed by less soluble aglycones. Although these aggregates are invisible, they can provide such non-canonical responses. When Figure 32.B was examined, the toxic effects of oxidative stress induced by H₂O₂ were seen. Though the aglycone showed some resistance at 100 nM concentration, cell viability was reduced. The stress by H₂O₂-induced predominated on the pure molecule.

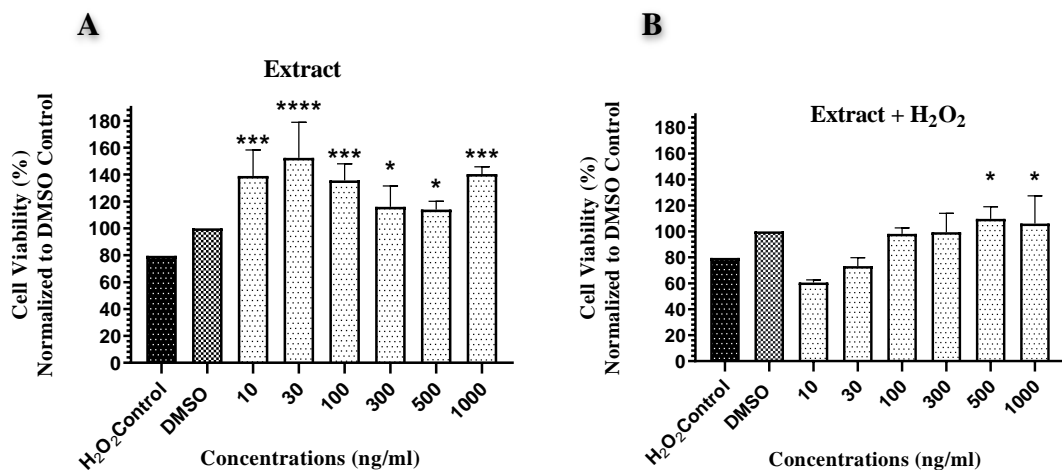


Figure 33. Proliferative effects of the standardized extract of *C. asiatica* on MRC-5 cell line under oxidative stress conditions at 24 h. Pre-treatment before exposure to H₂O₂ **A**), Treatment after exposure to H₂O₂ **B**) Each concentration was repeated as a triplicate. DMSO and H₂O₂ were used as control. The significant differences of all concentrations versus H₂O₂ control were defined: *p < 0.05, **p < 0.01, ***p < 0.001, ****p < 0.0001

The extract showed significant proliferative effects before being treated to exposure by H₂O₂ at ng/ml concentration levels. Reducing concentration levels did not affect the proliferative ability of the extract. Particularly, it almost reduplicated cell viability at 30 ng/ml concentration. Just as in Figure 31, non-canonical responses were observed again. Such non-canonical responses were seen in samples might be due to the reasons explained above. After being exposed to H₂O₂, surprisingly, it was noticed that the extract linearly developed a dose-dependent protection. The extract showed

statistically meaningful resistance to oxidative stress, especially at 500 and 1000 ng/ml concentrations, and showed a protective effect on cell viability. These findings showed that the standardized extract of *C. asiatica* could be useful preparation to harmful conditions in cellular metabolism such as oxidative stress. Based on these results, we concluded that the extract has protective effects against oxidative stress rather than reversing the damage due to oxidative stress.

3.3.3. Proliferative effects of major compounds (madecassoside, madecassic acid, asiaticoside, asiatic acid) on MRC-5 cell line via MTT assay

The effects of the major compounds (MS, MA, AS, AA) on the proliferation of MRC-5 cell lines were investigated using the MTT assay. Cells were treated with different concentrations (2, 10, 30, 100, 300 and 1000 nM) for 24 h. DMSO (0.2%) was used as a control. Cell viability was calculated by reading absorbances at 570 nm using a plate reader. Cell viability (%) versus concentration graphs were drawn using the GraphPad Prism 8 software and were shown in Figures 34 and 35, respectively.

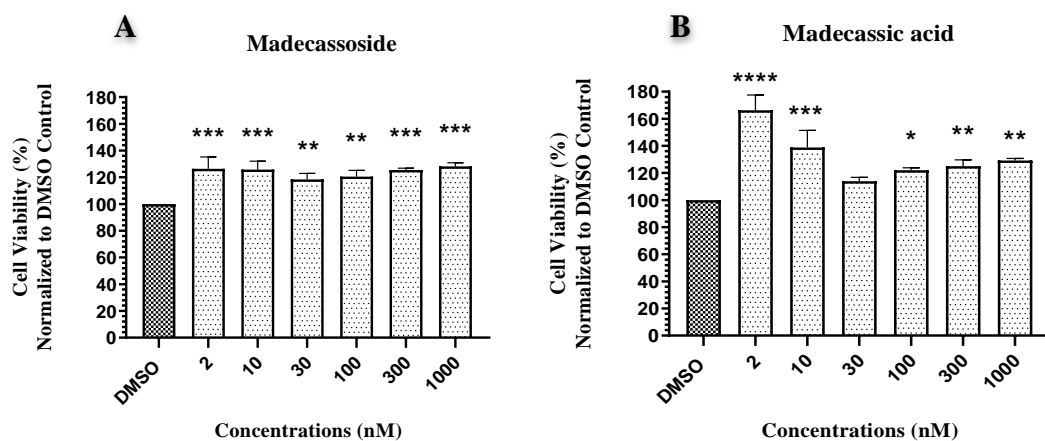


Figure 34. Proliferative effects of madecassoside (A) and madecassic acid (B) on MRC-5 cell line at 24 h. Each concentration was repeated as a triplicate. DMSO was used as control. The significant differences of all concentrations versus DMSO control were defined: * $p < 0.05$, ** $p < 0.01$, *** $p < 0.001$, **** $p < 0.0001$

MS and MA exhibited significant proliferative effects on the MRC-5 cell line. MS significantly and consistently increased viability by approximately 25% at all concentrations. Although, MS increased viability less compared to MA, its effectiveness at all concentrations may be an advantage providing a wide treatment range. Similarly, MA showed a proliferative effect at all concentrations (except 30 nM). Unlike MS, it showed a remarkably high proliferative effect at lower concentrations (about 60% at 2 nM). When the concentrations of MA increased, the effects on vitality decreased proportionally. Considering these results, possible effects should be observed by treating concentrations lower than 2 nM for MA.

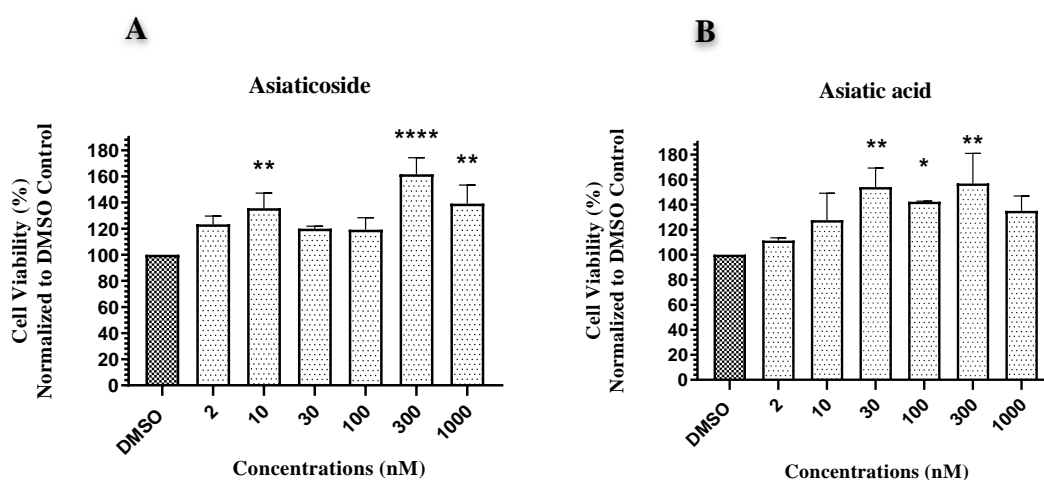


Figure 35. Proliferative effects of asiaticoside (A) and asiatic acid (B) on MRC-5 cell line at 24 h. Each concentration was repeated as a triplicate. DMSO was used as control. The significant differences of all concentrations versus DMSO control were defined: * $p < 0.05$, ** $p < 0.01$, *** $p < 0.001$, **** $p < 0.0001$

AS and AA at certain concentrations, especially 300 nM, significantly (about 50%) increased cell proliferation. The effects of AS increased in a dose-dependent manner. In contrast to MA, AA provided higher viability at higher doses. It should be discussed whether the absence/presence of the -OH group at C-6 position, which is the only difference between these two molecules, causes such a difference. Sugar moieties in glycosidic structures may interact with cells depending on the amount of their concentration, helping to accelerate cell migration. The graphs showed significant non-canonical responses (especially in AS). It was thought that the reason for such non-

canonical responses was due to colloidal structures formed by various compounds as above-mentioned or experimental errors rather than a compound-specific aggregation. Because glycosides such as AS and MS are more soluble but susceptible to actions of esterases to afford aglycones. Thus, further studies to explain colloid formation theory must be carried out.

3.3.4. Wound closure effects of madecassic acid, asiatic acid, and the standardized extract of *C. asiatica* on MRC-5 cell line via Scratch assay

Wound closure effects of MA, AA, and the standardized extract of *C. asiatica* on MRC-5 cell line were investigated by the Scratch assay. Cells were treated with different concentrations (2, 10, 30, 100, 300 nM, and ng/ml) for 36 h. DMSO (0.2%) was used as a control. Open wounds were regularly examined and photographed under a microscope at 24 and 36 h. Photographs were compared at certain times and closure percentages were calculated using the ImageJ and TScratch softwares. Wound closure (%) versus concentration graphs at 24 h were drawn on GraphPad Prism 8 software and shown in Figures 36, 37, and 38, respectively.

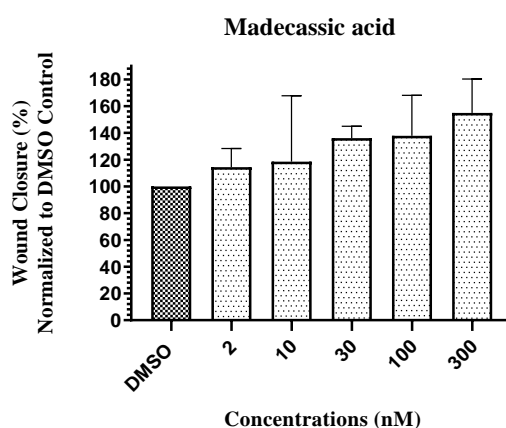


Figure 36. Wound closure effect of madecassic acid on MRC-5 cell line at 24 h. Each concentration was repeated as a triplicate. DMSO was used as control. The significant differences of all concentrations versus DMSO control were defined: * $p < 0.05$, ** $p < 0.01$, *** $p < 0.001$, **** $p < 0.0001$

It was observed that the madecassic acid, a known agent for its wound healing and proliferative effects, did not afford significant results on the opened wounds of MRC-5 cell line compared to the control. When the graph was examined, although it seemed to close the wound approximately 50% faster than the control, especially at the 300 nM concentration, its high standard deviation rendered the values to be meaningless. While MA showed significant effects on cell proliferation as in Figures 32.A and 34.B, the reason for not significant effects to cell migration on the scratch assay may be due to the factors mentioned previously. In further studies, administrating aglycones to the cell medium together with surfactants may facilitate in overcoming such problems and obtaining more consistent results.

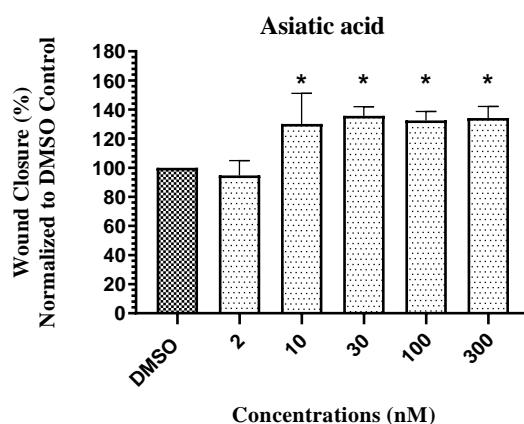


Figure 37. Wound closure effects of asiatic acid on MRC-5 cell line at 24 h. Each concentration was repeated as a triplicate. DMSO was used as control. The significant differences of all concentrations versus DMSO control were defined: * $p < 0.05$, ** $p < 0.01$, *** $p < 0.001$, **** $p < 0.0001$

Unsurprisingly, AA increased the cell migration in a dose-dependent manner (approximately 35%). Consistent with Figure 35.B, no effect was seen at 2 nM concentration, while the positive effects were observed at 30, 100, and 300 nM concentrations. Having superior lipophilic properties might be contributing to bioavailability; however, the above-mentioned explanation of colloidal particle formation becomes contradictory, and the results should be considered with intensely investigated further data. Besides these, it was also noteworthy to mention that while AA exhibited approximately 50% proliferation on MTT assay, it increased the cell migration rate by only 35%.

The extract covered the wound area by approximately 40% in the concentration range of 10 to 300 nM. Similar to Figure 33.A, while the effect reached its highest value at 10 and 30 nM concentrations, a slight reduction in the effects was detected at 300 nM concentration. While it shows significant effects even at μg levels, the low effects at 300 nM concentration were surprising. These results which both μg and ng levels are encouraging to perform further studies.

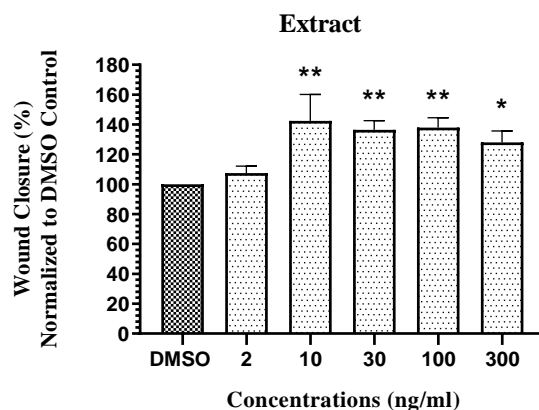


Figure 38. Wound closure effect of the standardized extract of *C. asiatica* on MRC-5 cell line at 24 h. Each concentration was repeated as a triplicate. DMSO was used as control. The significant differences of all concentrations versus DMSO control were defined: * $p < 0.05$, ** $p < 0.01$, *** $p < 0.001$, **** $p < 0.0001$

It is rational to state that the extract exhibits more consistent and meaningful results compared to the pure molecules, which might be because of aforementioned assumptions. Additionally, it should be taken into consideration that there are many compounds of minute quantities in the extract, which could influence the potency in bioactivity screening studies.

3.3.5. The effects of major compounds and the standardized extract of *C. asiatica* on hTERT protein level on HEK293T cell line via Immunoblotting assay

The effects of four major compounds (MS, MA, AS, AA) and the standardized extract of *C. asiatica* on hTERT protein level were examined using the immunoblotting

method. HEK293 cells were treated with different concentrations of major compounds (3, 30, 100, 300 nM) and the extract (10, 30, 100, 300, 1000 ng/ml) for 24 h. In chemiluminescence imaging, bands displayed on the PVDF membrane at approximately 120 kDa refer to the presence of the hTERT protein. β -actin and GAPDH were used as loading controls corresponding to bands at 42 kDa and 36 kDa, respectively. Densitometric analyzes of Western Blot scanning were performed using ImageJ software. Integral areas at each concentration were determined on ImageJ separately for hTERT and loading controls (GAPDH/ β -actin). The obtained values were calculated using Microsoft Excel software, the calculated values were normalized to DMSO control and graphs plotted relative level of hTERT versus concentration.

Western Blot gel images and densitometric analysis graphs obtained for major compounds (MS, MA, AS, AA) and the extract were given in Figures 39, 40, 41, 42, and 43, respectively.

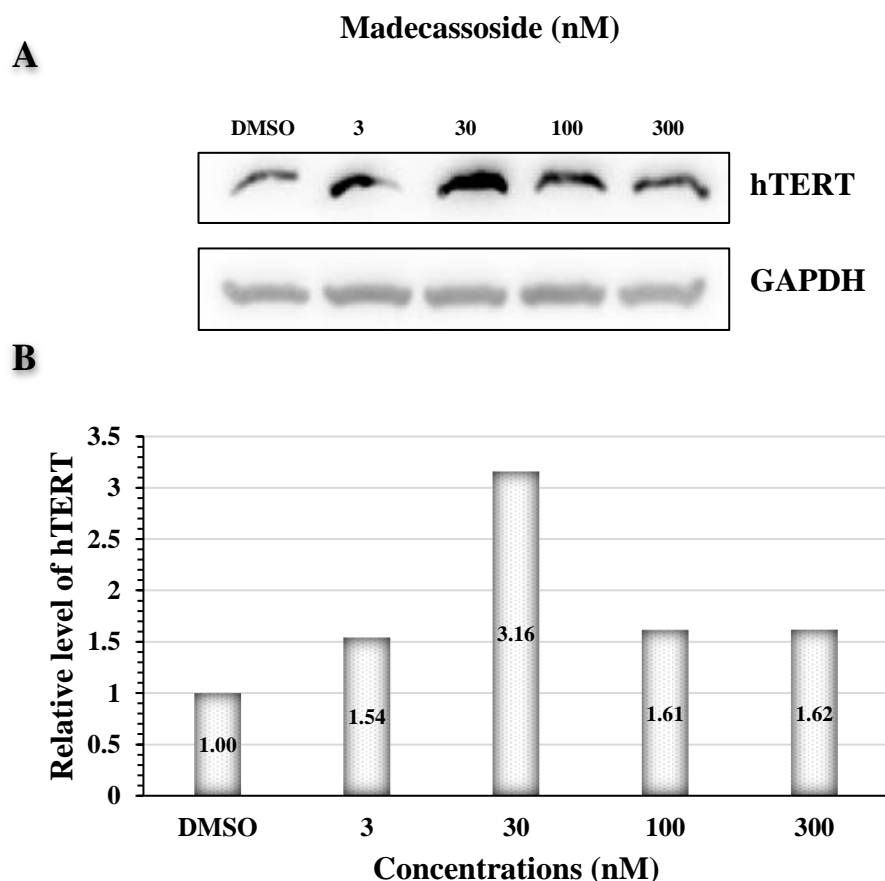


Figure 39. Effects of MS on hTERT protein level at 24 h. Each concentration was repeated as a triplicate. GAPDH was used as the loading control. DMSO was used as the control. A) Western blot gel image, B) Densitometric analysis graph

It was observed that HEK293 cells treated with DMSO used as control, increased the hTERT protein level to a certain extent. This is an expected result that cells endogenously affect the hTERT protein level. When the Western Blot gel image and its densitometric analysis graph were examined, MA increased the hTERT protein level at all concentrations compared to the control. Particularly, the thick band observed at the 30 nM concentration exhibited almost three times as high activity as the other concentrations. It was also highly consistent with the proliferation results in Figure 34.A.

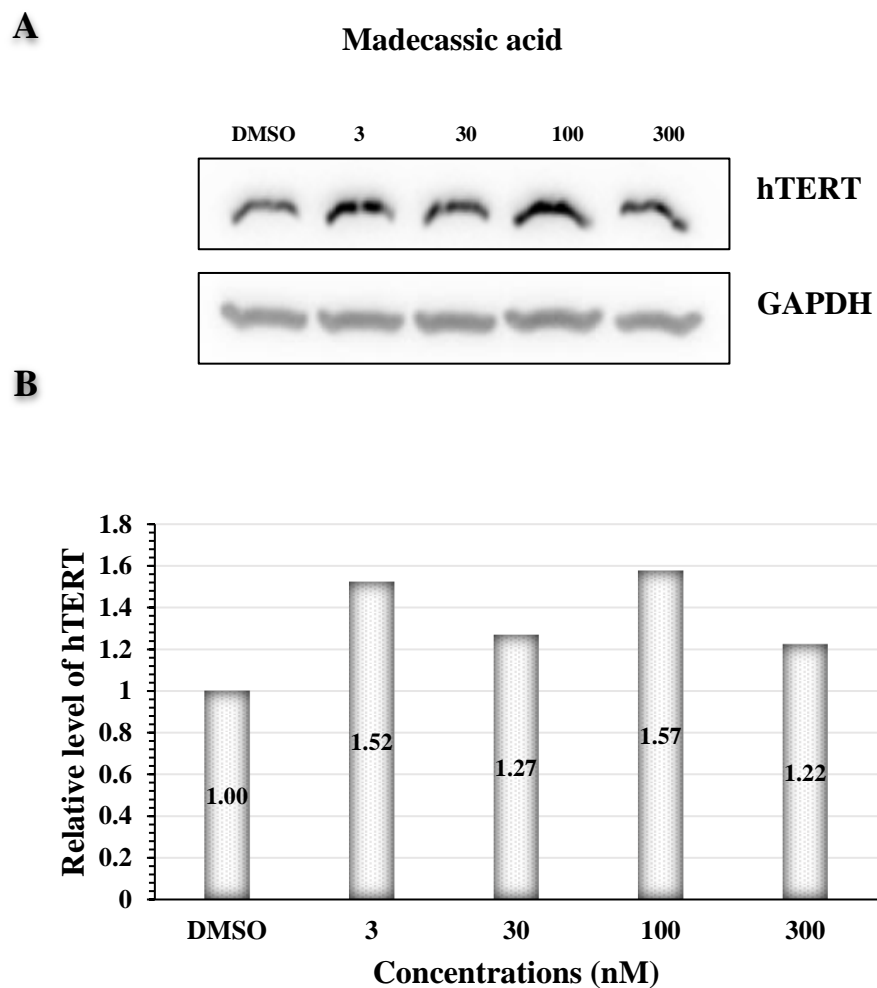


Figure 40. Effects of MA on hTERT protein level at 24 h. Each concentration was repeated as a triplicate. GAPDH was used as the loading control. DMSO was used as the control. **A)** Western blot gel image, **B)** Densitometric analysis graph.

Although MA slightly increased hTERT protein level at each concentration, no significant effects were observed. It might be necessary to further reduce the dose range to obtain greater effects with MA. Similar to the proliferation results, non-canonical responses were observed again.

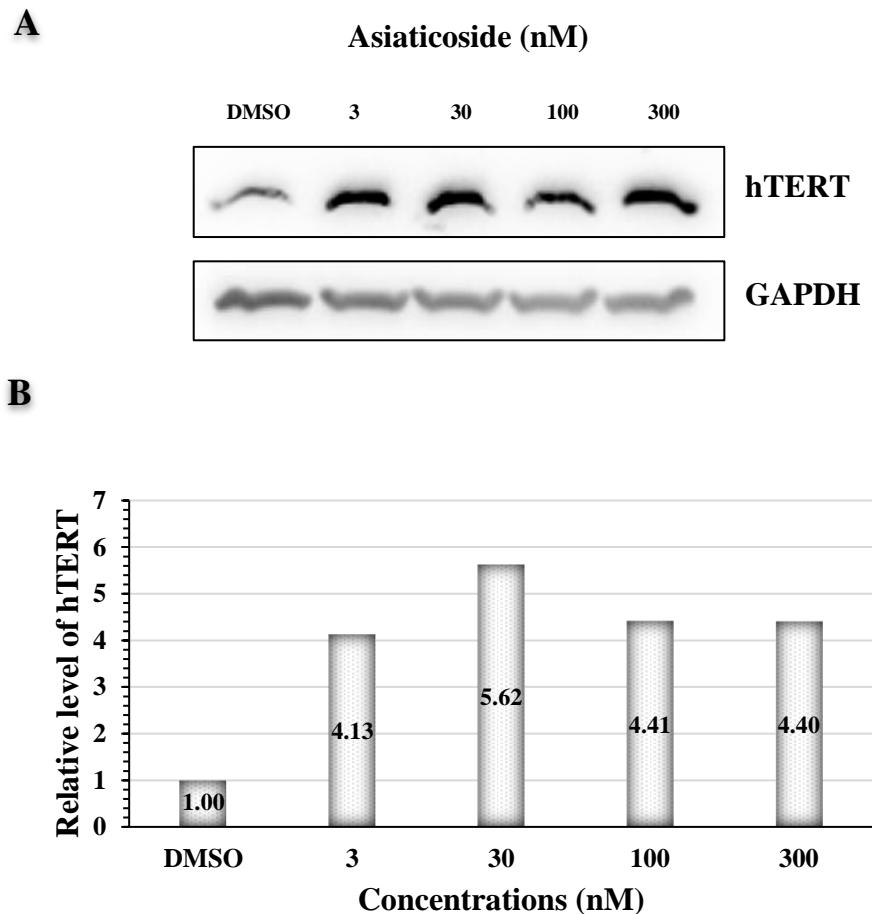


Figure 41. Effect of AS on hTERT protein level at 24 h. Each concentration was repeated as a triplicate. GAPDH was used as the loading control. DMSO was used as the control. **A)** Western blot gel image, **B)** Densitometric analysis graph

AS showed high activity (4 to 5 fold) in comparison to the DMSO control at all concentrations. Specifically, the hTERT protein level increased 5.62-fold versus the control at 30 nM concentration. These valuable data also supported the proliferation data in Figure 35.A. Non-canonical responses seen in proliferation data were not seen in the

immunoblotting assay. It was also noteworthy that higher effects of both AS and MS glycosides occurred at 30 nM concentrations.

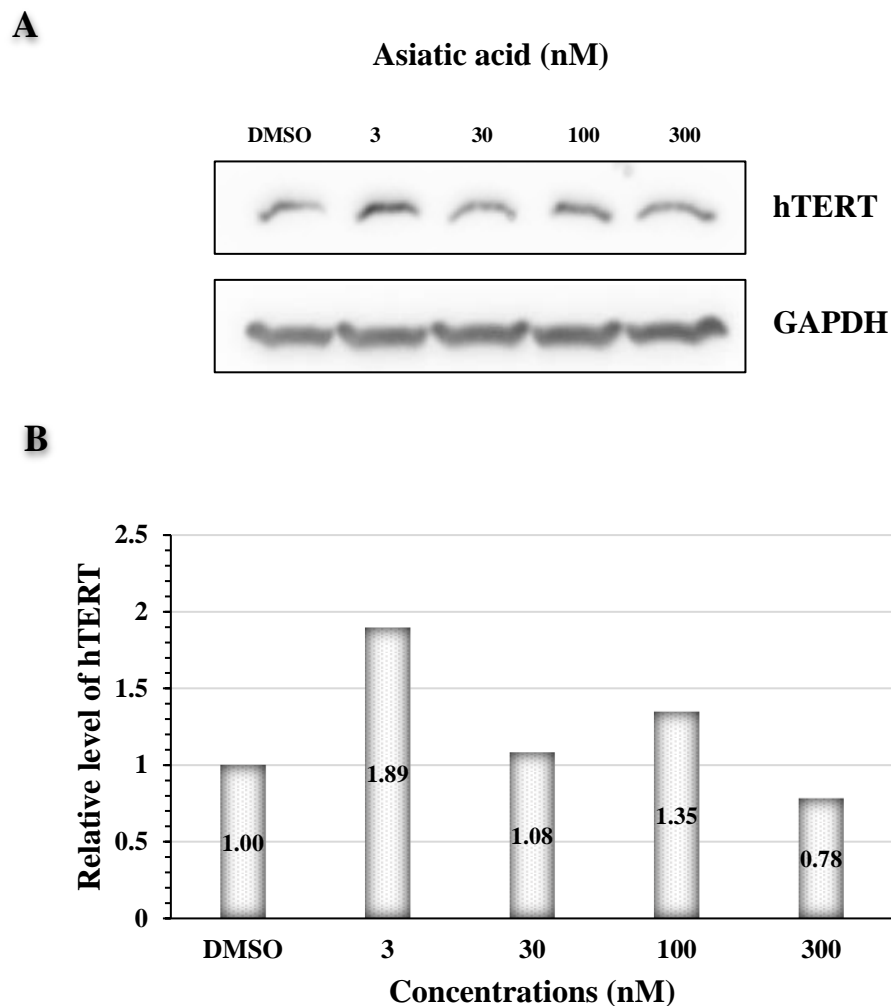


Figure 42. Effects of AA on hTERT protein level at 24 h. Each concentration was repeated as a triplicate. GAPDH was used as the loading control. DMSO was used as the control. **A)** Western blot gel image, **B)** Densitometric analysis graph

AA did not have a significant effect on the hTERT protein level like MA. It only showed an approximately two-fold (1.89) induction against DMSO at 3 nM concentration. Surprisingly, it showed activity at higher doses in proliferation and wound closure studies, while more significant activity at the lowest concentrations in the immunoblotting assay. The reason AA showed lower activity than expected might be due to the solubility issues again and/or not being held on to the loading control sufficiently.

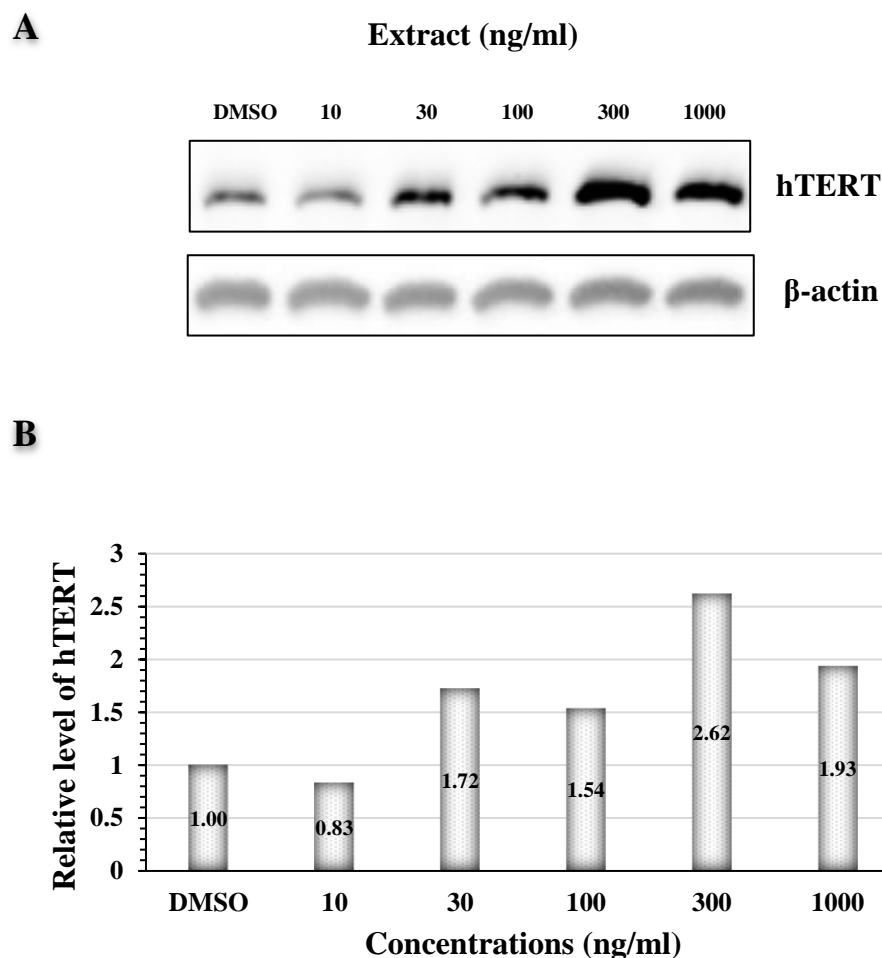


Figure 43. Effects of the standardized extract of *C. asiatica* on hTERT protein level at 24 h. Each concentration was repeated as a triplicate. β -actin was used as the loading control. DMSO was used as the control. **A)** Western bot gel image, **B)** Densitometric analysis graph

Unlike other samples, the concentration range of the extract was arranged between 10 and 1000 ng/ml. Observing lower activity than the control at the 10 ng/ml concentration was most likely due to an experimental error or failure to bind to the loading control. When the gel images were examined, it was seen that as the concentration of the extract increased, the hTERT protein levels were up directly in a dose-dependent manner. The peak value was observed at 300 ng/ml (2.62-fold) concentration. The reason for the decrease in the hTERT protein level activity at 1000 ng/ml concentration could be due to exceeding the optimum concentration range. The significant effects of the standardized extract at higher concentrations were also consistent with the results obtained in previous biological activity studies (Figure 31, 33.A, and 39). Considering these results, it was

demonstrated that the standardized extract of *C. asiatica* increased the hTERT protein level in a dose-dependent manner.

Saponin glycosides (MS and AS) contain an ester bond at C-28 and three sugar moieties extending from this position. Ester bonds can easily be cleaved by esterase enzymes (Shao et al., 2017). The standardized extract of *C. asiatica* has many compounds glycosidic in nature. When treating the extract to a cell medium, sugar moieties could rise solubility and thus help transportation of the extract through the cell membrane. The esterase enzymes in the cell might have easily cleave the ester bond transforming the compounds into aglycone forms. The aglycones and their synergistic interactions upon reaching the cell might be leading to higher activity. However, when aglycones were treated directly into the cell medium, non-canonical responses can occur as colloidal structures forming. Eventually, it is proposed herein that the sugar moieties do not have any effect on the biological activity; however, they assist to get over solubilization and so aggregation issues.

CHAPTER 4

CONCLUSION

Traditionally used *C. asiatica* plant as a well-known medicine has various pharmacological benefits including anti-diabetic, anti-bacterial, anti-inflammatory, anti-cancer, anti-oxidant, cognitive function, hepatoprotective, and wound healing. Many *in vitro* and *in vivo* studies have proven that *C. asiatica* has beneficial effects on the body's wound healing process. Based on these studies, a number of commercial wound healing products have been developed and introduced to the market worldwide (Chandrika & Kumara., 2015; Azis et al., 2017). Recent findings have shown that the standardized extract of *C. asiatica* might be a potential telomerase activator (Tsoukalas et al., 2019). The remarkable biological activities of the standardized extract of *C. asiatica* are thought to be originating from two major triterpenic saponins (MS and AS) and their aglycones (MA and AA), constituting more than 80% of its phytochemical composition.

In this thesis, pure major saponins (MS and AS) were isolated from the standardized powder extract of *C. asiatica* using chromatographic methods, and their aglycones (MA and AA) were prepared by alkaline hydrolysis reaction followed by purification. The chemical structures of the purified compounds were established by spectroscopic methods (1D-, 2D-NMR, and HR-ESI-MS). *In vitro* MTT and scratch assay's were performed on the purified compounds and the standardized extract of *C. asiatica* using MRC-5 cell line to examine the proliferative and cell migration effects, which provide information towards the treatment of skin-related disorders. Afterward, to examine the potential of *C. asiatica* as a telomerase activator, the effects of four pure compounds, and the standardized extract of *C. asiatica* on the hTERT protein level, a telomerase marker, were investigated by *in vitro* immunoblotting assay on HEK293T cell line.

All flow charts and amounts of the fractions isolated from the standardized extract of *C. asiatica* by chromatographic methods were given in Figures 11 and 14. The amounts of the compounds, their chemical structures, and the codes of the fractions used in biological activity studies were shown in Table 8. Since it is a growth-promoted cell line known to be frequently used *in vitro* wound healing experiments, cell proliferation and

migration studies have been conducted with MRC-5 cell line. HEK293 is used on immunoblotting studies because it is a cell line used as a gold model in molecule screenings towards telomerase activation. The level of hTERT protein does not directly prove telomerase activation, but it is suggested to be one of the key markers.

MS, a triterpenic saponoside, consistently increased the proliferation of the MRC-5 cell line at all concentrations (approximately 25%) compared to control (DMSO). While it slightly increased the hTERT protein level on HEK293 cell line at all concentrations, the increase was 3.16-fold at 30 nM concentration. AS significantly increased cell proliferation at certain concentrations (10, 300, and 1000 nM, about 50%), but exhibited non-canonical responses at 30 and 100 nM concentrations. Although it is suggested to be a bioavailable compound, the reason for such non-canonical results may be due to the concentration-specific aggregation behavior of AS or may indicate a mistake during experiments. Asiaticoside (AS) strikingly increased the hTERT protein level of the HEK293 cell line by more than 4-fold at each concentration. The fact that the protein level increased 5.62-times at 30 nM, the highest activity observed, was quite valuable data supporting the potential of AS to be a telomerase activator.

One of the aglycones, MA, increased cell proliferation by approximately 60% at low concentrations (2, and 10 nM), but caused cell death by generating a toxic effect at $\mu\text{g/ml}$ concentration levels. Surprisingly, it did not increase the cell migration significantly on scratch assay studies versus the control group. It is hypothesized that the aglycone backbone forms colloidal structures that are invisible in the cell medium, leading to non-canonical responses. MA did not show any protective effects under H_2O_2 -induced oxidative stress conditions. Although hTERT level slightly increased, the effects were found to be low. The other aglycone derivative, AA, increased proliferation and migration dose-dependently on the MRC-5 cell line (approximately 50%) compared to MA. However, it similarly showed no significant effect on the hTERT protein level. One of the notable results of this thesis was that the effects of aglycone derivatives were lower than those of glycosides and the standardized extract.

The standardized extract of *C. asiatica* showed proliferative effects on MRC-5 cell line at concentrations ranging from 5 to 100 $\mu\text{g/ml}$. It also provided statistically meaningful results at 500-1000 ng/ml concentrations under H_2O_2 -induced oxidative stress conditions. Although the extract was not effective to reverse the stress conditions, it was found to be cell protective. It accelerated cell migration in a dose-dependent manner (approximately 40%), and showed consistent data at all concentrations. The extract also

increased the hTERT protein level significantly on HEK293 cell line at each concentration (except 10 ng/ml). It was seen that hTERT protein level was enhanced up to 3-times (2.62) compared to the control at 300 ng/ml. The standardized extract exhibited significant activities in all biological activity screenings, providing more consistent results than pure major molecules. However, the fact that it did not display a high effect on the increase of hTERT protein level like saponosides was an important finding in terms of understanding the effective fractions/components of *C. asiatica*.

As mentioned above, the standardized extract of *C. asiatica* and glycosides (MS and AS) revealed higher activities and more consistent results than aglycone derivatives (MA and AA). In fact, aglycones that are generally treated in low concentration ranges are expected to exhibit significant activities. Based on the obtained results and our group's preliminary screenings with other members of triterpenoids, it is thought that the lower and non-canonical activities of the aglycones might be due to the formation of colloidal particles mentioned earlier. A reasonable explanation for the glycosides exhibiting more favorable results than aglycone derivatives would be: they are more soluble due to the presence of sugar moieties in their structures preventing aggregate formation, and increasing their bioavailabilities. Another hypothesis is: there are minor quantities of the aglycones in the extract, aggregation of which could be prevented due to the presence of saponin glycosides as surface-active agents, in turn increasing the bioavailability. If it is so, the sugar moieties do not contribute to biological activities. On the other hand, polar monodesmosidic saponin glycosides (AS and MS) possessing ester bond between C-28 and sugar chain are susceptible to the action of esterase enzymes that results in cleavage and in turn formation of aglycones. Thus, it is proposed that all biological effects are due to aglycones, and their glycosidic forms are similar to pro-drugs responsible for in solution stability and transport. Additionally, it should be taken into consideration that there are many compounds of minute quantities in the extract, which could be highly active and enhance the potency in screening studies. One should also keep in mind that major glycosides and the other minor components of the extract may have synergistic effects from bioactivity point of view. This synergism might enable the extract to exert higher activities even over a wide range of concentrations.

Although the standardized extract of *C. asiatica* and pure major compounds were administered without any formulation, a number of valuable results were obtained. To have deep insight, further studies are warranted especially to optimize the activities of the extract, crude fractions as well as the major compounds by developing various

formulations. In addition, to shed light on the mechanism of action not only the pure compounds but combinations of them need to be studied *in vitro* and *in vivo* utilizing different models of tissue regeneration and aging. Additively, new target-specific derivatives of saponins/sapogenins originating from *C. asiatica* should be synthesized using methods such as semi-synthesis, biotransformation as well as click chemistry, and the effects of new derivatives on telomerase activation should be examined. Especially, the biotransformation studies will also provide valuable information regarding metabolism products of the triterpenoids from *C. asiatica*, including possible esterase metabolites.

Lastly, the hTERT protein level results reveal that overriding basis of *C. asiatica* products for their wound healing properties, could likely be deriving from telomerase activation. The fact that there are a few telomerase activators available in the market makes telomerase activation studies on *C. asiatica* even more meaningful. It is clear that a new formulation with optimized telomerase activation can be produced from the standardized extract of *C. asiatica*, and its major compounds (MS, AS, MA, and AA) might have significant market values as single entities or in combination. However, studies on telomerase activation of *C. asiatica* are still very limited, and further mechanistic studies are especially necessary. This study, which is performed on HEK293T cell line to detect the hTERT protein level, is the first one with *C. asiatica*. Our results are believed to have significant impact in the field particularly encouraging future research.

REFERENCES

- Ahmed, A. S., Taher, M., Mandal, U. K., Jaffri, J. M., Susanti, D., Mahmood, S., & Zakaria, Z. A. (2019). Pharmacological properties of *Centella asiatica* hydrogel in accelerating wound healing in rabbits. *BMC Complementary and Alternative Medicine*, 19(1), 1–7.
- Alfarra, H. Y., & Omar, M. N. (2013). *Centella asiatica*: from folk remedy to the medicinal biotechnology-a state revision. *International Journal of Biosciences*, 3(6), 49–67.
- Amiri, M. S., Yazdi, M. E. T., & Rahnama, M. (2021). Medicinal plants and phytotherapy in Iran: Glorious history, current status and future prospects. *Plant Science Today*, 8(1), 95–111.
- Anulika, N. P., Ignatius, E. O., Raymond, E. S., Osasere, O.-I., & Abiola, A. H. (2016). The chemistry of natural product: Plant secondary metabolites. *Int. J. Technol. Enhanc. Emerg. Eng. Res*, 4(8), 1–9.
- Augustin, J. M., Kuzina, V., Andersen, S. B., & Bak, S. (2011). Molecular activities, biosynthesis and evolution of triterpenoid saponins. *Phytochemistry*, 72(6), 435–457.
- Azerad, R. (2016). Chemical structures, production and enzymatic transformations of sapogenins and saponins from *Centella asiatica* (L.) Urban. *Fitoterapia*, 114, 168–187.
- Azis, H. A., Taher, M., Ahmed, A. S., Sulaiman, W. M. A. W., Susanti, D., Chowdhury, S. R., & Zakaria, Z. A. (2017). *In vitro* and *In vivo* wound healing studies of methanolic fraction of *Centella asiatica* extract. *South African Journal of Botany*, 108, 163–174. <https://doi.org/https://doi.org/10.1016/j.sajb.2016.10.022>
- Babu, T. D., Kuttan, G., & Padikkala, J. (1995). Cytotoxic and anti-tumour properties of certain taxa of Umbelliferae with special reference to *Centella asiatica* (L.) Urban. *Journal of Ethnopharmacology*, 48(1), 53–57.
- Basu, N., & Rastogi, R. P. (1967). Triterpenoid saponins and sapogenins. *Phytochemistry*, 6(9), 1249–1270.
- Beserra, F. P., Rozza, A. L., Vieira, A. J., Gushiken, L. F. S., & Pellizzon, C. H. (2016). Antiulcerogenic compounds isolated from medicinal plants. In *Studies in Natural Products Chemistry* (Vol. 47, pp. 215–234). Elsevier.

- Bonte, F., Dumas, M., Chaudagne, C., & Meybeck, A. (1994). Influence of asiatic acid, madecassic acid, and asiaticoside on human collagen I synthesis. *Planta Medica*, 60(02), 133–135.
- Bradwejn, J., Zhou, Y., Koszycki, D., & Shlik, J. (2000). A double-blind, placebo-controlled study on the effects of Gotu Kola (*Centella asiatica*) on acoustic startle response in healthy subjects. *Journal of Clinical Psychopharmacology*, 20(6), 680–684.
- Brinkhaus, B., Lindner, M., Schuppan, D., & Hahn, E. G. (2000). Chemical, pharmacological and clinical profile of the East Asian medical plant *Centella asiatica*. *Phytomedicine*, 7(5), 427–448.
- Butler, M. S. (2004). The role of natural product chemistry in drug discovery. *Journal of Natural Products*, 67(12), 2141–2153.
- Chandrika, U. G., & Kumara, P. A. A. S. P. (2015). Gotu Kola (*Centella asiatica*): nutritional properties and plausible health benefits. *Advances in Food and Nutrition Research*, 76, 125–157.
- Cheng, C. L., Guo, J. S., Luk, J., & Koo, M. W. L. (2004). The healing effects of Centella extract and asiaticoside on acetic acid induced gastric ulcers in rats. *Life Sciences*, 74(18), 2237–2249.
- Chin, G., & Lansing, C. S. (2004). *The biological sciences collaboratory*. Pacific Northwest National Lab.(PNNL), Richland, WA (United States).
- Cooper, R., & Nicola, G. (2014). *Natural products chemistry: sources, separations and structures*. CRC press.
- Das, A. J. (2011). Review on nutritional, medicinal and pharmacological properties of *Centella asiatica* (Indian pennywort). *Journal of Biologically Active Products from Nature*, 1(4), 216–228.
- Das, T. K., Banerjee, D., Chakraborty, D., Pakhira, M. C., Shrivastava, B., & Kuhad, R. C. (2012). Saponin: Role in animal system. *Veterinary World*, 5(4), 248.
- Dias, D. A., Urban, S., & Roessner, U. (2012). A historical overview of natural products in drug discovery. *Metabolites*, 2(2), 303–336.
- Du, Q., Jerz, G., Chen, P., & Winterhalter, P. (2004). Preparation of ursane triterpenoids from *Centella asiatica* using high speed countercurrent chromatography with step-gradient elution. *Journal of Liquid Chromatography & Related Technologies*, 27(14), 2201–2215.
- Faizal, A., & Geelen, D. (2013). Saponins and their role in biological processes in plants.

- Phytochemistry Reviews*, 12(4), 877–893.
- George, M., & Joseph, L. (2009). Anti-allergic, anti-pruritic, and anti-inflammatory activities of *Centella asiatica* extracts. *African Journal of Traditional, Complementary and Alternative Medicines*, 6(4).
- Giardini, M. A., Segatto, M., Da Silva, M. S., Nunes, V. S., & Cano, M. I. N. (2014). Telomere and telomerase biology. *Progress in Molecular Biology and Translational Science*, 125, 1–40.
- Gnanapragasam, A., Ebenezar, K. K., Sathish, V., Govindaraju, P., & Devaki, T. (2004). Protective effect of *Centella asiatica* on antioxidant tissue defense system against adriamycin induced cardiomyopathy in rats. *Life Sciences*, 76(5), 585–597.
- Gohil, K. J., Patel, J. A., & Gajjar, A. K. (2010). Pharmacological review on *Centella asiatica*: a potential herbal cure-all. *Indian Journal of Pharmaceutical Sciences*, 72(5), 546.
- Guo, S. al, & DiPietro, L. A. (2010). Factors affecting wound healing. *Journal of Dental Research*, 89(3), 219–229.
- Haralampidis, K., Trojanowska, M., & Osbourn, A. E. (2002). Biosynthesis of triterpenoid saponins in plants. *History and Trends in Bioprocessing and Biotransformation*, 31–49.
- Hengjumrut, P., Anukunwithaya, T., Tantisira, M. H., Tantisira, B., & Khemawoot, P. (2018). Comparative pharmacokinetics between madecassoside and asiaticoside presented in a standardised extract of *Centella asiatica*, ECa 233 and their respective pure compound given separately in rats. *Xenobiotica*, 48(1), 18–27.
- Hiyama, E., & Hiyama, K. (2007). Telomere and telomerase in stem cells. *British Journal of Cancer*, 96(7), 1020–1024.
- Hostettmann, K., & Terreaux, C. (2000). Medium-pressure liquid chromatography. *Wilson ID (Chief Ed) Encyclopedia of Separation Science*. Academic, San Diego, 3296–3303.
- Inamdar, P. K., Yeole, R. D., Ghogare, A. B., & De Souza, N. J. (1996). Determination of biologically active constituents in *Centella asiatica*. *Journal of Chromatography A*, 742(1–2), 127–130.
- James, J. T., & Dubery, I. A. (2009). Pentacyclic triterpenoids from the medicinal herb, *Centella asiatica* (L.) Urban. *Molecules*, 14(10), 3922–3941.
- Jamwal, K., Bhattacharya, S., & Puri, S. (2018). Plant growth regulator mediated consequences of secondary metabolites in medicinal plants. *Journal of Applied*

- Research on Medicinal and Aromatic Plants*, 9, 26–38.
- Jeong, B.-S. (2006). Structure-activity relationship study of asiatic acid derivatives for new wound healing agent. *Archives of Pharmacal Research*, 29(7), 556–562.
- Kai, G., Pan, J., Yuan, C., & Yuan, Y. (2008). Separation of madecassoside and madecassic acid isomers by high performance liquid chromatography using β -cyclodextrin as mobile phase additive. *Bulletin of the Korean Chemical Society*, 29(3), 551–554.
- Kräutler, B., & Sahu, N. P. (2008). *Fortschritte der Chemie organischer Naturstoffe/Progress in the Chemistry of Organic Natural Products* (Vol. 89). Springer Science & Business Media.
- Lee, J., Jung, E., Kim, Y., Park, J., Park, J., Hong, S., Kim, J., Hyun, C., Kim, Y. S., & Park, D. (2006). Asiaticoside induces human collagen I synthesis through TGF β receptor I kinase (T β RI kinase)-independent Smad signaling. *Planta Medica*, 72(04), 324–328.
- Lin, X., Huang, R., Zhang, S., Wei, L., Zhuo, L., Wu, X., Tang, A., & Huang, Q. (2013). Beneficial effects of asiaticoside on cognitive deficits in senescence-accelerated mice. *Fitoterapia*, 87, 69–77.
- Mahato, S. B. (2000). Bioactive saponins from some plants used in Indian traditional medicine. In *Saponins in Food, Feedstuffs and Medicinal Plants* (pp. 13–23). Springer.
- Mahato, S. B., Sarkar, S. K., & Poddar, G. (1988). Triterpenoid saponins. *Phytochemistry*, 27(10), 3037–3067.
- Mangas, S., Moyano, E., Hernandez-Vazquez, L., & Bonfill, M. (2009). *Centella asiatica* (L) Urban: An updated approach. *Plant Secondary Terpenoids, Research Signpost*, 37(661), 2.
- Mathur, A., Mathur, A. K., Yadav, S., & Verma, P. (2007). *Centella asiatica* (L.) Urban- Status and scope for commercial cultivation. *J Med Arom Plant Sci*, 129, 151–162.
- Mazid, M., Khan, T. A., & Mohammad, F. (2011). Role of secondary metabolites in defense mechanisms of plants. *Biology and Medicine*, 3(2), 232–249.
- Milgate, J., & Roberts, D. C. K. (1995). The nutritional & biological significance of saponins. *Nutrition Research*, 15(8), 1223–1249.
- Moore, D., Robson, G. D., & Trinci, A. P. J. (2020). *21st century guidebook to fungi*. Cambridge University Press.
- Moses, T., Papadopoulou, K. K., & Osbourn, A. (2014). Metabolic and functional

- diversity of saponins, biosynthetic intermediates and semi-synthetic derivatives. *Critical Reviews in Biochemistry and Molecular Biology*, 49(6), 439–462.
- Nalini, K., Aroor, A. R., Rao, A., & Karanth, K. S. (1992). Effect of *Centella asiatica* fresh leaf aqueous extract on learning and memory and biogenic amine turnover in albino rats. *Fitoterapia*, 63(3), 231–238.
- Nasir, M. N., Habsah, M., Zamzuri, I., Rammes, G., Hasnan, J., & Abdullah, J. (2011). Effects of asiatic acid on passive and active avoidance task in male Sprague–Dawley rats. *Journal of Ethnopharmacology*, 134(2), 203–209.
- Netala, V. R., Ghosh, S. B., Bobbu, P., Anitha, D., & Tarte, V. (2015). Triterpenoid saponins: a review on biosynthesis, applications and mechanism of their action. *International Journal of Pharmacy and Pharmaceutical Sciences*, 24–28.
- Oleszek, W. A. (2002). Chromatographic determination of plant saponins. *Journal of Chromatography A*, 967(1), 147–162.
- Osborn, A. E. (2003). Saponins in cereals. *Phytochemistry*, 62(1), 1–4.
- Pan, J., Kai, G., Yuan, C., & Jin, R. (2007). Separation and determination of the structural isomers of madecassoside by HPLC using β -cyclodextrin as mobile phase additive. *Chromatographia*, 66(1), 121–123.
- Pan, S.-Y., Litscher, G., Gao, S.-H., Zhou, S.-F., Yu, Z.-L., Chen, H.-Q., Zhang, S.-F., Tang, M.-K., Sun, J.-N., & Ko, K.-M. (2014). Historical perspective of traditional indigenous medical practices: the current renaissance and conservation of herbal resources. *Evidence-Based Complementary and Alternative Medicine*, 2014.
- Park, B. C., Bosire, K. O., Lee, E.-S., Lee, Y. S., & Kim, J.-A. (2005). Asiatic acid induces apoptosis in SK-MEL-2 human melanoma cells. *Cancer Letters*, 218(1), 81–90.
- Pitinidhipat, N., & Yasurin, P. (2012). Antibacterial activity of *Chrysanthemum indicum*, *Centella asiatica* and *Andrographis paniculata* against *Bacillus cereus* and *Listeria monocytogenes* under osmotic stress. *Assumption University Journal of Technology*, 15(4), 239–245.
- Pittella, F., Dutra, R. C., Junior, D. D., Lopes, M. T. P., & Barbosa, N. R. (2009). Antioxidant and cytotoxic activities of *Centella asiatica* (L) Urb. *International Journal of Molecular Sciences*, 10(9), 3713–3721.
- Prakash, V., Jaiswal, N., & Srivastava, M. (2017). A review on medicinal properties of *Centella asiatica*. *Asian J Pharm Clin Res*, 10(10), 69.
- Prasad, A., Mathur, A. K., & Mathur, A. (2019). Advances and emerging research trends for modulation of centelloside biosynthesis in *Centella asiatica* (L.) Urban-A

- review. *Industrial Crops and Products*, 141, 111768.
- Punturee, K., Wild, C. P., Kasinrerak, W., & Vinitketkumnuen, U. (2005). Immunomodulatory activities of *Centella asiatica* and *Rhinacanthus nasutus* extracts. *Asian Pacific Journal of Cancer Prevention*, 6(3), 396.
- Puttarak, P., & Panichayupakaranant, P. (2012). Factors affecting the content of pentacyclic triterpenes in *Centella asiatica* raw materials. *Pharmaceutical Biology*, 50(12), 1508–1512.
- Rao, N. J., Subash, K. R., & Kumar, K. S. (2012). Role of phytotherapy in gingivitis: A review. *Int J Pharmacol*, 8, 1–5.
- Ray F. Evert, S. E. E. (2016). *Raven Bitki Biyolojisi* (8th ed.). Palme Yayinevi.
- Roy, D. C., Barman, S. K., & Shaik, M. M. (2013). Current updates on *Centella asiatica*: phytochemistry, pharmacology and traditional uses. *Medicinal Plant Research*, 3.
- Rush, W. R., Murray, G. R., & Graham, D. J. M. (1993). The comparative steady-state bioavailability of the active ingredients of Madecassol. *European Journal of Drug Metabolism and Pharmacokinetics*, 18(4), 323–326.
- Ruszymah, B. H. I., Chowdhury, S. R., Manan, N. A. B. A., Fong, O. S., Adenan, M. I., & Saim, A. Bin. (2012). Aqueous extract of *Centella asiatica* promotes corneal epithelium wound healing *in vitro*. *Journal of Ethnopharmacology*, 140(2), 333–338.
- Sainath, S. B., Meena, R., Supriya, C., Reddy, K. P., & Reddy, P. S. (2011). Protective role of *Centella asiatica* on lead-induced oxidative stress and suppressed reproductive health in male rats. *Environmental Toxicology and Pharmacology*, 32(2), 146–154.
- Saxena, M., Saxena, J., Nema, R., Singh, D., & Gupta, A. (2013). Phytochemistry of medicinal plants. *Journal of Pharmacognosy and Phytochemistry*, 1(6).
- Schaneberg, B. T., Mikell, J. R., Bedir, E., Khan, I. A., & Nachname, V. (2003). An improved HPLC method for quantitative determination of six triterpenes in *Centella asiatica* extracts and commercial products. *Die Pharmazie-An International Journal of Pharmaceutical Sciences*, 58(6), 381–384.
- Seevaratnam, V., Banumathi, P., Premalatha, M. R., Sundaram, S. P., & Arumugam, T. (2012). Functional properties of *Centella asiatica* (L.): a review. *Int J Pharm Pharm Sci*, 4(5), 8–14.
- Shao, W., Cao, X., Shen, L., Zhang, F., & Yu, B. (2017). A convergent synthesis of the triterpene saponin asiaticoside. *Asian Journal of Organic Chemistry*, 6(9), 1270–

1276.

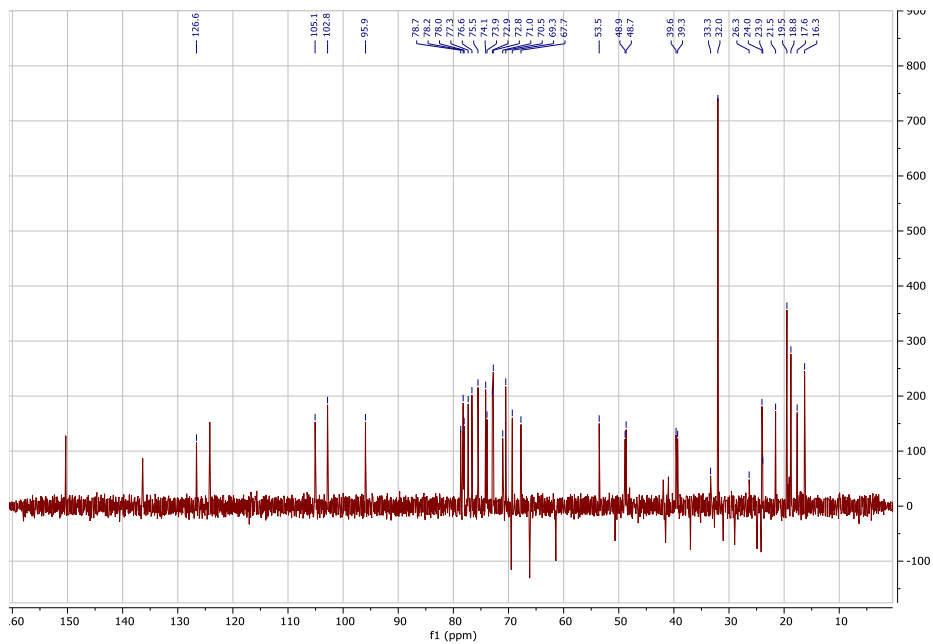
- Shukla, A., Rasik, A. M., Jain, G. K., Shankar, R., Kulshrestha, D. K., & Dhawan, B. N. (1999). *In vitro* and **in vivo** wound healing activity of asiaticoside isolated from *Centella asiatica*. *Journal of Ethnopharmacology*, *65*(1), 1–11.
- Somchit, M. N., Sulaiman, M. R., Zuraini, A., Samsuddin, L., Somchit, N., Israf, D. A., & Moin, S. (2004). Antinociceptive and antiinflammatory effects of *Centella asiatica*. *Indian Journal of Pharmacology*, *36*(6), 377.
- Sparg, S. G., Light, M. E., & Van Staden, J. (2004). Biological activities and distribution of plant saponins. *Journal of Ethnopharmacology*, *94*(2–3), 219–243.
- Sun, B., Wu, L., Wu, Y., Zhang, C., Qin, L., Hayashi, M., Kudo, M., Gao, M., & Liu, T. (2020). Therapeutic potential of *Centella asiatica* and its triterpenes: a review. *Frontiers in Pharmacology*, *11*, 1373.
- Sun, H., Fang, W.-S., Wang, W.-Z., & Hu, C. (2006). Structure-activity relationships of oleanane-and ursane-type triterpenoids. *Botanical Studies*, *47*(4), 339–368.
- Thakur, M., Melzig, M. F., Fuchs, H., & Weng, A. (2011). Chemistry and pharmacology of saponins: special focus on cytotoxic properties. *Botanics: Targets and Therapy*, *1*, 19–29.
- Theodorou, V., Skobridis, K., Tzakos, A. G., & Ragoussis, V. (2007). A simple method for the alkaline hydrolysis of esters. *Tetrahedron Letters*, *48*(46), 8230–8233.
- Tiwari, R., & Rana, C. S. (2015). Plant secondary metabolites: a review. *International Journal of Engineering Research and General Science*, *3*(5), 661–670.
- Tsoukalas, D., Fragkiadaki, P., Docea, A. O., Alegakis, A. K., Sarandi, E., Thanasoula, M., Spandidos, D. A., Tsatsakis, A., Razgonova, M. P., & Calina, D. (2019). Discovery of potent telomerase activators: Unfolding new therapeutic and anti-aging perspectives. *Molecular Medicine Reports*, *20*(4), 3701–3708.
- Ullah, M. O., Sultana, S., Haque, A., & Tasmin, S. (2009). Antimicrobial, cytotoxic and antioxidant activity of *Centella asiatica*. *Eur J Sci Res*, *30*(2), 260–264.
- Van Loc, T., Nhu, V. T. Q., Van Chien, T., Thao, T. T. P., & Van Sung, T. (2018). Synthesis of madecassic acid derivatives and their cytotoxic activity. *Zeitschrift Für Naturforschung B*, *73*(2), 91–98.
- Wu, T., Geng, J., Guo, W., Gao, J., & Zhu, X. (2017). Asiatic acid inhibits lung cancer cell growth *in vitro* and *in vivo* by destroying mitochondria. *Acta Pharmaceutica Sinica B*, *7*(1), 65–72.
- Yoosook, C., Bunyaphatsara, N., Boonyakiat, Y., & Kantasuk, C. (2000). Anti-herpes

- simplex virus activities of crude water extracts of Thai medicinal plants. *Phytomedicine*, 6(6), 411–419.
- Yoshida, M., Fuchigami, M., Nagao, T., Okabe, H., Matsunaga, K., Takata, J., Karube, Y., Tsuchihashi, R., Kinjo, J., & Mihashi, K. (2005). Antiproliferative constituents from Umbelliferae plants VII. Active triterpenes and rosmarinic acid from *Centella asiatica*. *Biological and Pharmaceutical Bulletin*, 28(1), 173–175.
- Yu, Q.-L., Duan, H.-Q., Takaishi, Y., & Gao, W.-Y. (2006). A novel triterpene from *Centella asiatica*. *Molecules*, 11(9), 661–665.
- Zheng, C. J., & Qin, L. (2007). Chemical components of *Centella asiatica* and their bioactivities. *Zhong Xi Yi Jie He Xue Bao= Journal of Chinese Integrative Medicine*, 5(3), 348–351.

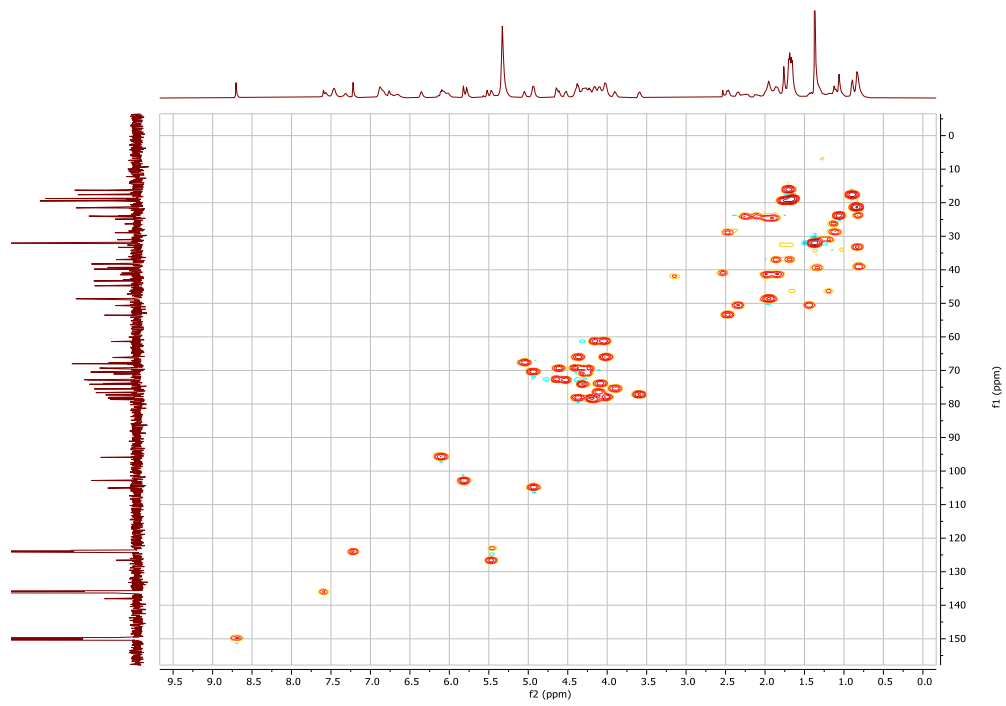
APPENDICES

APPENDIX A.

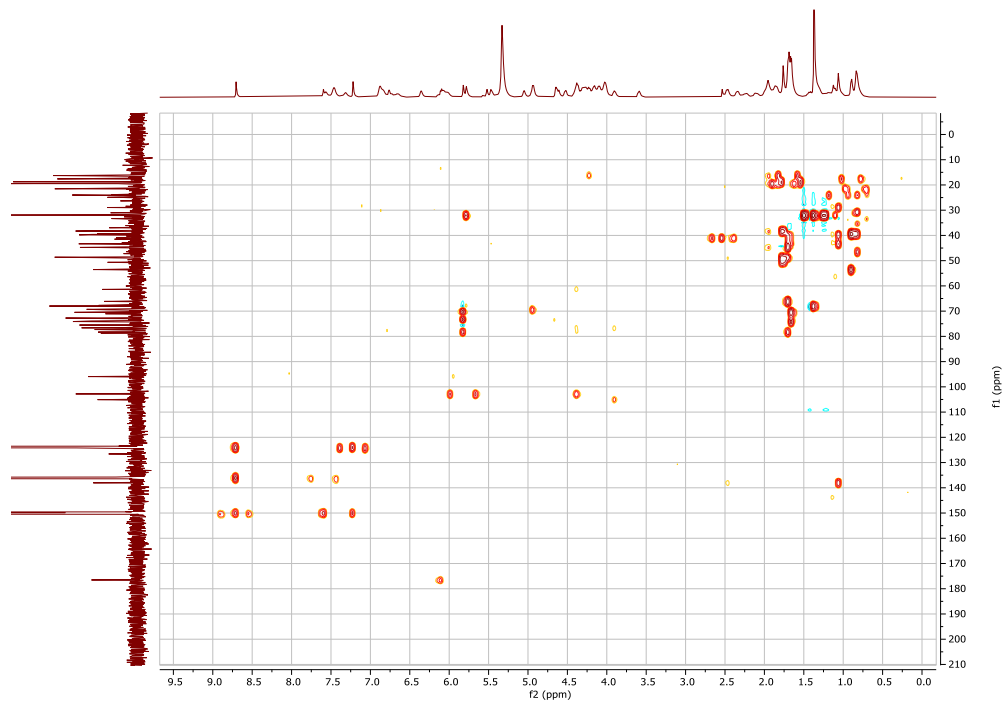
SPECTRUMS OF DD-GK-01, DD-GK-02, DD-GK-03, DD-GK-04



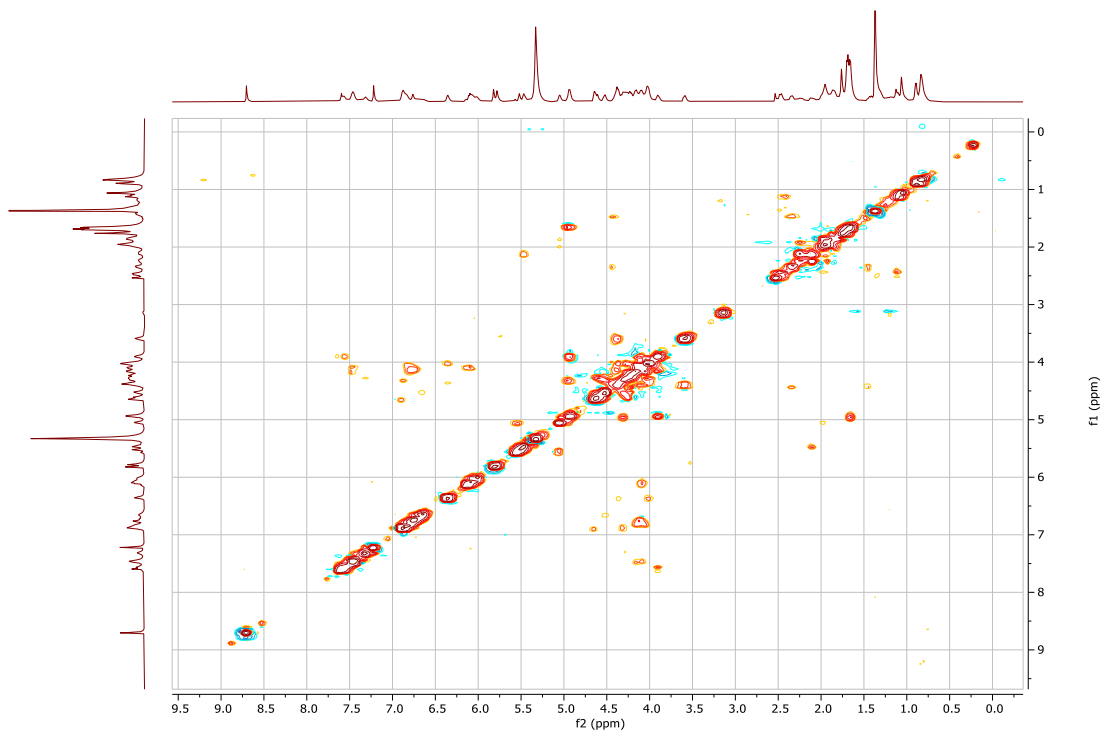
Spectrum 9. DEPT135 spectrum of DD-GK-01



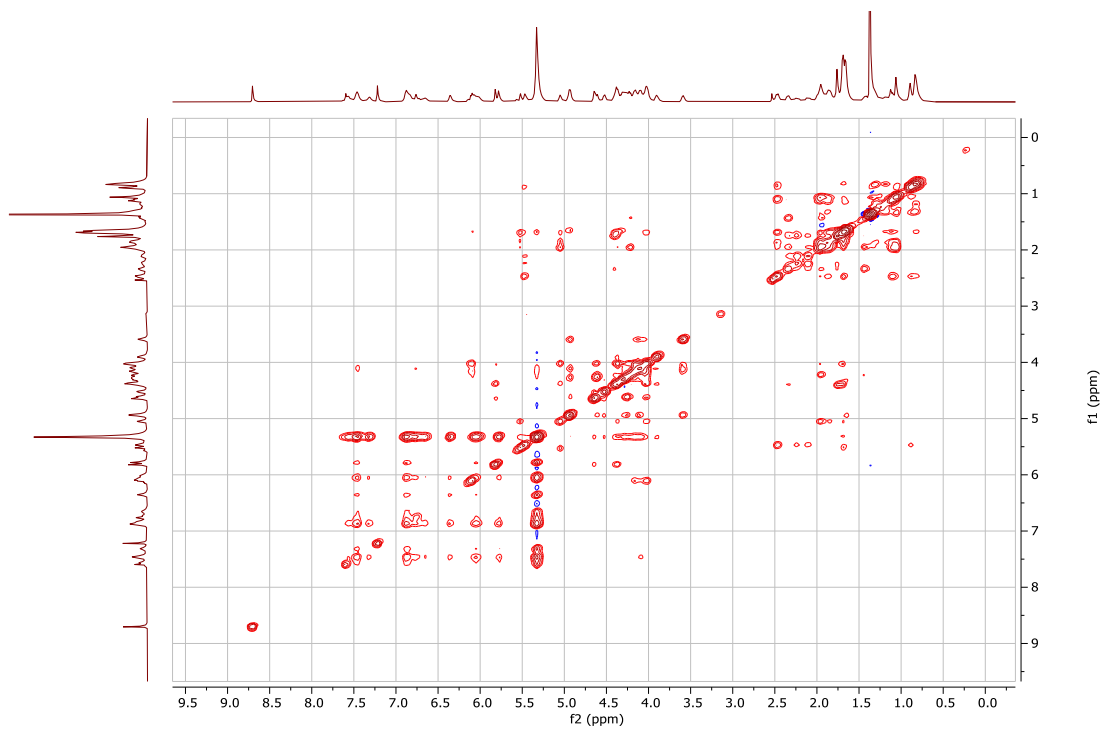
Spectrum 10. HSQC spectrum of DD-GK-01



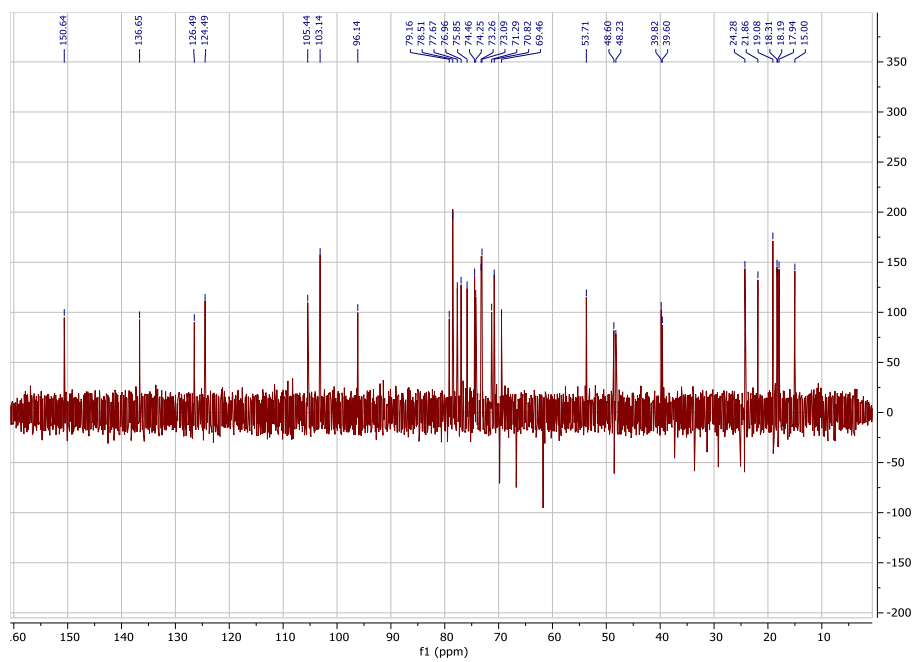
Spectrum 11. HMBC spectrum of DD-GK-01



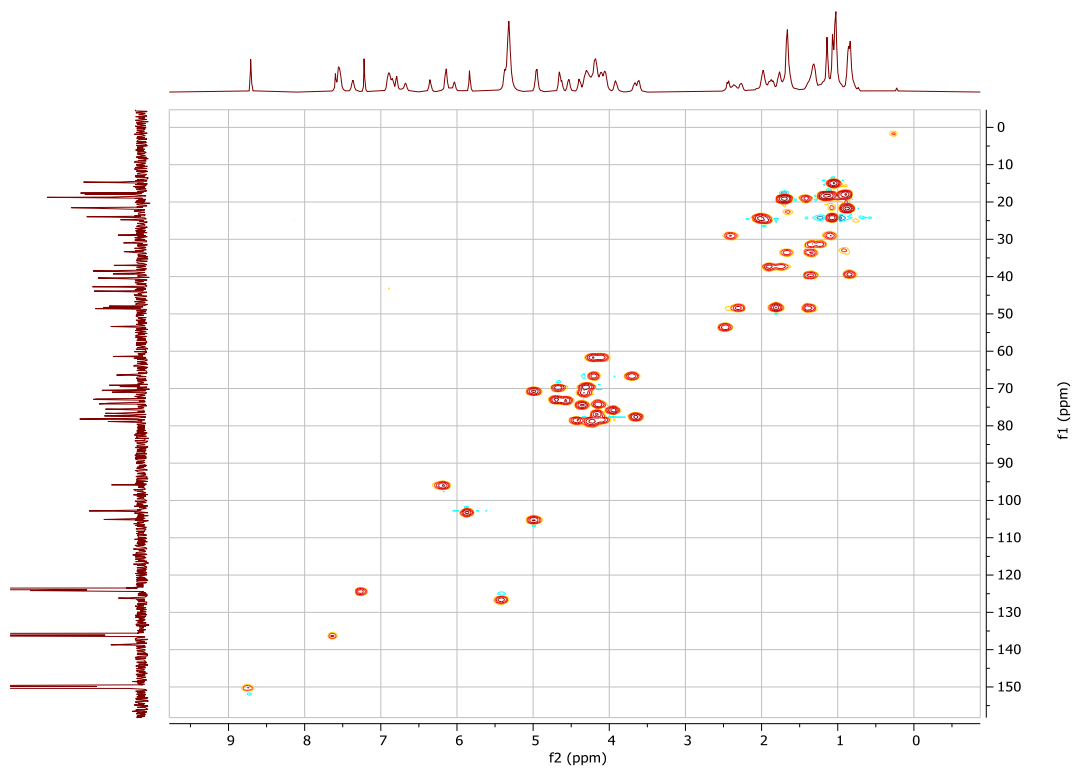
Spectrum 12. COSY spectrum of DD-GK-01



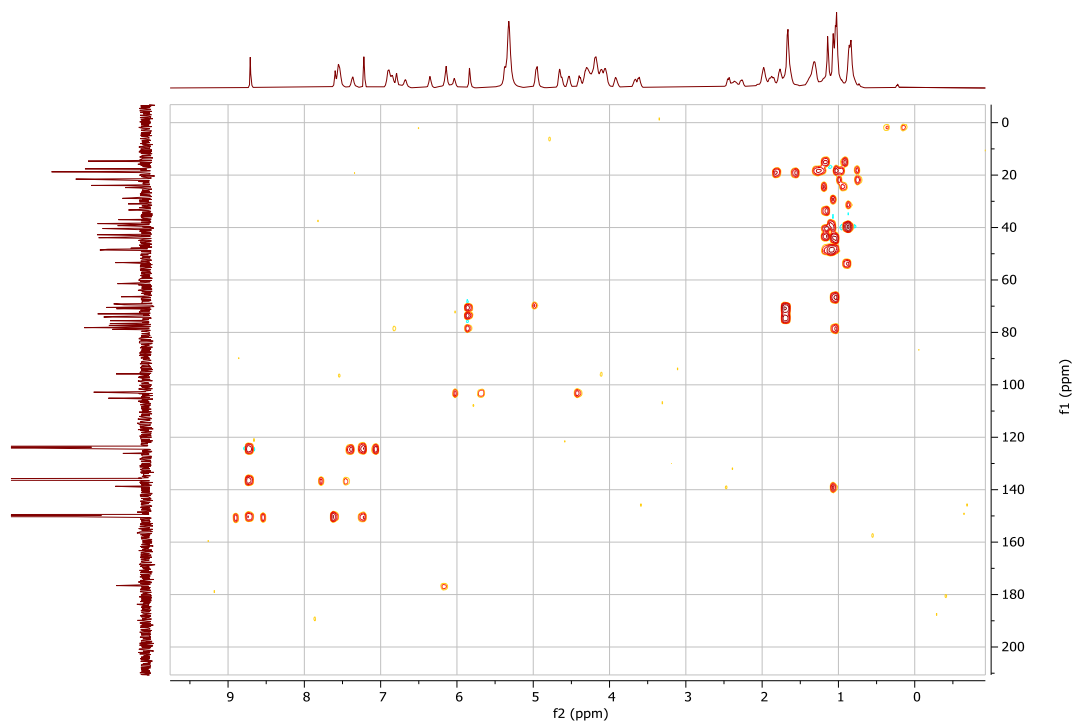
Spectrum 13. NOESY spectrum of DD-GK-01



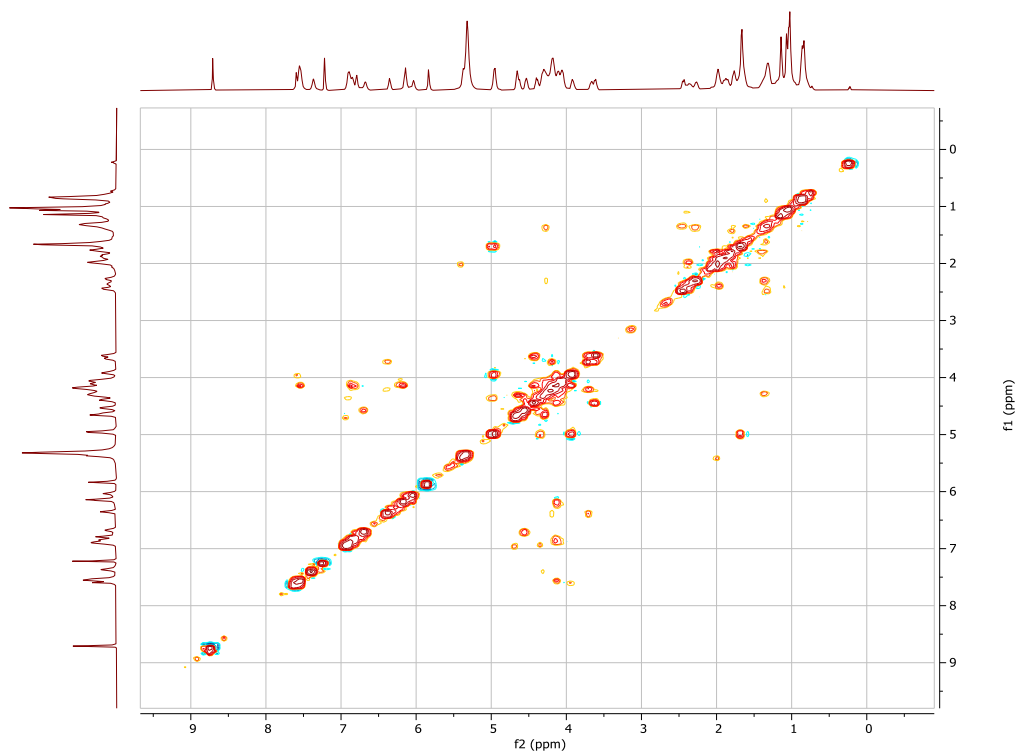
Spectrum 14. DEPT135 spectrum of DD-GK-02



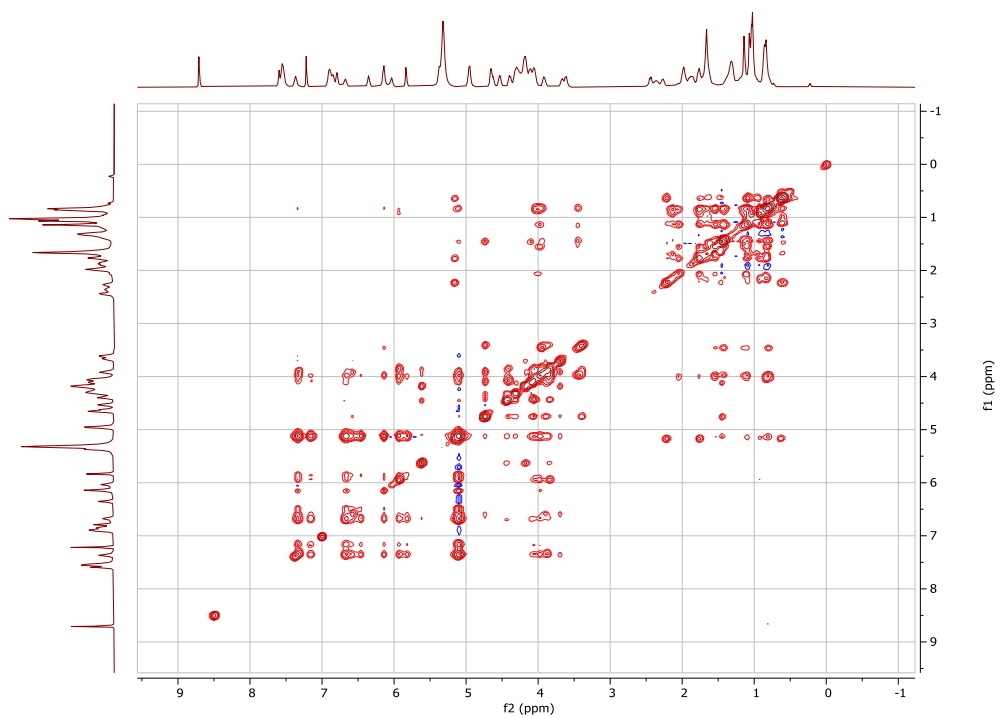
Spectrum 15. HSQC spectrum of DD-GK-02



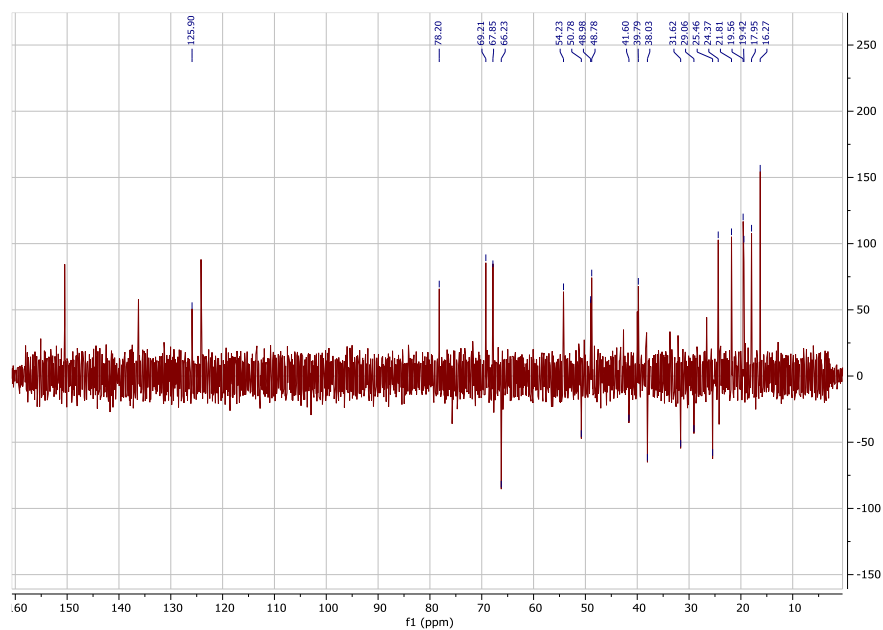
Spectrum 16. HMBC spectrum of DD-GK-02



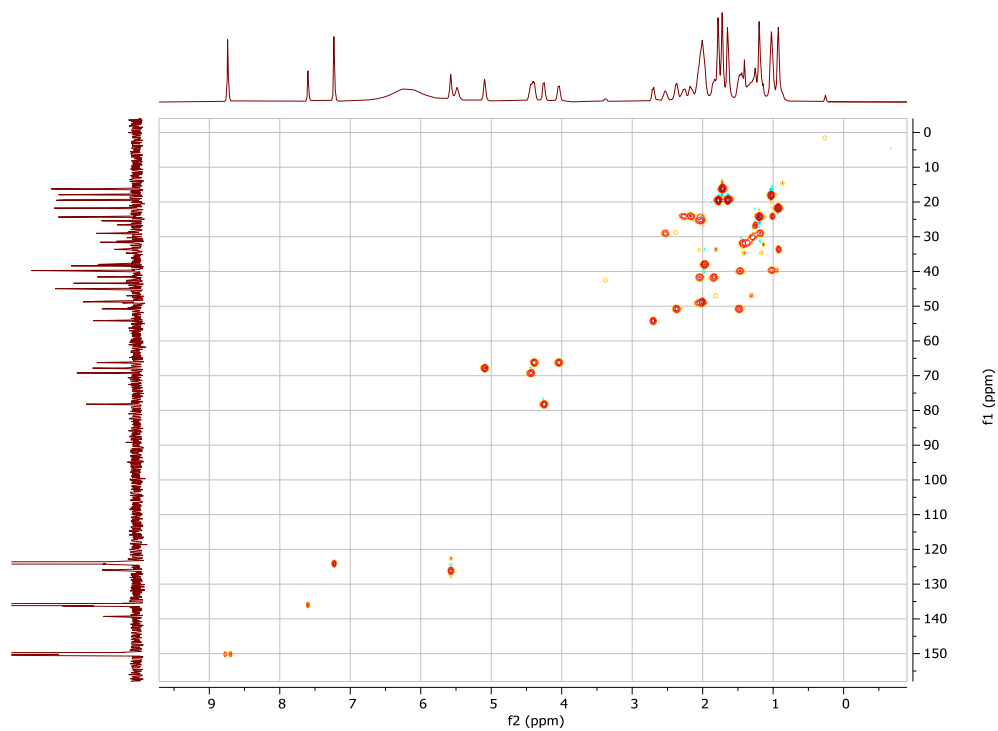
Spectrum 17. COSY spectrum of DD-GK-02



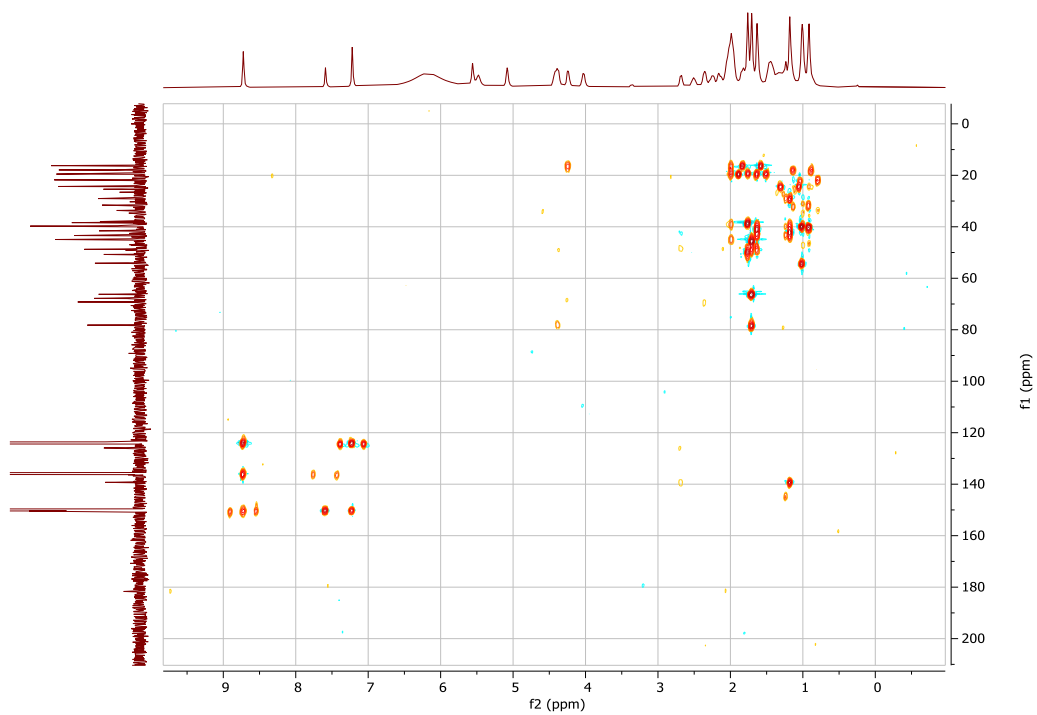
Spectrum 18. NOESY spectrum of DD-GK-02



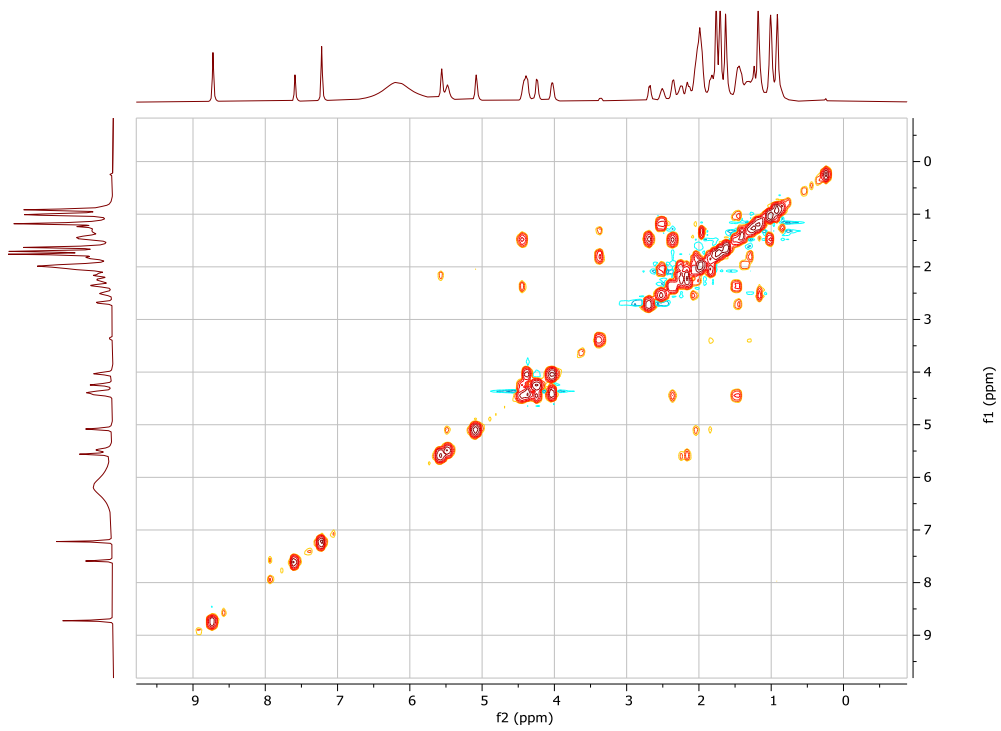
Spectrum 19. DEPT135 spectrum of DD-GK-03



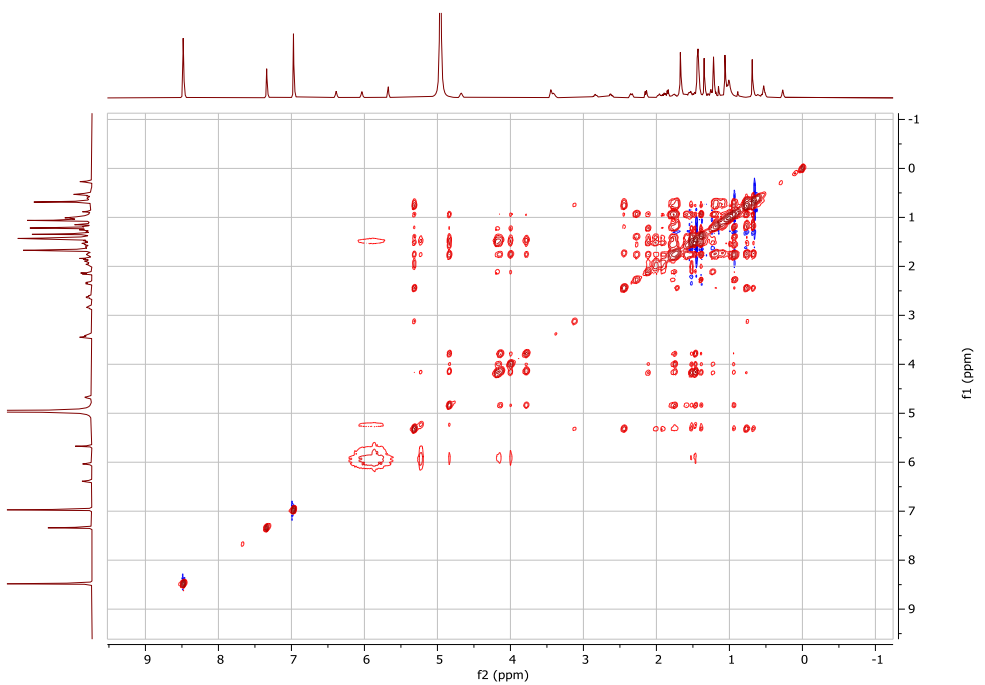
Spectrum 20. HSQC spectrum of DD-GK-03



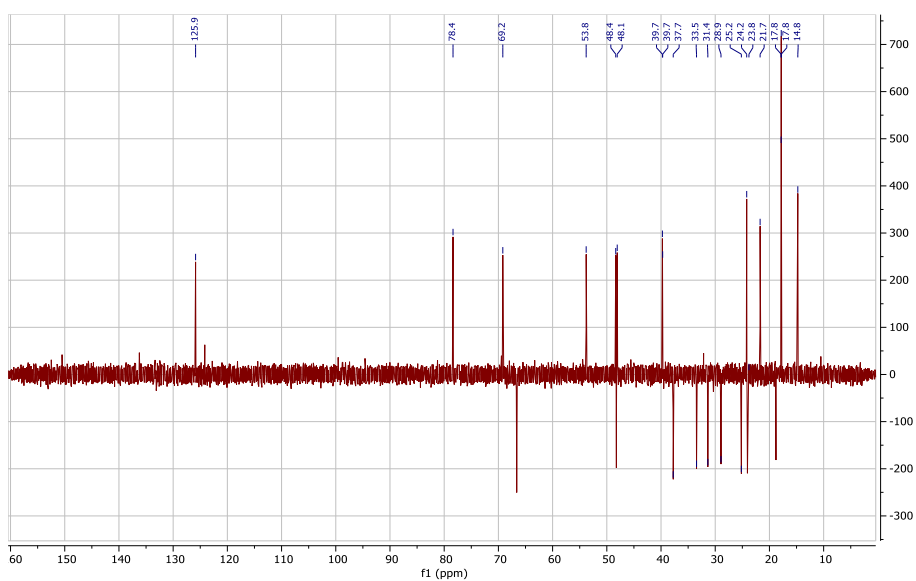
Spectrum 21. HMBC spectrum of DD-GK-03



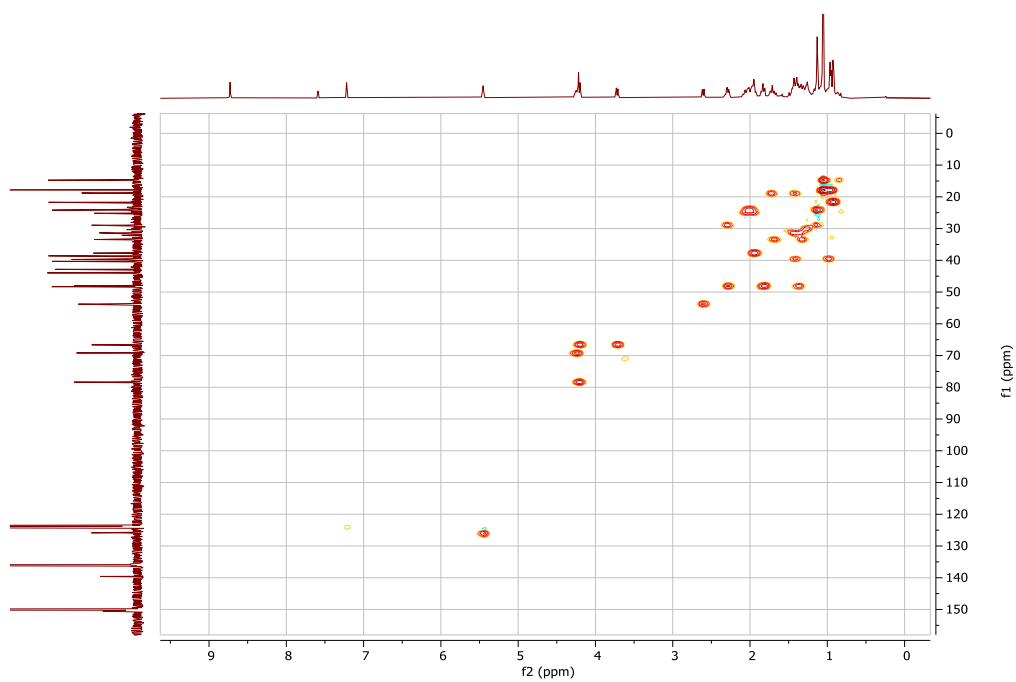
Spectrum 22. COSY spectrum of DD-GK-03



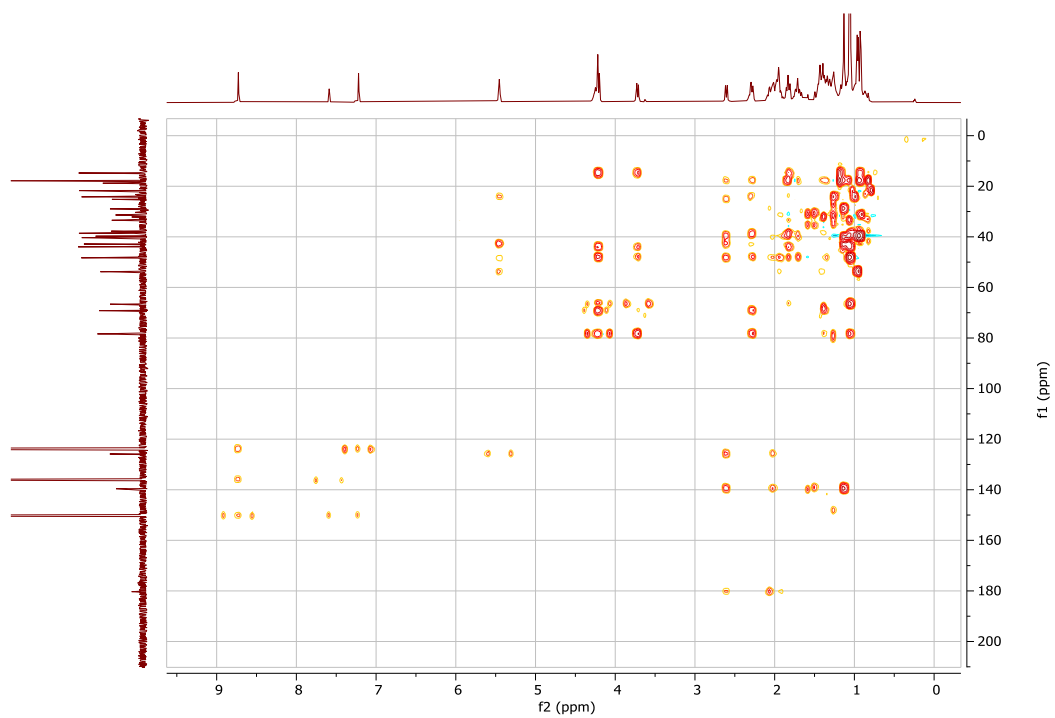
Spectrum 23. NOESY spectrum of DD-GK-03



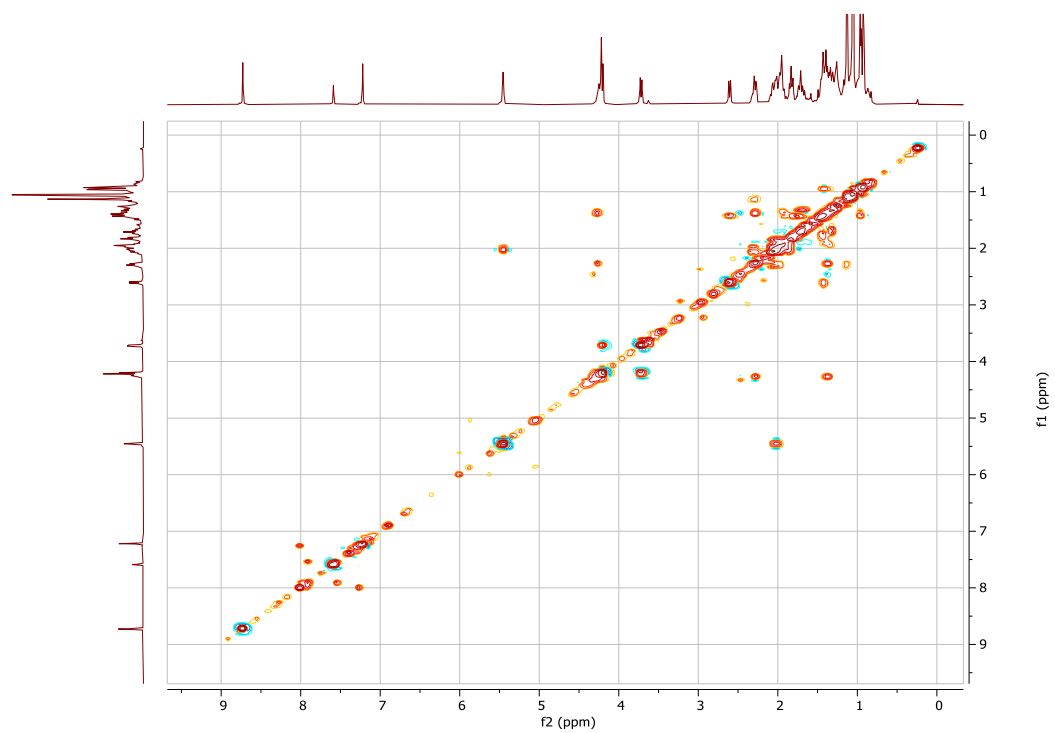
Spectrum 24. DEPT135 spectrum of DD-GK-04



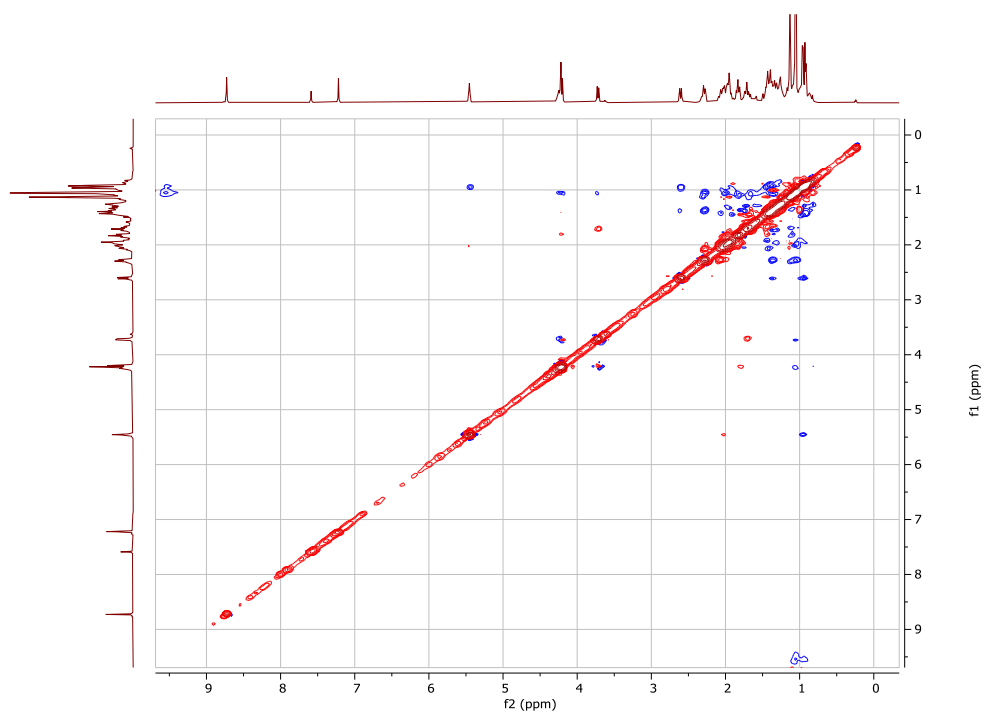
Spectrum 25. HSQC spectrum of DD-GK-04



Spectrum 26. HMBC spectrum of DD-GK-04



Spectrum 27. COSY spectrum of DD-GK-04



Spectrum 28. NOESY spectrum of DD-GK-04

APPENDIX B.

OPEN WOUND IMAGES OF MADECASSIC ACID, ASIATIC ACID, AND THE EXTRACT

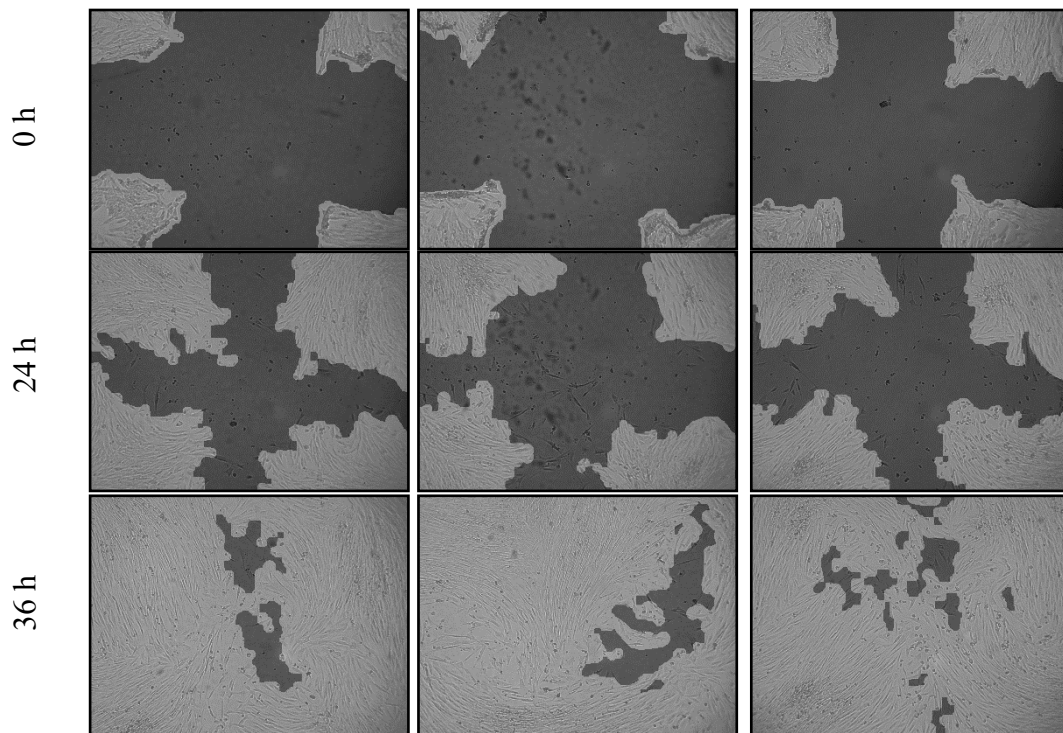


Figure 44. Open wound images of DMSO control at 0, 24, and 36 h

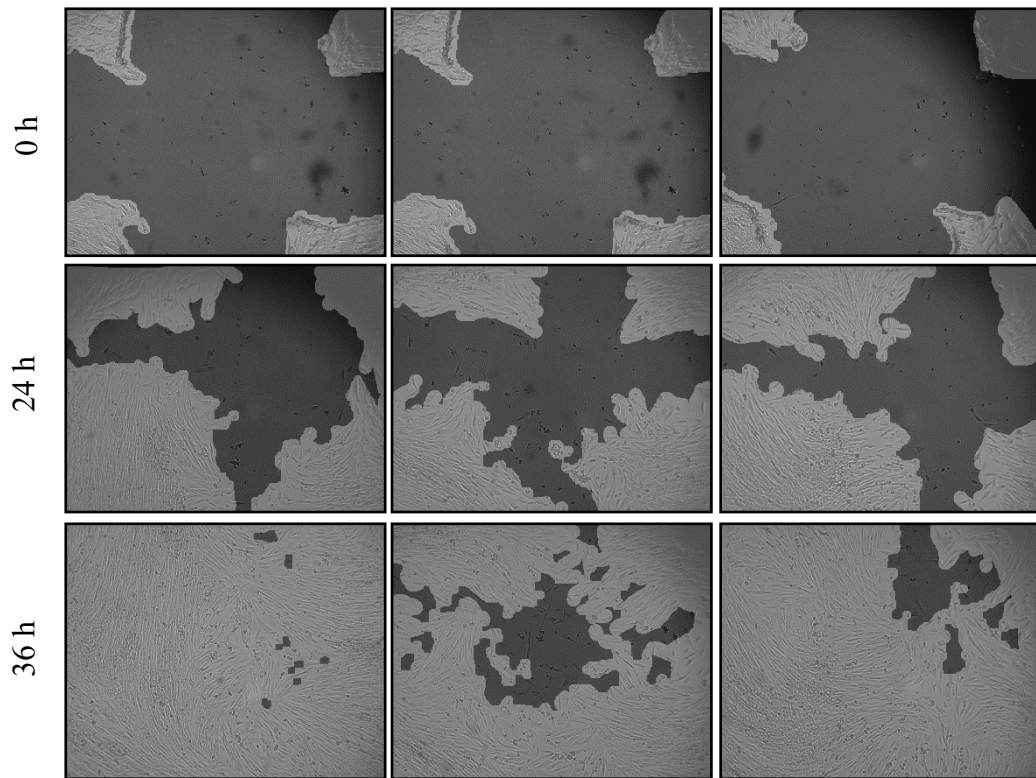


Figure 45. Open wound images of MA (2nM) at 0, 24, and 36 h

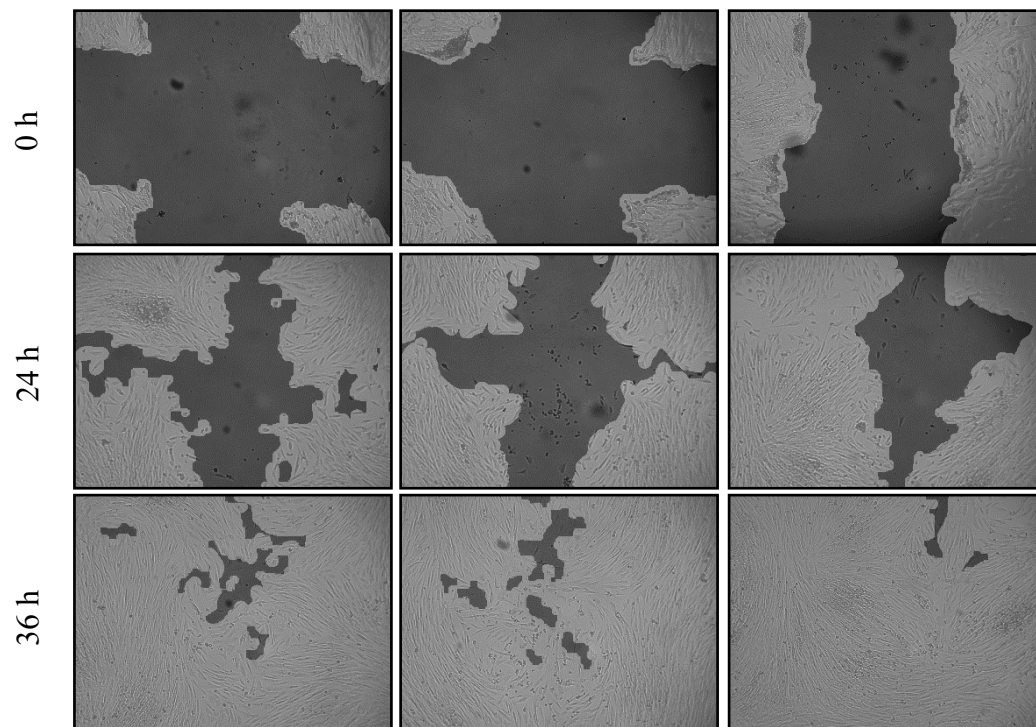


Figure 46. Open wound images of MA (10nM) at 0, 24, and 36 h

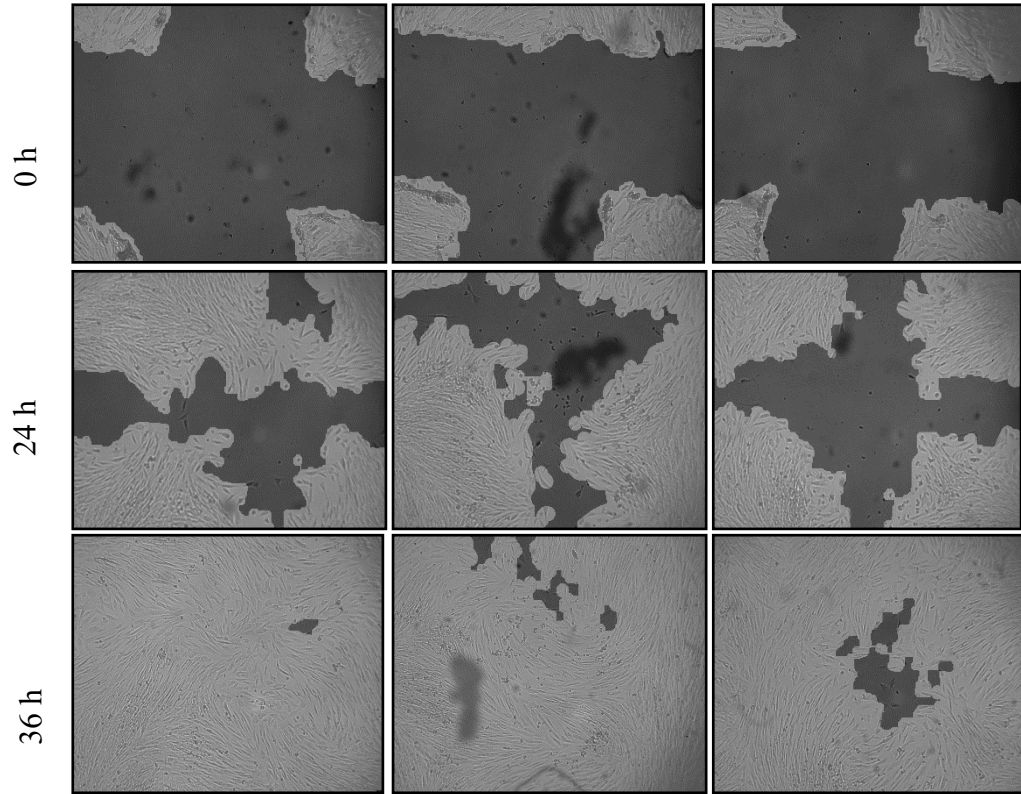


Figure 47. Open wound images of MA (30nM) at 0, 24, and 36 h

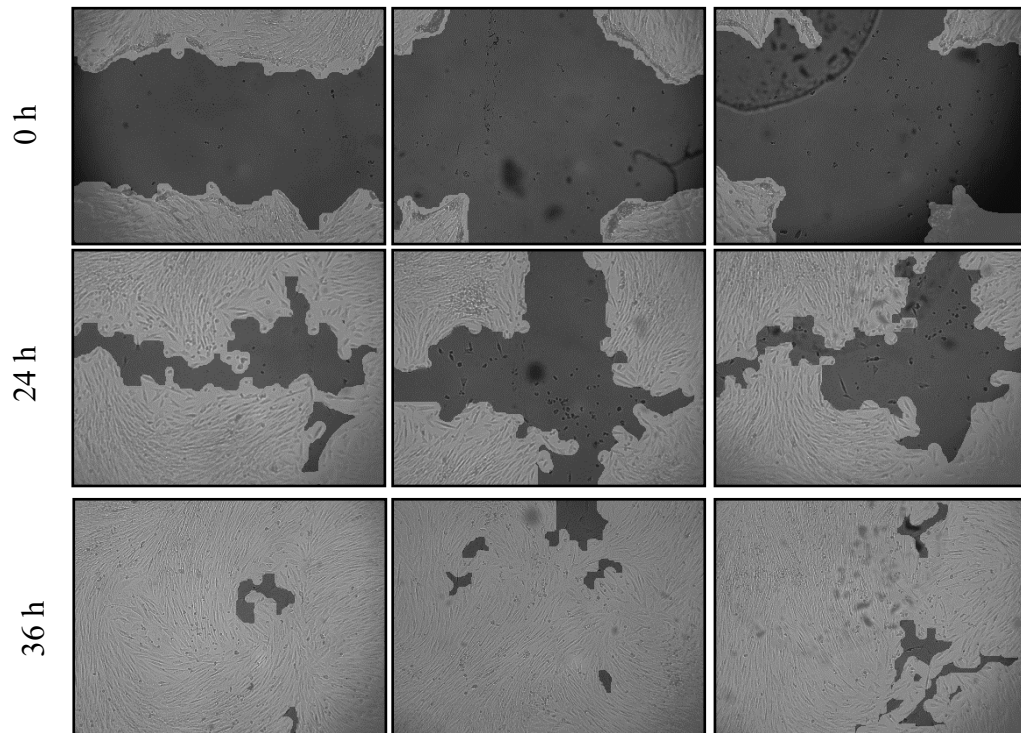


Figure 48. Open wound images of MA (100nM) at 0, 24, and 36 h

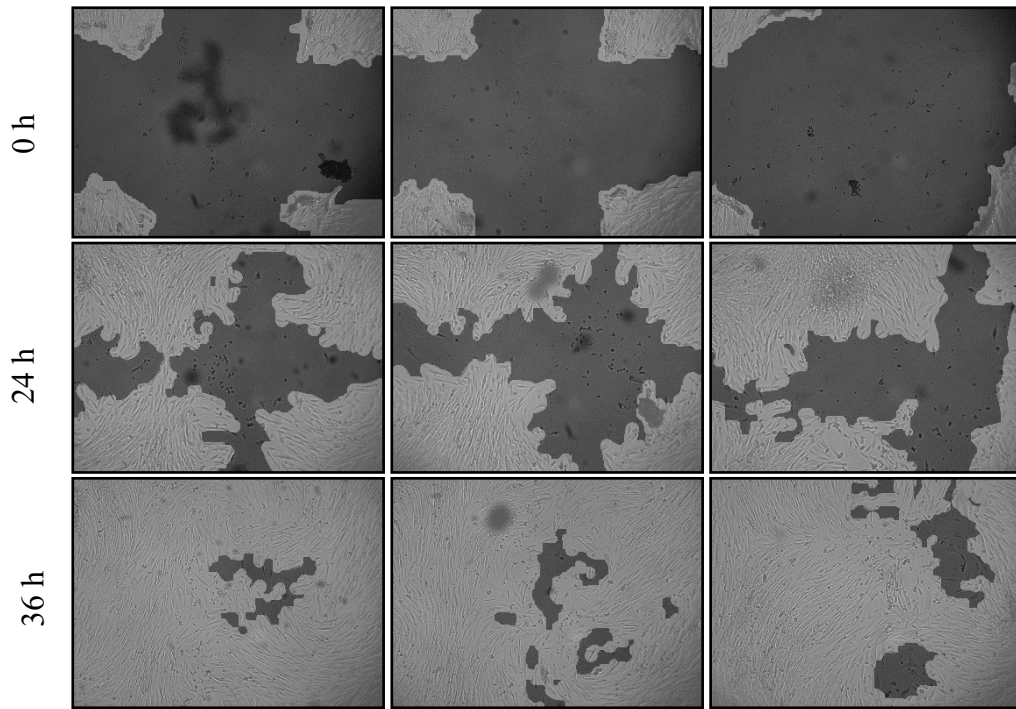


Figure 49. Open wound images of MA (300 nM) at 0, 24, and 36 h

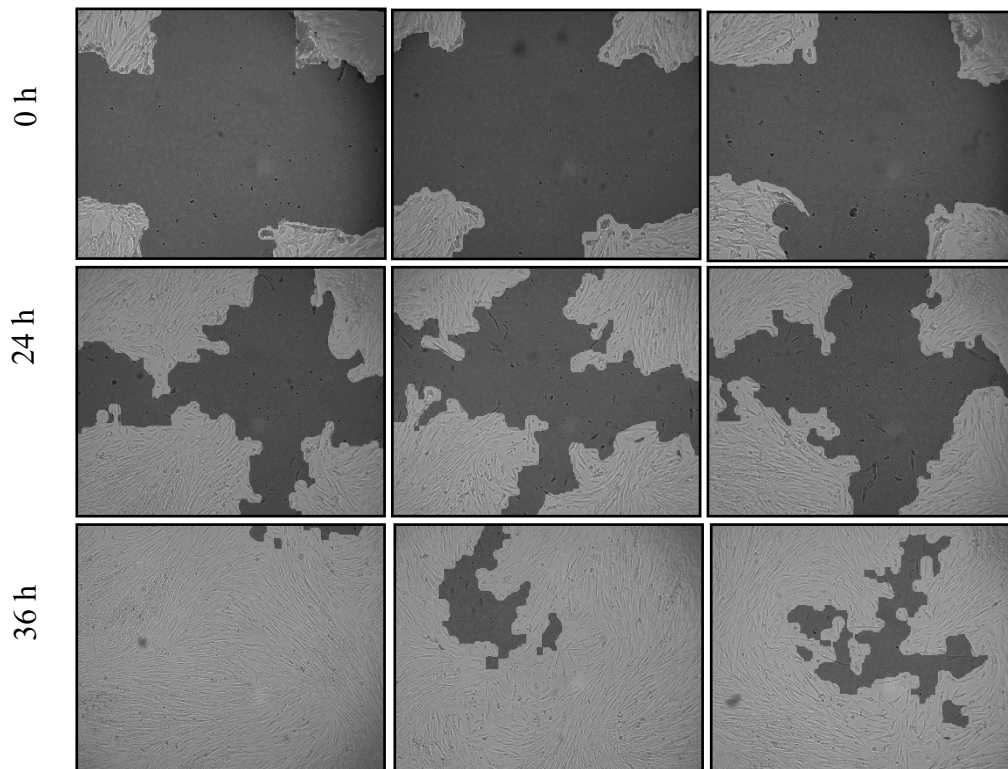


Figure 50. Open wound images of AA (2 nM) at 0, 24, and 36 h

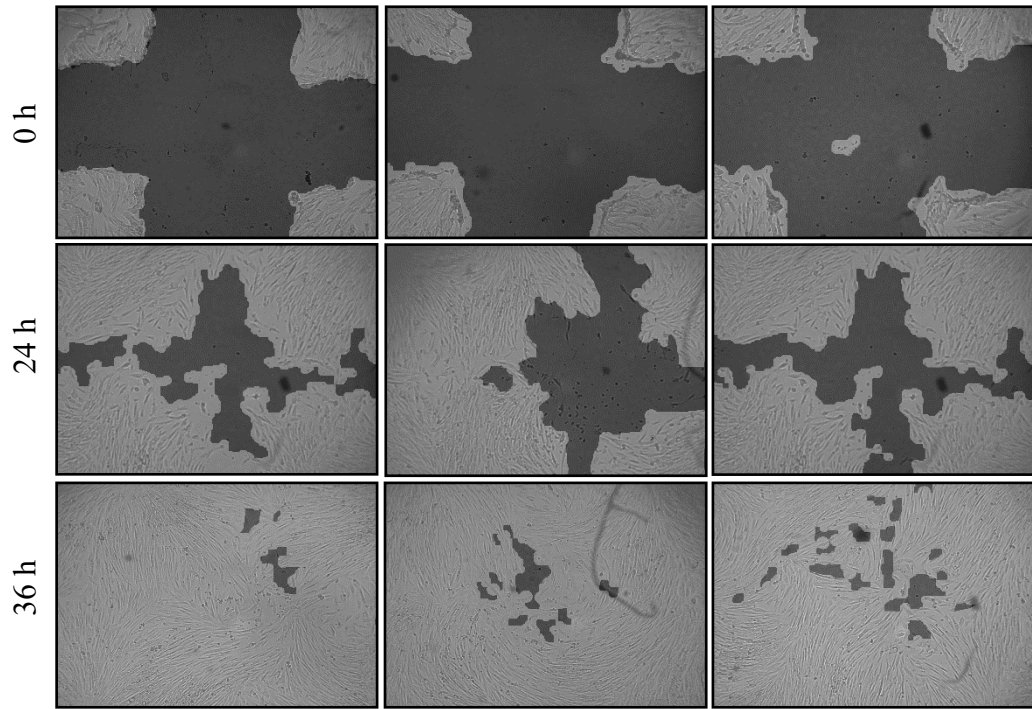


Figure 51. Open wound images of AA (10 nM) at 0, 24, and 36 h

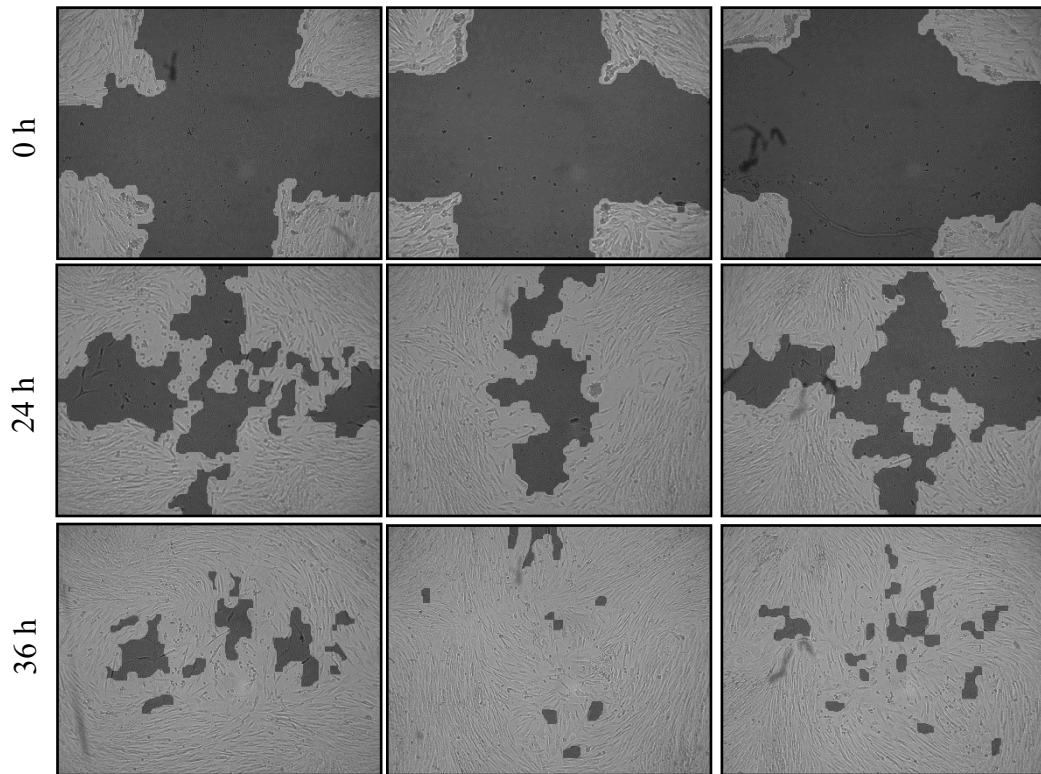


Figure 52. Open wound images of AA (30 nM) at 0, 24, and 36 h

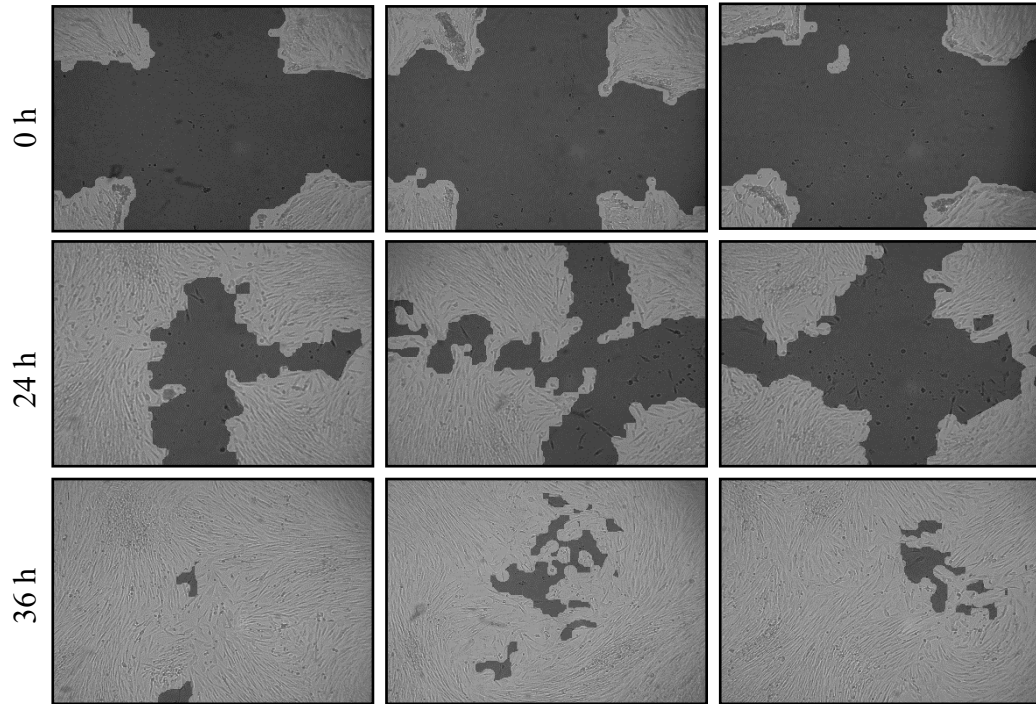


Figure 53. Open wound images of AA (100 nM) at 0, 24, and 36 h

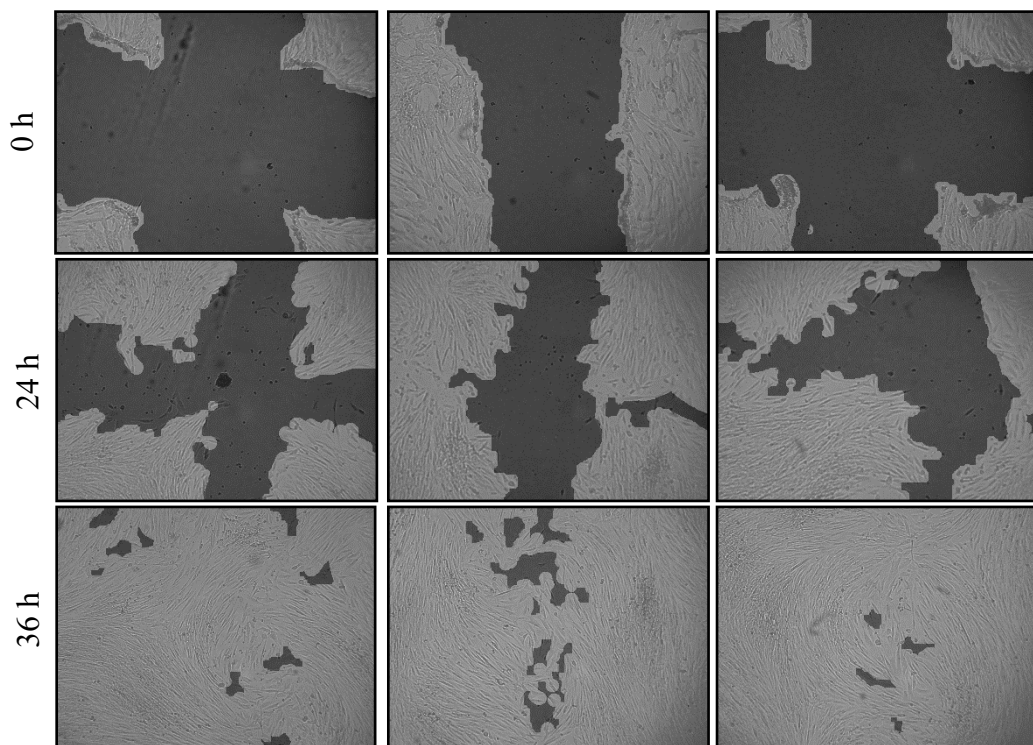


Figure 54. Open wound images of AA (300 nM) at 0, 24, and 36 h

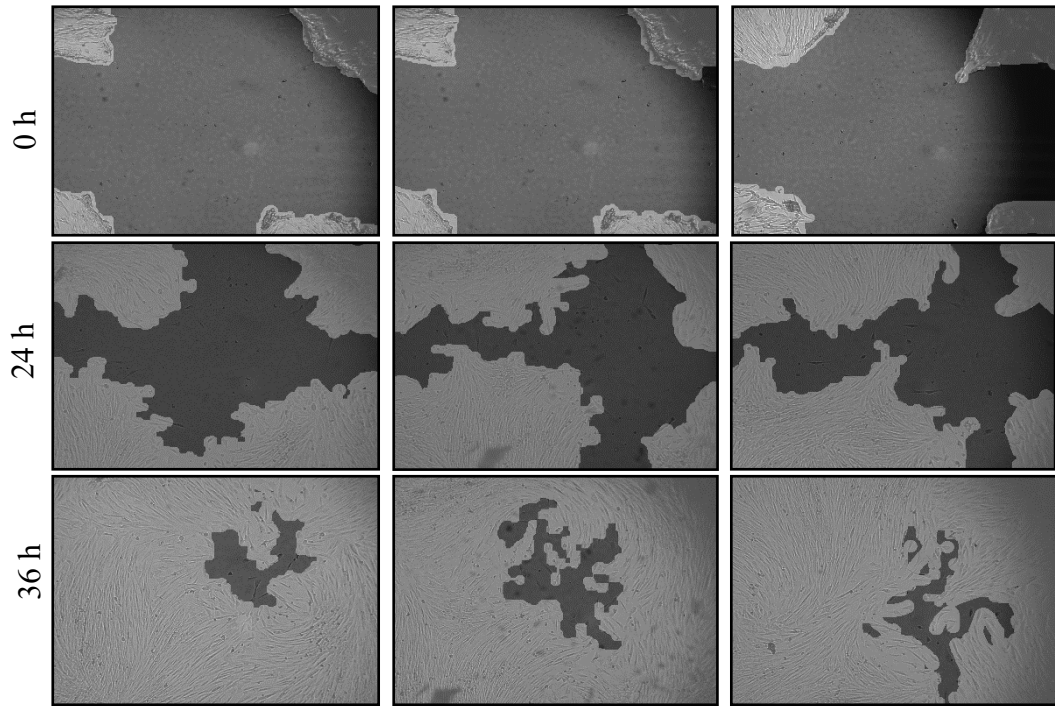


Figure 55. Open wound images of the extract (2 nM) at 0, 24, and 36 h

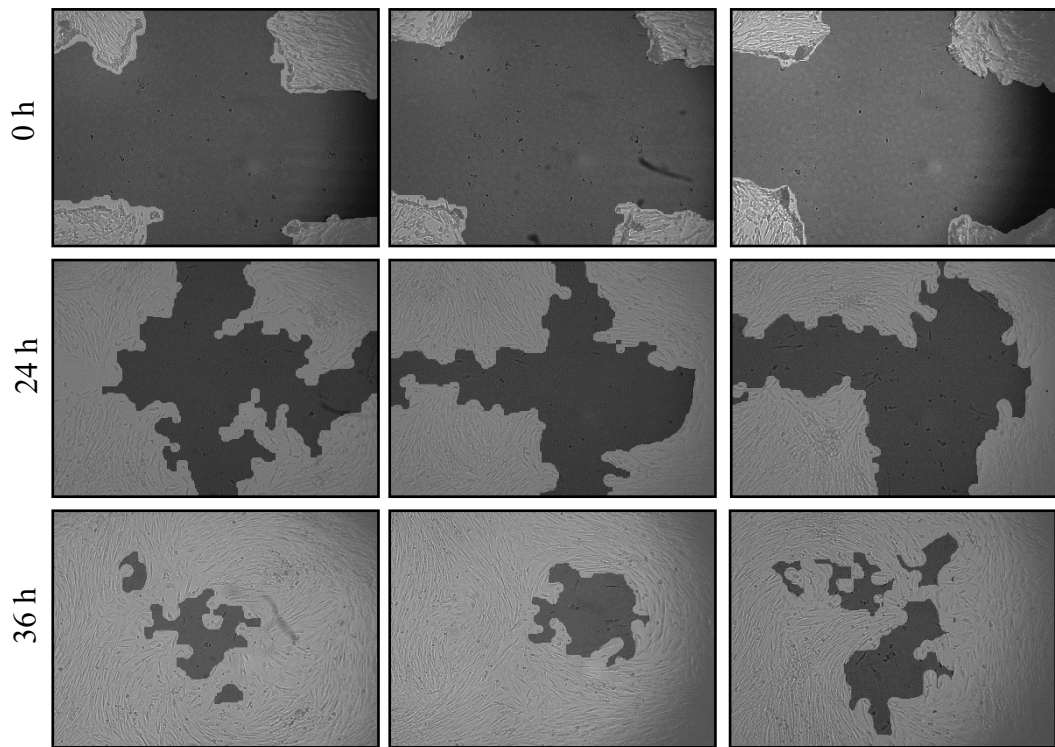


Figure 56. Open wound images of the extract (10 nM) at 0, 24, and 36 h

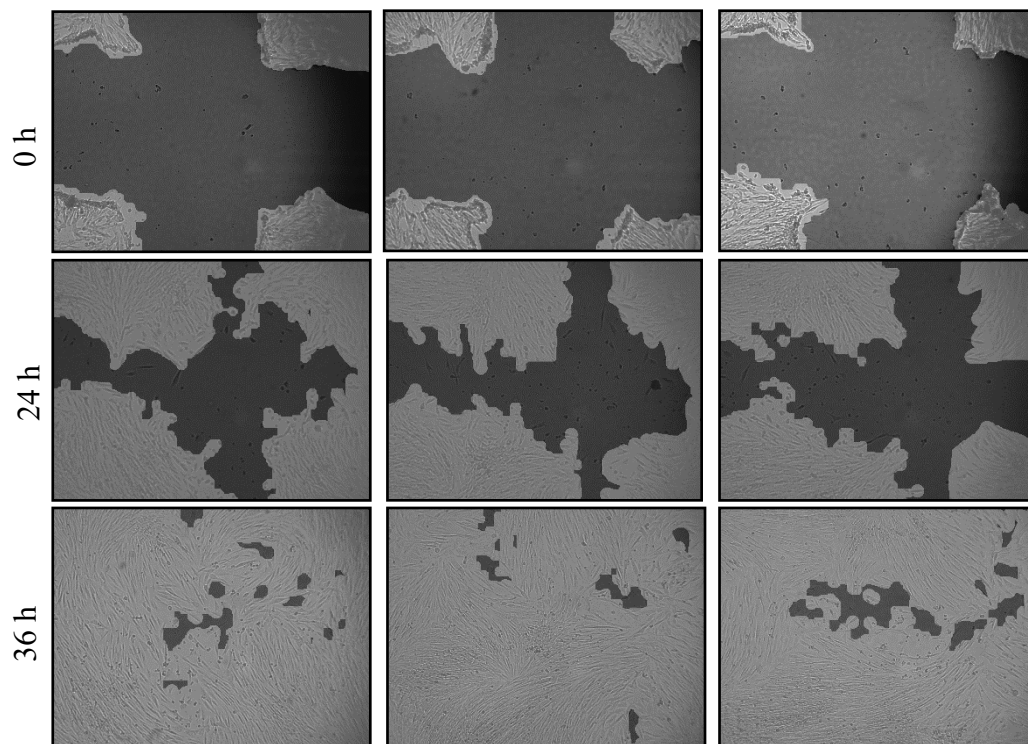


Figure 57. Open wound images of the extract (30 nM) at 0, 24, and 36 h

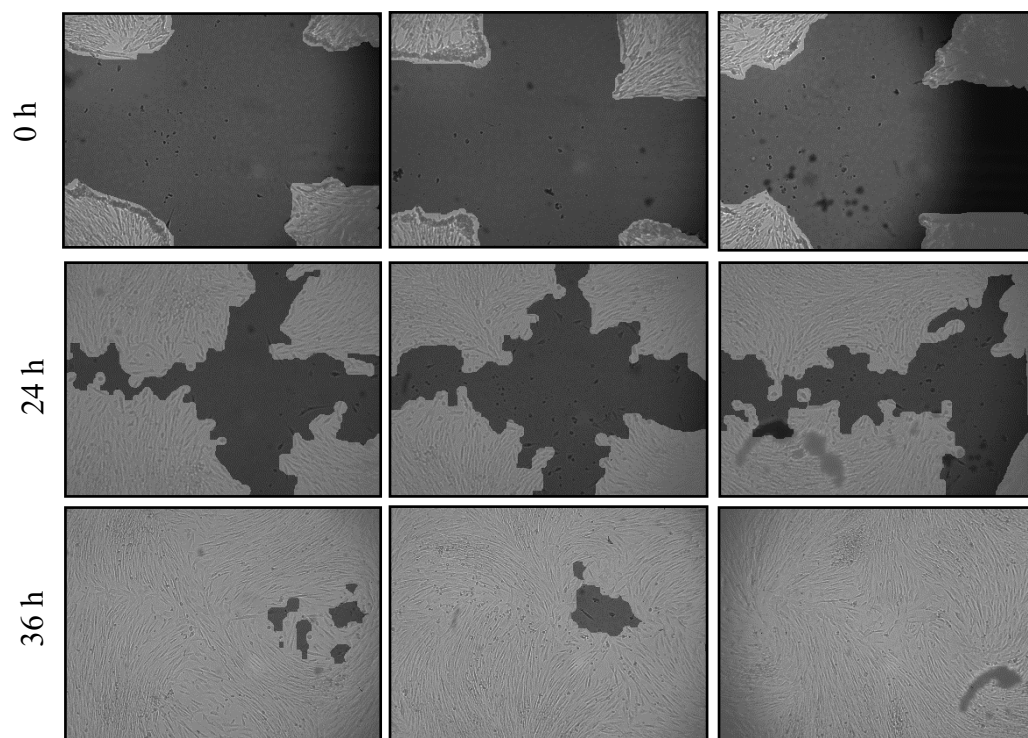


Figure 58. Open wound images of the extract (100 nM) at 0, 24, and 36 h

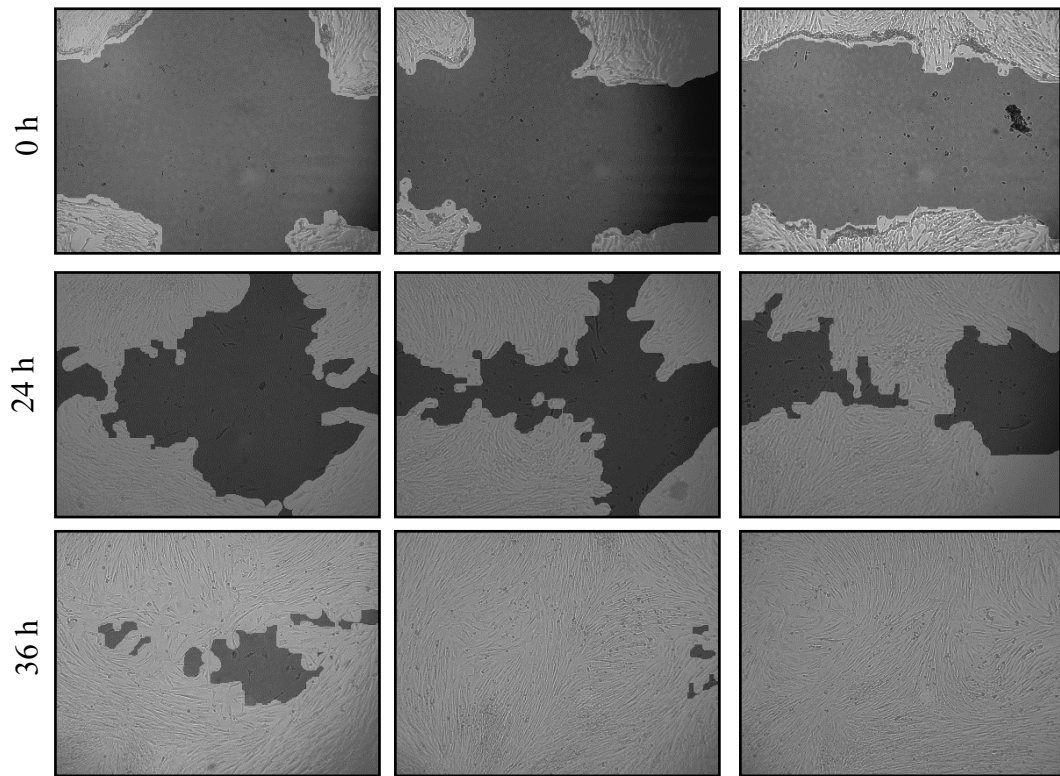


Figure 59. Open wound images of the extract (300 nM) at 0, 24, and 36 h